INTERACTIONS BETWEEN RABIES VIRUS (GLYCOPROTEIN) AND ITS HOST CELL RECEPTOR PEPTIDE ANALOGUES AS ANTIVIRAL STRATEGIES

Thesis

Submitted to the

DEEMED UNIVERSITY

Indian Veterinary Research Institute

Izatnagar – 243 122 (U.P.), India

Dr. BASAVARAJ SAJJANAR
Roll No. 1236

IN PARTIAL FULFILLMENT OF THE REQUIREMENTS

FOR THE DEGREE

OF

Doctor of Philosophy

(Animal Biotechnology)

March, 2015

भारतीय पशु चिकित्सा अनुसंधान संस्थान
(सम विश्वविद्यालय)
इज़्ज़तनगर -243122,(उ.प्र.),भारत

DIVISION OF VETERINARY BIOTECHNOLOGY
INDIAN VETERINARY RESEARCH INSTITUTE
(Deemed University)
IZATNAGAR - 243 122, U.P., INDIA

Dr. Satish Kumar, PhD
Principal Scientist
In-Charge CIF, Bioengg

Dated: 07-03 2015

Certificate

This is to be certified that the research work embodied in this thesis entitled "**Interactions between the rabies virus (glycoprotein) and host cell receptor peptide analogues as antiviral strategy**" *submitted by* **Dr. Basavaraj Sajjanar, Roll No.1236,** *for the award of* **Doctor of Philosophy** *Degree in* **Animal Biotechnology** *at Indian Veterinary Research Institute, Izatnagar, is the original work carried out by the candidate herself under my supervision and guidance.*

It is further certified that **Dr. Basavaraj Sajjanar, Roll No. 1236,** *has worked for more than 30 months in the Institute and has put in more than 300 days attendance under me from the date of registration for Doctor of Philosophy Degree in this Deemed University, as required under the relevant ordinance.*

(SATISH KUMAR)
Chairman
Advisory Committee

Certificate

We the undersigned members of Advisory Committee of ***Dr. Basavaraj Sajjanar, Roll No. 1236,*** *a candidate for the degree of* **Doctor of Philosophy** *with the major discipline in* **Animal Biotechnology** *agree that the thesis entitled* **"Interactions between rabies virus (glycoprotein) and its host cell receptor peptide analogues as antiviral strategy"** *may be submitted in partial fulfillment of the requirement for the degree.*

We have gone through the contents of the thesis and are fully satisfied with the work carried out by the candidate, which is being presented for the award of **Doctor of Philosophy** *Degree of this Institute.*

It is further certified that the candidate has completed all the prescribed requirements governing the award of **Doctor of Philosophy** *Degree of the Deemed University, Indian Veterinary Research Institute, Izatnagar.*

.....

( )

External Examiner

Date:...10-04-2015

.....

(Satish Kumar)

Chairman

Advisory Committee

Date:.....07.03.2015

MEMBERS OF STUDENT'S ADVISORY COMMITTEE	
Dr. Dr. A. K. Tiwari, Principal Scientist & Head Division of Biological Standardization, IVRI	.....
Dr. Bhaskar Sharma, Principal Scientist Division of Animal Biochemistry, IVRI	.....
Dr. P. Joshi, Principal Scientist & Head Division of Animal Biochemistry, IVRI	.....
Dr. G. Taru Sharma, Principal Scientist & Head CAS Physiology and Climatology, IVRI	.....
Dr. P. Saravanan, Senior Scientist, Immunology Section, IVRI	.....

Acknowledgement

The work presented in this thesis would not have been possible without my close association with many people who were always there when I needed them the most. I take this opportunity to acknowledge them and extend my sincere gratitude for helping me achieve this.

Words are not enough to acknowledge my advisor ***Dr. Satish Kumar,*** *Principal Scientist, In-Charge, CIF-Bioeng, IVRI for his incredible affection, patience, constant support and encouragement during the course of this study. His astute scientific advice helped me to tread the path of science. With profound gratitude towards him, I feel proud to be one of his disciples.*

I express my warm regards and sincere thanks to the other learned members of my advisory committee ***Dr. A. K. Tiwari,*** *Principal scientist and Head, Division of Biological Standardization;* ***Dr. P. Joshi****, Principal scientist and Head, Animal Biochemistry;* ***Dr. Bhaskar Sharma****, ICAR, National Professor;* ***Dr. G. Taru Sharma****, Principal scientist and Head, CAS, Physiology& Climatology Division;* ***Dr P. Saravanan****, Senior Scientist, Immunology Section.*

I express my sincere thanks to ***Dr. Rajendra Singh****, Head, Division of Pathology and* ***Dr. R.P.Singh****, Principal Scientist, B.P. Division for extending lab facility to work without which my research work would not have completed.*

I am grateful to ***Dr. P.S. Minhas****, Director NIASM, Baramati, Pune, MH for providing me study leave to complete my PhD. I sincerely thank and always cherish the kind help from* ***Dr. S. K. Bal , Dr. N. P. Singh and Satish*** *who stood for me in difficult times.*

I express a note of thanks to all the scientists of Division of Veterinary Biotechnology for the help and moral support during the course of the research work.

I would express my special deep sense of gratitude to ***Dr .GVPPS Ravikumar, Dr. Adity Sahoo, Dr. Ajay Kumar, Dr. Karuna, Dr. Mukesh*** *(Biochemistry) for their valuable advice to my research problems and also being constant support during my stay at IVRI.*

I couldn't have made it through this PhD research without the help of my lab members, ***Dr. Vikas Dighe, Dr. Dimpal and Dr. Vinay Joshi*** *who had provided me all the necessary guidance and support during initial period as I came on study leave to continue PhD research after long gap. I sincerely acknowledge help received from* ***Dr.Arvind.*** *He had shared and taught me many lab skills during this period.*

*I remain indebted to both **Ms Shika** and **Deepika** for their kindness and belongingness. Their ever ready helping hands gave me lot of strength. They not only created working environment, but often made lighter moments which I always treasure for ever.*

*My heartfelt gratitude towards all the staff of CIF, **Surendranath Sir, Subashji, Hariji, and Bablaji** who were always there to help and assist. Their constant support made me comfortable and sail through this journey at CIF, IVRI. I remember with immense grievance the experimental animals sacrificed during the research work.*

*I am grateful to all my **friends at Kannada balaga** for their brotherly care, love and respect. The ease and ambience in the mess always made me feel like home. I cherish those moments for rest of my life.*

This present endeavor could not have possible without the encouragement of my sister and brother. Blessings of my parents and their patience, sacrifices made me to come this far and I dedicate this work to them.

Date: 07.03.2015
Place: IVRI, Izatnagar

(Basavaraj Sajjanar)

List of Abbreviations

AuNPs	Gold nanoparticles
BSA	Bovine serum albumin
CD	Circular Dichroism
CNS	Central nervous system
DAPI	4',6-diamidino-2-phenylindole
DCM	Dichloromethane
DIPC	N,Ndiisoprpoyl carodiimide
DMAP	Dimethlyamino pyridine
DMEM	Dulbecco's Modified Eagles medium
DMF	Dimethylformamide
EDT	1,2-ethanedithiol
FFIT	Fluorescent Focus Inhibition Test
FFU	Fluorescent focus units
FITC	Fluorescin isothiocyanate
HBTU	2-(1H-benzotriazolyl-1-yl)-1,1,3,3-Ttetramethly uroniumhexafluoro phosphate
HoBT	1-hydroxy benztriazole
MALDI	Matrix Associated Laser Desorption Ionization
MTT	[3-(4,5-Dimethyl thiozole-2-yl)-2,5-Diphenyl tetra zolium bromide]
OD	Optical Density
PBS	Phosphate buffer saline
PEG	Poly ethylene glycol
RTCIT	Rabies tissue culture infection test
RV	Rabies Virus
RVG	Rabies virus glycoprotein
SPPS	Solid Phase Peptide Synthesis
TEM	Transmission electron microscopy
TFA	Trifluoroacetic acid
TFE	Trifluoroethanol
TVG	Trypsin-Versene-Glucose
v/v	Volume/volume

List of Tables

List of Figures

Contents

Introduction

Viruses are obligate intracellular parasites. Hence they must bind and enter host cells in order to exploit cellular machinery required for their replication (Thorely *et al*., 2010). There are two broad categories of viruses, enveloped viruses bound by a lipid bilayer and non-enveloped viruses with a proteinaceous capsid. In a typical productive virus life cycle, there are well recognized steps from attachment and entry of the host cells to the release of progeny viruses.

Among all other stages of virus life cycle, attachment and entry of the virus into the host cells is critical in establishing virus infection (Marsh and Helenius, 2006). The initial adsorptions of the virus to the host cells may be mediated by nonspecific weak electrostatic interactions which primarily serve to catch hold the virus on the host cell (Grove and Marsh, 2011). The subsequent entry of virus particles require specific interactions between host cell molecules, or receptors and viral encoded envelope or capsid proteins (Thorley *et al*., 2010). Over a period of time viruses have adapted to target certain host cell types leading to their specificity in tissue and species tropism. This specificity is frequently, but not always, mediated by the first step in the viral replication cycle, attachment of viral surface proteins to receptors expressed on susceptible cells (Vlasak *et al*., 2005).

The viral surface proteins/viral attachment proteins (VAP) are the polypeptides forming the coat of enveloped viruses and capsid of non-enveloped viruses. The virus receptor is a normal constituent associated with the host cell membrane. These receptors may be proteins/carbohydrates/lipids/combination of these components (Grove and Marsh, 2011). Many viruses can use more than one attachment receptor, and indeed may sequentially engage multiple receptors or co-receptors to infect a cell.

Virus binding and cross-linking with their specific receptors can also lead to activation of downstream signaling that promote entry and prepare the cell for invasion (Greber, 2002). Both enveloped viruses and non-enveloped viruses have evolved complex mechanisms to enter cells. The sequence of events and entry mechanisms are now only beginning to be understood (Jolly and Sattentau, 2011). Molecular details of virus -host interactions may help in adopting different strategies to design and develop novel agents to fight viral infections in both human and animals.

Antivirals are the agents that obstruct one or more steps in the virus life cycle. The first step, attachment of the virion to host cells receptors represents ideal target for the agents that prevent the infection (Lentz, 1988). In recent years, several host cell receptors have been identified including their domains binding to the viral surface proteins (Morizono and Chen, 2011). This knowledge serves as the basis for the rational development of agents that block the interaction of viruses with the host cell receptors.

Two groups of agents in theory should block the virus entry into the host cells. The first group includes agents which mimic VAP and compete with the virus for binding to the host cell receptor. For example, surface proteins of Human Immunodeficiency Virus (HIV), SARS Corona and Hepatitis B Virus (HBV) virus were shown to have antiviral effect (Root and Steger, 2004; Bo-Jian *et al*., 2005; Do-Hyoung *et al*., 2008). Second group of agents specifically resemble binding domain of the receptors including designed receptor mimics also called molecular decoys (Lentz, 1990). The later could be synthetic peptides representing the binding domain of the receptor. In case of influenza virus, sialic acid containing glycoprotein had antiviral effect (Pritchett *et al*., 1987). N-terminal fragments of CD4 molecule and synthetic peptides of CD4 residues 25 to 58 and benzylated 83 to 94 peptides reduced HIV-1 infectivity and were able to prevent virus induced cell fusion (Chao *et al*., 1989; Jameson *et al*., 1988; Lifson *et al*., 1988).

Recently random peptide libraries in the form of M13 filamentous phage display, ribosome display or yeast two hybrid screening methods are utilized to identify specific peptides against whole viruses as targets (Hamzeh-Mivehroud *et al*., 2013). These identified peptides mimic host cell receptor binding sites and specifically interact with VAP.

In natural viral infection of cells, the receptor mimic peptides may prevent binding of virus particles to host cell receptors may prove to be strong antiviral agents (Huang *et al*., 2012). By binding to the conserved domains of VAP, these agents would be effective against different strains of viruses. Random phage display library screening techniques were used to identify receptor mimic antiviral peptides against Newcastle disease virus (NDV), avian influenza virus, West Nile Virus (WNV) and Andes virus (ANDV) (Ozawa *et al*., 2005; Jeremy *et al*., 2006; Fengwei *et al*., 2007; Pamela *et al*., 2009). Further, the designed receptor mimetic peptides could suppress or delay infection sufficiently long for the normal defensive mechanism to clear the virus. These peptides can be produced in large quantities by recombinant DNA techniques or by chemical synthesis. It is also possible that their analogues can be designed rationally to bind even with higher affinity as compared to the native receptors, making them potential antiviral peptides.

Rabies is the oldest and devastating disease that has been feared by mankind for more than 4000 years (Knobel *et al*., 2005). Rabies disease is fatal once clinical symptoms appear in several species of mammals including humans. The disease remains huge burden for the developing countries. A recent World Health Organization (WHO) report estimates a total of 55,000 annual deaths from rabies encephalomyeilits, with India alone reporting 20,000 deaths annually (WHO, 2010). Further large number of rabies deaths go without reported and more than 40% of total deaths include children making it seventh most important global infectious disease (Cleaveland *et al*., 2002).

Rabies virus (RV) is a member of Lyssavirus genus of the *Rhabdoviridae* family with single stranded RNA genome. It is an enveloped virus with outer membrane glycoproteins. The attachment of RV to the host cells essentially requires viral glycoprotein and these proteins also play a major role both in fusion to the host cell membrane and release of the virions inside the cells (Pulmanausahakul *et al*., 2008).

It is less clear about the host molecule to which the RV glycoprotein binds. Nicotinic Acetylcholine receptor (nAChR) was the first identified receptor for RV (Lentz *et al*., 1982). Other potential receptors for RV include low-affinity nerve growth factor receptor ($p75^{NTR}$) (Tuffereau *et al*., 1998) and neuronal cell adhesion molecule (NCAM) (Lafon, 2005). The interaction of purified torpedo nAChR with the RV was confirmed in different studies (Bracci *et al.,* 1988; Maria *et al*., 1996).

Further it was found that synthetic peptides of different lengths from nAChRα-subunit were able to bind RV at the range of micro molar concentrations (Lentz, 1990). One of these peptides was also found to inhibit RV infection in human neuroblastoma cells (IMR-32) (Lentz *et al.,* 1997).

Large numbers of rabies deaths are primarily due to the absence of optimal post-exposure treatment protocols and serotherapy (Wilde *et al*., 2002). RV immunoglobulins of human or equine origin are in short supply worldwide and completely unaffordable in many developing countries (Hemachuda *et al*., 2013). Even though significant developments were achieved in RV vaccines, cheaper and more effective vaccines for rabies are always in demand. It is also urgent to find alternative solution to treat the initial phase of the RV exposure. Local treatment with the virucidal drug would solve this problem, and development of anti-rabies peptides may be of great interest in this respect.

In view of the above mentioned facts, the present work has been planned with the following objectives:

1. **To design and synthesize peptide ligands for rabies virus (glycoprotein).**
2. **To assess peptide ligands for binding to the RV.**
3. **To study anti-rabies effect of peptides in cell culture and by mice inoculation test.**

2 Review of Literature

GENERAL FEATURES OF VIRAL LIFE CYCLE:

Viruses are obligate intracellular parasites for the very reason that they lack their own complete biosynthetic machinery. The optimum conditions allow every single virus to infect the cells, replicate and give rise to many progeny viruses (Jolly and Sattentau, 2011). These viruses can infect other neighboring cells. Even though different viruses have their unique mechanism of overtaking cellular machinery for their own benefit, there are well recognized common steps that most of the viruses follows while infecting their particular host cells.

The model viral life cycle follows typical stages; viz attachment (adsorption), penetration, uncoating, gene expression (synthesis of viral RNA and viral proteins), genome replication, virion assembly/maturation and release of new infectious viruses (by lysis of host cells or budding from the cell membranes). Understanding of the life cycle of viruses causing disease is significant not only to satiate intellectual curiosity but also very critical for the control and treatment of viral infections in human and animals. The recent studies have unraveled different events in the virus life cycle in minute details. Simultaneously based on these understandings at the molecular levels, novel strategies are being developed to interfere at any of the possible stages of virus life cycle (Chang and Yang, 2013).

Infection of cells by viruses begins with the attachment of the virus to the surface of host cells (Marsh and Helenius, 1989). Viruses are constructed as metastable molecular assemblages that can be unlocked during entry by specific molecular and/or cellular environmental cues, with minimal energetic input (Marsh and Helenius, 2006).

Virus receptors have been defined as structures on the cell surface to which virus attachment is followed by a biologically relevant response, usually infection of cells (Tardieu *et al.*, 1982). Attachment and entry is the first step in the virus life cycle which is very critical. Cellular membranes present a barrier between the viral particle and intracellular sites of replication in the cytosol or nucleus (Marsh and Helenius, 2006) . Both enveloped viruses and non-enveloped viruses have evolved complex and often poorly defined mechanisms to enter cells.

The attachment and entry of the virus requires specific interactions between host cell and viruses. The events are mediated through viral surface components, either membrane glycoproteins or sites on a viral capsid along with the host cell components like glycolipid /glycoprotein attachment factors, such as heparan sulfate proteoglycans (de Haan *et al*., 2005; Vlasak *et al*., 2005). The initial interactions may be non-specific involving weak electrostatic interactions and primarily serve for just holding of virus on the host cells. From these events, the viruses may eventually recruit specific receptors that drive the reactions leading to entry of viruses into the cells.

Virus receptors can efficiently target viruses for endocytosis or they may critically involve in activating specific signaling pathways that facilitate entry of the viruses (Greber, 2002). Receptor molecules may also be involved directly in fusion/ penetration events at the surface of a target cell or within endocytic compartments by inducing conformational changes in key virus surface structures (Kalia and Jameel, 2011).

Identification of the virus receptors proved difficult until recently, because the virus particles can adhere many of the substances, including inert materials. This makes it hard to distinguish between the non-specific binding and biologically relevant binding. Attachment of the virus particles to the receptors brings them in intimate physical contact with the cell surface and sets the stage for crossing the membrane. Viruses then enter the cells either by direct fusion with the plasma membrane or by absorptive or receptor- mediated endocytosis (Marsh and Helenius, 1989).

In adsorptive endocytosis, the receptor-virus complex is internalized in clathrin-coated pits and delivered to the endosomes. The acidic interior of the endosome triggers the conformation changes in viral fusion protein (Roche *et al.,* 2008). Exposed hydrophobic sequences induce fusion of the viral membrane with the endosome membrane allowing the viral genome to escape into the cytoplasm (Winfried *et al*., 2007). Some viruses require proteolytic cleavage of a fusion protein by host proteases which expose a new hydrophobic N- terminal region of viral protein before fusion and entry of the virus into the host cells.

Earlier it was considered that virus and host cell receptor interactions resemble the interactions of simple ligands with their receptors, defined largely by factors such as ionic strength, pH, and temperature (Lonberg-Holm and Philipson, 1974; Lonberg-Holm, 1981). This has gradually changed to a view of a more dynamic multistep process (Haywood, 1994). For some viruses, this means that initial binding might be followed by a secondary binding step involving other sites or components on the virus and the cell. Each of these steps might entail conformational changes in viral and cellular components that are necessary to promote subsequent stages of binding and entry (Haywood, 1994). Different strategies employed by the viruses for host cell attachment and entry are depicted in figure 2.1.

Despite the importance of virus receptors, relatively few of them are presently known or widely accepted. Also, in most of the cases, there is only scant information available concerning the molecular mechanisms that underlie virus binding and entry (Schweighardt and Atwood, 2001). Carbohydrates, lipids and proteins can act as virus receptors.

Polyoma virus and orthomyxoviruses bind to the sialyloligosaccharides of glycoproteins and glycolipids (gangliosides) (Liu *et al*., 1998). Vesicular stomatitis virus recognizes phosphatidylserine and phosphatidylinositol. Most of other viruses attach to protein associated with the cell surface. Some of these receptors belong to immunoglobulin superfamily including CD4 molecule which serves as human immunodeficiency virus (HIV-1) receptors (Maddon *et al*., 1986). Rhinovirus and poliovirus utilize intracellular adhesion molecule 1(ICAM-1) as receptor (Mendelsohn *et al*., 1989; Greve *et al*., 1986).

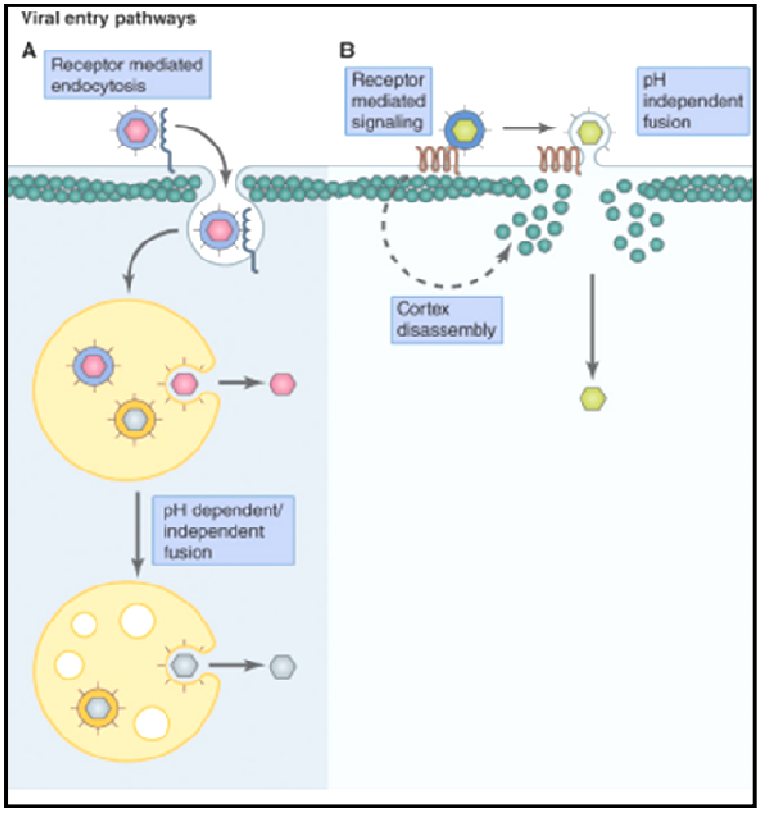

Figure 2.1: Virus entry strategies. Viruses attach and enter host cells with the help of specific receptors and employ different mechanism of entry. Virus-receptor interaction leads to endocytosis followed by pH dependent/independent fusion of endocytic compartment (A). Fusion and release may also occur at host cell plasma membrane by receptor mediated signaling coupled with membrane destabilization (B). (adapted from Grove & Marsh, 2011).

Many of the virus receptors also physiologically function as receptors for hormones or neurotransmitters. These include epidermal growth factor receptor for vaccinia virus (Eppstein *et al*., 1985), β adrenergic receptor for reovirus 3 (Co *et al*., 1985) and the acetylcholine receptor for RV (Lentz *et al.,* 1982). Different host cell receptors of other animal viruses are listed along with their entry mechanisms involved at Swiss Bioinformatics Institute database (Expasy, ViralZone).

ANTIVIRAL AGENTS TARGETING ATTACHEMENT OF VIRUS TO HOST CELL RECEPTOR:

Historically the development of antiviral drugs has been largely fortuitous, inspired by the success of antibiotics, drug companies have launched random screening of large number of compounds with little success. Chemists constantly modify the lead compounds for enhancing their bioactivity along with other properties like specificity, solubility, toxicity etc (Eric, 2002).

Rational drug design may be possible using structure of the target molecule in complex with a known inhibitor and biochemical knowledge to theoretically design a better inhibitor. Modern docking programs or software packages (Q site finder, Ligand explorer, Rasmol, MOE etc) can be utilized to find the active site on target molecule and choose best ligands theoretically possible (Roberta, 2009).

Combinatorial chemistry represents another method where enormous numbers of compounds generated from limited number of subunits are tested for their bioactivity. Any active agent is considered as lead compound for further screening (Real *et al.,* 2004).

Though different steps in the virus life cycle can be targeted to design antiviral agents, the binding of virus to host cell receptor offers potential advantages. There are two classes of agents that should in theory prevent virus entry into cells by blocking the attachment of virus particles to host cell receptors (Erik, 2002). The first group of agents resembles structurally or conformationally the binding domain on the VAP which competitively inhibit binding of VAP to the cellular receptor. These agents for example include receptor antibodies. The second group of agents represent those resembling the binding domain on the receptors to which VAP binds (Lentz, 1990). Receptor mimetic peptides classically belong to this group of agents. The antiviral mechanism of these two groups of agents is depicted in figure 2.2.

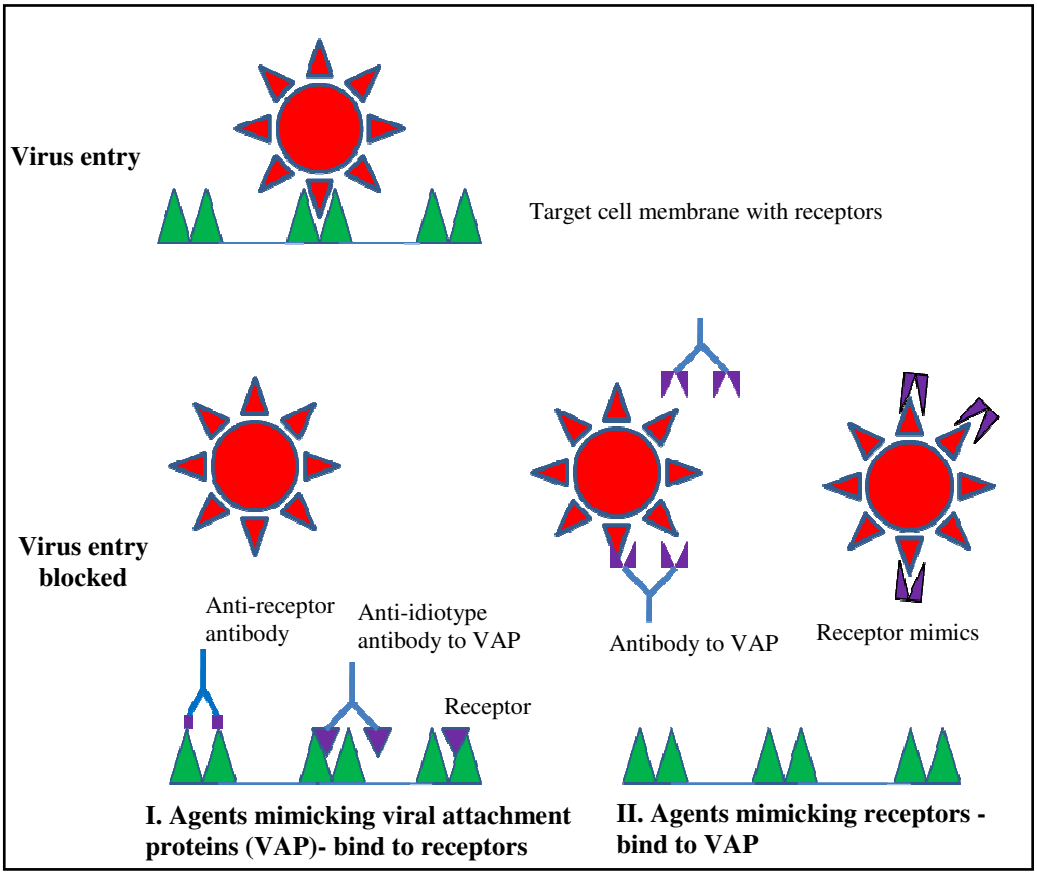

Figure 2.2: Schematic representation of Antiviral strategies to overcome attachment and entry of the virus on the target host cell membranes.

I. Protein and peptide mimics of the VAP:

The examples of mimics of VAP include antibodies directed against binding site of the receptor, natural ligands of the receptor and designed ligand mimics. The later could be represented by synthetic peptides of the VAP.

In one of the example a gp120 octapeptide (peptide T) was able to inhibit HIV infection in human T cells *in vitro* (Pert *et al*., 1986). Later the same peptide was found to improve the conditions of AIDS patients (Bridge *et al.,* 1989). A peptide (Fuzeon) developed from the gp41 surface protein of HIV was found to be a potent HIV- inhibitor (Root and Steger, 2004). This Fuzeon peptide designed was corresponding to the trimeric helical bundle portion of gp41 which mediates binding of HIV to host cells (Chan and Kim, 1998).

Hepatitis B Virus (HBV) preS1 surface proteins were found to involve in the initial viral attack on the hepatocytes. This indicated that peptide derived from this protein hold a great promise as effective HBV-blocking agent (Engelke *et al*., 2006). Acylated analog of a preS1 fragment, a 21 residue lio-peptide from genotype C HBV was produced based on the previous structural study was shown potently inhibiting the HBV infection with an IC_{50} value of 20nM (Do-Hyoung *et al*., 2008). In an attempt to develop antiviral peptides against SARS Corona virus, four 20-mer synthetic peptides were designed to span sequence variation hotspots of spike protein of SARS Corona Virus. These peptides exhibited significant antiviral activities in a cell line. SARS-CoV infectivity was reduced over 10,000-folds through pre-incubation with two of these peptides, while it was completely inhibited in the presence of three peptides (Bo-Jian *et al*., 2005).

II. Protein and peptide mimics of the receptor:

The agents resembling the binding domain on the receptor to which viral attachment protein binds (VAP) can prevent attachment of the virus to host cell receptors. These agents include antibodies produced against VAP, receptor molecule itself and designed receptor mimics. The later could be synthetic peptide of the binding domain of the receptor.

In CD4 receptor based therapies for HIV, soluble CD4 (sCD4) or recombinant truncated CD4 (rsCD4) tested to compete with the binding of the virus to CD4 at the cell surface. It was found that both of these molecules were able to efficiently block the infection of human cells by the laboratory strains of HIV *in vitro* (Daar *et al*., 1990). rsCD4 also studied *in vivo* showed reduction in HIV antigen in affected patients (Schooley *et al*., 1990).

In a modified approach a recombinant molecule was produced in which the two N-terminal Ig-like regions of CD4 were joined by genetic engineering to the constant (Fc) portion of an antibody molecule. The resulting molecule referred as immune-adhesion or CD4-IgG; showed advantages over sCD4 and anti-HIV antibodies (Byrn *et al*., 1990). CD4-IgG possess higher half life than sCD4 and equally capable of crossing the primate placenta (Capon *et al*., 1989).

In another study, pretreatment of chimpanzees CD4-IgG was found to prevent the HIV infection in them (Ward *et al*., 1991). Synthetic peptide segments of the CD4 molecule, which might be expected to act much like sCD4, were also found to block HIV infection and inhibit syncytium formation *in vitro* (Lifson *et al*., 1988). The structure of these peptides is based on amino acids spanning between 81^{th} to 92^{nd} positions of CD4. It is hoped that small CD4-derived peptides with anti-HIV activity might have unique clinical potential by gaining access to organ compartments that exclude sCD4.

The interaction of virus and cellular entry factors was utilized as promising target for novel peptide drug against Hepatitis C Virus (HCV). Peptide inhibitors for HCV entry were identified by screening a library of overlapping peptides covering host cell entry factors (CD81, scavenger receptor BI, CLDN1 and occludin). An 18–amino acid peptide (designated as CL58) that was derived from the CLDN1 intracellular and first transmembrane region inhibited both *de novo* and established HCV infection *in vitro* (Si *et al*., 2012).

Random peptides library screening methods including two hybrid yeast screening, phage display technology and ribosome display methods are recently exploited to identify highly specific peptide that bind to the viral attachment protein and inhibits virus binding to the cellular receptors (Huang *et al*., 2012; Hamzeh-Mivehroud *et al*., 2013).

A disulphide constrained random heptapeptide library displayed on the filamentous bacteriophage M13 was used to identify specific peptide sequence which binds to Newcastle disease virus (NDV). The peptides in linear and cyclic forms were able to inhibit hemolytic activity of the virus as well as its propagation in embryonated chicken eggs (Ramanujam *et al*., 2002; Ozawa *et al*., 2005).

Similarly antiviral peptides were selected against Andes virus (ANDV) which causes Hantavirus cardiopulmonary syndrome. Cysteine-constrained cyclic nonapeptide-bearing phage display library was panned against the density gradient- purified, UV-treated ANDV strain CHI-7913. Three highly specific peptides identified by iterative rounds of panning were found to inhibit ANDV infection to a significant level (Pamela *et al*., 2009).

A murine phage display library was probed against the envelope protein of the West Nile Virus (WNV) to identify antiviral peptides. The specific peptide obtained was able to inhibit not only WNV infection but also related flavivirus including dengue virus *in vitro.* Moreover, mice challenged with WNV that had been incubated with identified peptide had reduced viremia and fatality compared with control animals (Fengwei *et al*., 2007). A disulfide constrained heptapeptide phage display library was biopanned against purified avian influenza virus sub-type H9N2 virus particles in order to select peptides targeting three surface protein; hemagglutinin (HA), neuraminidase (NA) and one ion channel protein M2. The phage displaying the peptide NDFRSKT possessed good anti-viral properties *in vitro* and *in ovo.* Further it was confirmed that the above peptide was specifically binding to the HA protein (Rajik *et al*., 2009).

In one of the exhaustive method of identifying antiviral peptides against RV by targeting phosphoprotein (P), Ele´onore *et al* (2004) used yeast two hybrid screening to identify peptides which inhibit P protein function in viral replication. Among screened peptides, four peptides provided highest percentage (More than 80%) of infection inhibition. Many other recent studies have proved peptides as having potential therapeutic value. A natural antimicrobial peptide (AMP), Ltc 1 had shown significant inhibitory effects against dengue NS2B-NS3pro and virus replication in the infected cells (Rothan *et al*., 2014).

RABIES VIRUS (RV):

Structure and genome organization:

Rabies virus (RV) belongs to the genus lyssavirus in the *Rhabdoviridae* family. RV is divided into two phylogroups with a total of 11 genotypes. Genotype 1, which contains the so called classical RV is the most prevalent and is responsible for most animal and human infections and deaths (Nadin-Davis *et al*., 2008).

RV has negative sense single stranded RNA genome of about 12 kb sizes. The genome is tightly encapsidated in the nucleocapsid and encodes five proteins (Conzelmann *et al*., 1990). The ribonucleoprotein is the functional template for transcription and replication. The viral polymerase consists of RNA dependent RNA polymerase (RdRP) and phosphoprotein.

The nucleocapsid is further surrounded by matrix protein and glycoprotein. Matrix protein serves as a bridge between ribonucleocapsid and virion membrane (Mebatsion *et al*., 1999). RV glycoprotein forms trimer and play important role in viral attachment, entry, membrane fusion and virion release (Gaudin *et al*., 1992).

Life cycle of RV:

Three distinct phases of RV life cycle includes the first phase of virus binding to the host cell receptor followed by the entry of virus with endocytic pathway and release from the endosomes (Baer, 2007). The virions travel in retrograde from axonal end to cell body after entering at the neuromuscular junction of the motor neuron (Kelly and Strick, 2000). Second phase involves the production of virion components by transcription, translation and replication. In the third phase ribonucleocapsid assembles and reach membrane for budding and release from the host cell to start new cycle of infection.

RV receptors and entry mechanism:

In the first step of RV life cycle, virus glycoprotein binds to host cell receptor molecule and mediates its entry into cells. Importance of glycoprotein can be appreciated by the fact that RV with a deletion in the gene encoding the glycoprotein that are trans-complemented with the glycoprotein infect cells efficiently but cannot spread from the infected cell *in vivo* or *in vitro* (Etessami *et al*., 2000).

There is evidence of at least three RV receptors including nicotinic acetyl choline receptor (nAChR), Neuronal Cell Adhesion Molecule-1 (NCAM-1) and and low- affinity p75 neurotropin receptor ($p75^{NTR}$). However, it is less clear which host cell molecule or receptor specifically interacts with the RV glycoprotein and mediates its entry into cells.

Nicotinic acetylcholine receptor (nAChR) was the first identified potential receptor for RV (Lentz *et al.*, 1982). A segment of the RV glycoprotein possesses amino acid sequence similar to curaremimetic snake venom neurotoxins which bind specifically with high affinity to the nAChR (Lentz *et al*., 1984). ^{35}S-labeled RV and ^{125}I-labeled RV glycoprotein have been shown to bind to purified torpedo nAChR (Bracci *et al.,* 1988).

Further a synthetic peptide comprising residues 173-204 of the α-subunit of the nAChR was investigated for its binding to the RV. It was found that receptor peptides were able to bind the ^{125}I-labeled virus at micromolar concentration. Different nAChRα-subunit peptides including torpedo, rat, bovine/calf and human were analyzed for their ability to bind to the RV. Competition studies with shorter α-subunit peptides indicated that the highest affinity virus binding determinants are located within the residues 179-192 (Lentz, 1990).

These findings indicate that synthetic peptides of the receptors which bind to the RV glycoprotein may represent useful antiviral agents targeting the recognition event between the VAP and host cell receptor. Because nAChRs are located at the postsynaptic muscle membrane and not at the presynaptic nerve membrane (Lafon, 2005), it is unlikely that this receptor is used for the initial entry into motor neurons. Instead, it is possible that nAChR enriches RV at the neuromuscular junction to enable more efficient infection of the connected motor neuron. Moreover, as RV might initially replicate in striated muscle cells, nAChRs could be used to infect muscle cells (Murphy and Bauer, 1974).

All cell lines susceptible to RV infection appear to contain the NCAM receptor, which is a cell adhesion glycoprotein of the immunoglobulin superfamily on their surface; NCAM was not found on the surface of resistant cell lines (Thoulouze *et al*., 1998). It has been shown that virus-resistant cell lines are permissive to RV infection after NCAM expression and that NCAM-specific antibodies and NCAM ligand treatment reduce RV infection. However, mice in which the gene that encodes NCAM was deleted were still susceptible to infection with the virus, although the disease was delayed. This indicates that although the receptor might not be essential for infection, it has a role in the infection process (Thoulouze *et al*., 1998). Furthermore, soluble NCAM neutralized RV infection, indicating that occupation of the receptor on target cells. When RV resistant L cells were transfected with NCAM cDNA, cells become susceptible to RV infection. NCAM receptor is localized in presynaptic membranes hence it is well positioned for internalization of RV by receptor mediated endocytosis into vesicles (Lafon, 2005).

The function of $p75^{NTR}$ in RV entry is less clear. Similarly to NCAM, expression of $p75^{NTR}$ enables non-permissive cells to be infected with a RV field isolate, but there is no difference in disease progression between $p75^{NTR}$-deficient and wild-type mice (Tuffereau *et al*., 1998). Moreover, only 25% of the primary dorsal root ganglions that express p75NTR were infected by RV *ex vivo*, indicating that $p75^{NTR}$ might only function in combination with another cell surface molecule (Tuffereau *et al*., 2007). $p75^{NTR}$ is not present at the neuromuscular junction and it is mainly present in the dorsal horn of the spinal cord, suggesting that it could be involved in trafficking of RV by sensory pathway (Lafon, 2005).

The multiple potential receptors identified are not essential for *in vitro* infection by the RV. Simultaneous use of two or more receptors by the virus may be the possible mechanism involved, this speculation is evidenced by the fact that single point mutation in the virus glycoprotein render the RV non-neurotropic and reduce its uptake speed (Dietzschold *et al*., 1985). Differences in speed of uptake and spread in tissue culture of bat-derived RV and a RV vaccine strain also suggest that different receptors may be used (Pulmanausahakul *et al*., 2008).

RV enters cells by receptor mediated endocytosis and found in the clathrin coated pits, uncoated vesicles and lysosomes at subsequent time of infection. Fusion and release of the virus from these vesicles requires change in pH (Superti *et al*., 1984). Glycoprotein is solely responsible for both these events of attachment and pH dependent membrane fusion (McGettigan *et al*., 2001).

Glycoprotein combines features of both class-I and class-II fusion proteins (Roche *et al*., 2006). The fusion is optimum around pH 5.8-6.0 and is not detected above pH 6.3. Pre-incubation of the virus below pH 6.75 in the absence of membrane leads to inhibition of viral fusion. However this inhibition is reversible and readjusting pH to above 7 leads to the complete recovery of the initial fusion activity. This is the main difference between Rhabdoviruses and other viruses fusing at lower pH for which low pH induced fusion inactivation is irreversible (Roche *et al*., 2008).

Schnell et al (2010) hypothesized the probable entry mechanisms of the RV at the neuromuscular junctions and the stealth mechanism it employs to reach the CNS (Figure 2.3).

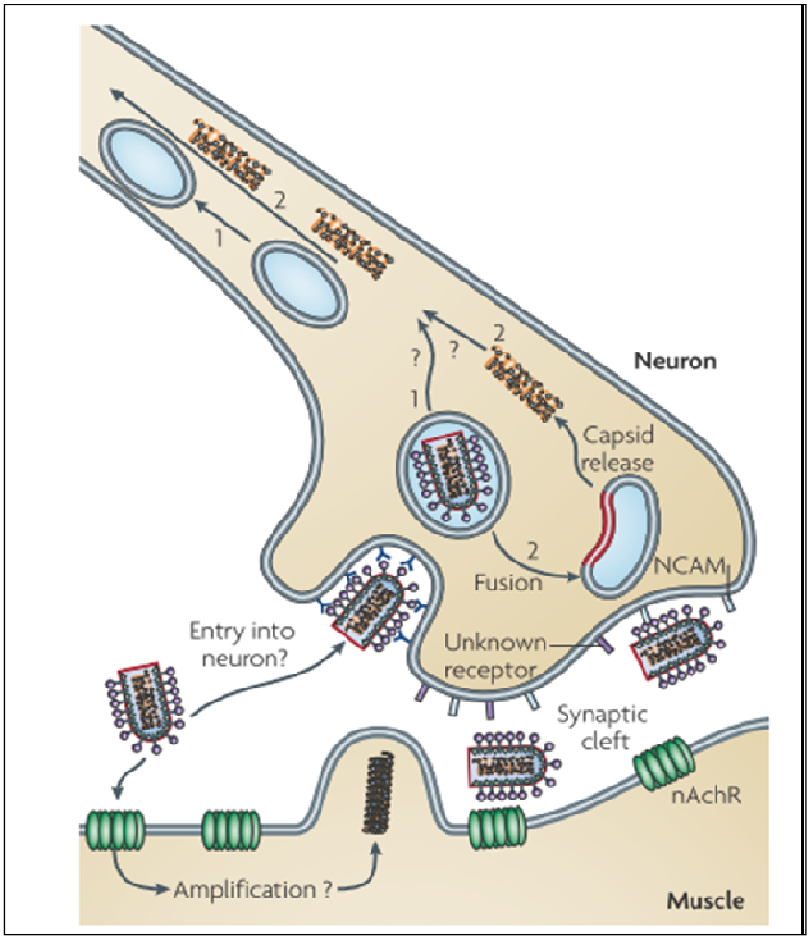

Figure 2.3: RV entry into neurons and intra-neuronal transport (Adopted from Schnell *et al*., 2010).

Intracellular RV transport:

After entry at the neuronal axon, the RV has to reach to neuronal cell body for its replication and transcription and protein synthesis (Malgaroli *et al*., 2006). Two mechanisms were described include transport of nucleocapsid alone or entire virion. The transport of nucleocapsid requires uncoating of virion and specific interaction with the transport machinery.

It was found that interaction between RV phosphoprotein and the dynein light chain 8 (LC8), which indicate the role of cytoplasmic dynein motor complex for intracellular transport of nucleocapsid towards neuronal cells body (Jacob *et al*., 2000).

A recent study used a capsid- and envelope-labeled RV and showed that the whole virion is transported to the cell body in an endosomal vesicle (Klingen *et al*., 2008). Transport depends on the RV glycoprotein, as retroviral vectors trans-complemented with the RV glycoprotein are transported in a similar manner as RV (Mazarakis *et al*., 2001).

Assembly and budding of RV:

Assembly of the viral components and release of virions require the inner core of the virions or capsid must be engulfed by the host cell membrane. Budding of RV takes place at the plasma membrane, but it is unknown how the capsid is transported to the site of budding. Both the RV matrix protein and glycoprotein play an important part in budding. Deletion of the cytoplasmic domain of the RV glycoprotein led to a six fold decrease in the release of virions and revealed a specific interaction between RV glycoprotein and matrix protein (Mebatsion *et al*., 1999). Unlike the glycoprotein of vesicular stomatitis virus (VSV), the cytoplasmic domain of RV glycoprotein is required for the incorporation of foreign glycoproteins into the virion (Schnell *et al*., 1998).

RABIES PROPHYLACTICS:

In 1885 Louis Pasteur developed a crude desiccated nervous tissue vaccine after attenuating it intracranially by serial passaging. Pasteur's crude vaccine was later modified by Fermi and Semple. Most of the nerves tissue vaccines are being discontinued as they cause post vaccinal nervous symptoms and death in some vaccinated animals. However the nervous tissue vaccines are still used in mass vaccination campaign in Africa, Latin America, Caribbean till recently (Cliquet and Picard-Meyer, 2004).

Human diploid cell rabies vaccines (HDCV) are being used in much of the developed world (Vodopija and Clark, 1991). A purified Vero cell rabies vaccine (Verorab^{R}) is one of the latest generation human rabies vaccines.

A low cost purified chick embryo cell rabies vaccine (Rabipur^{R}) has also been produced. The vaccinia-RV glycoprotein vaccine was first recombinant rabies vaccine developed and field tested and helped in controlling rabies in wild foxes in Belgium (Brochier *et al*., 1991).

Rabies Vaccination regimen:

Pre-exposure vaccination is recommended for persons in high risk groups, such as veterinarians, animal handlers, cave explorers and rabies laboratory and vaccine production unit workers etc. Pre-exposure porphylaxis regimen consists of three doses of rabies vaccine given on days 0, 7, and 21 or 28. Post-exposure treatment of rabies following the bite of an infected mammal, in humans, required as recommended by the World Health Organization (WHO, 2010).

The treatments depend on the type of contact with the suspected rabid animal which include category I (touching or feeding animals, licks on intact skin (that is, no exposure), category II (nibbling of uncovered skin, minor scratches or abrasions without bleeding) and category III (single or multiple transdermal bites or scratches, contamination of mucous membrane with saliva from licks, licks on broken skin, exposures to bats). For category I exposures, no prophylaxis is required; for category II, immediate vaccination is recommended; and for category III, immediate vaccination and administration of rabies immunoglobulin are recommended. For categories II and III, thorough washing and flushing (for about 15 minutes, if possible) with soap or detergent and copious amounts of water of all bite wounds and scratches should be done immediately. Where available, an iodine-containing, or similarly viricidal, topical preparation should be applied to the wound (WHO, 2010).

Rabies Immunoglobulins:

Rabies immunoglobulin for passive immunization is administered only once, preferably at, or as soon as possible after the initiation of post-exposure vaccination. Beyond the seventh day after the first dose, rabies immunoglobulin is not indicated because an active antibody response to the cell culture vaccine is presumed to have occurred (Khawplod *et al*., 1996).

The use of human rabies immunoglobulins (HRIG) and of purified pepsin-digested equine products (equine rabies immunoglobulin, or ERIG) have since saved the lives of countless patients who would have died if treated with vaccine alone (Wilde *et al*., 2002). RIG serves to neutralize virus at the inoculation (bite) sites. It reduces the virus load that can replicate in muscle cells and later invade nerve endings. RIG thus closes the gap until endogenous antibodies elicited by active immunization appear (Hemachuda and Mitrabhakdi, 2000).

The dose of human rabies immunoglobulin is 20 IU/kg body weight; for equine immunoglobulin and F(ab')2 products, it is 40 IU/kg body weight. All of the rabies immunoglobulin, as much as anatomically possible, should be administered into or around the wound site or sites. The remaining immunoglobulin, if any, should be injected intramuscularly at a site distant from the site of vaccine administration (Nigg and Walker, 2009). Rabies immunoglobulin may be diluted to a volume sufficient for all wounds to be effectively and safely infiltrated (Hemachuda *et al*., 2013).

3 Materials and Methods

3.1. Buffers and chemicals:

The details of the media, buffers and other solutions used in this study are given in the appendix. The molecular biology grade reagents/chemicals were used for the preparation of various buffers and reagents.

3.1.1. Biochemicals and reagents:

The biochemicals and molecular biology reagents were obtained from Sigma (USA), Life Technologies. Inc. (USA), New England Biolabs, Beverly, MBI Fermentas, QIAGEN (Germany) and Merck (Germany). Reagents for preparation of buffers used in cell culture work such as $MgCl_2$, NaOH, $NAHCO_3$, Na_2CO_3, Na_3HPO_4, KH_2PO_4 were form Sigma (USA). Cell culture medium Dulbecco's Modified Eagles medium (DMEM) and Fetal bovine serum were from Gibco (USA). The sterile plastic wares like microfuge tubes, microtips, cell culture plates, flasks, pipettes and immunoplates were from Axygen (USA) and Nunc (USA). The general plastic wares were from Tarsons (India).

3.1.2. Equipments:

Thermal cycler (Biometra, UK), Real-time qPCR (BI 7500 machine, Applied Biosystems, Foster City, CA), Microcentrifuge (Biofuge fresco Heraeus, USA), Spectrophotometer (CECIL, CE7450, USA). Spectropolarimeter (Jasco J-810, UK), fluorescence spectrometer (Perkin Elmer, LS55, UK), HPLC (Shimadzu, UFLC, Japan) with PDA detector, Laminar flow (Bio-Class IIA, Telstar, USA), Electrophoresis apparatus (BIORAD, USA), Inverted bright field and Inverted fluorescence microscope (Nikon Eclipse Ti, Japan), Electronic balance (Sartorious, Germany), Spectramax M5 (Molecular Devices, USA), Speed Vac concentrator (Eppendorf, Germany), CO_2 incubator (New Brunswick, USA), Orbital shaker (GallenKamp, Germany), Ultra low temperature freezer (New Brunswick, U101 innova, USA).

3.2 Peptide synthesis:

Solid phase peptide synthesis (SPPS) invented by Merrifield (Merrifield, 1963) was used for synthesis of peptides. The principal of SPPS is the stepwise addition of amion protected amino acids on a solid support. Peptide sequences were synthesized by SPPS using standard 9-fluorenylmethoxycarbonyl (Fmoc) chemistry. The successive Fmoc amino acids were added as per sequence using HOBt- HBTU as coupling reagents. All the peptides were prepared as amides at the C-terminal therefore Rink amide resins (loading efficiency: 0.42 mmol/g of 100-200 μm size) were used as solid support.

Solvents for peptide synthesis:

Analytical grade and dried solvents such as Dimethylformamide (DMF), Dichloromethane (DCM), dried ethanol, methanol and diethyl ether were obtained from SD's Fine Chemicals (India). Dimethly Amino Pyridine (DMAP), piperidine and Thioanisol were from Spectrochem (India). Trifluoroacetic acid (TFA) and N,N, Diisoprpoyl Carodiimide (DIPC) used were form Sigma (USA). Coupling reagents such as 1-hydroxy benztriazole (HOBt) was form Fluka (Germany), 2-(1H-benzotriazolyl-1-yl)-1,1,3,3-tetramethlyuronium hexafluoro phosphate (HBTU) was purchased from GL Biochem (Shanghai, China) and Nova Biochem (Switzerland). The SPPS protocol depicted in figure 3.1 and involved following steps.

3.2.1 Loading of first Fmoc-amino acid to Rink amide Resin:

1. 1g of Rink amide resin beads were taken in modified a Merrifield apparatus, added sufficient amount of DMF and allowed to swell for 1hr.
2. First Fmoc-amino acid at C-terminal of the sequence was taken 3 equivalent excess and dissolved separately in 5ml of dry DMF and cooled at 0^{o}C over ice bath.
3. For activation of amino acid, 3eq.HOBt and 2.9eq.HBTU were added to Fmoc amino acid dissolved in DMF and kept at 0^{o}C for 15min to form active esters.
4. Then the *in situ* active esters solution was added to Rink amide resin in reaction vessel and stirred for 2hr at room temperature (25^{o}C) at 160rpm.

The Rink amide resin was washed 5times with DMF and 5times with DCM to remove un-reacted Fmoc derivatives and coupling reagents.

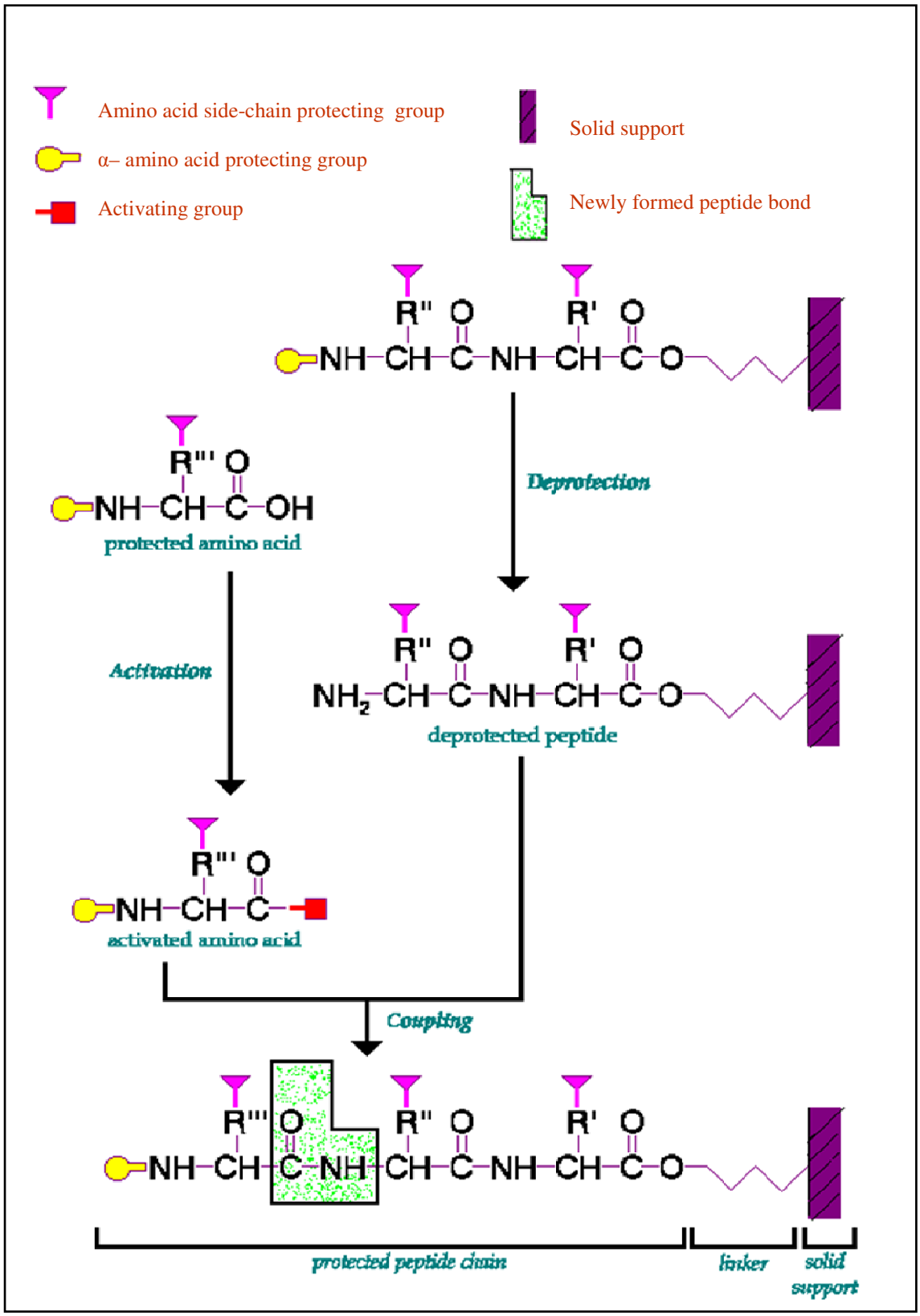

Figure 3.1 Steps in Solid Phase Peptide Synthesis (SPPS)

3.2.2 Estimation of loading efficiency of first amino acid:

1. 20mg of Rink amide resin was taken from the reaction vessel and washed 5times with dry diethyl ether and dried under vacuum.
2. About 1mg of dried Rink amide resin was taken and 3ml of 20% piperidine solution was added to it with occasional swirling for 5min. Resin was allowed to settle at the bottom. At least three repeat samples were taken.
3. The supernatant solutions were taken in silica UV cell of 10mm path length.
4. The absorbance at 290nm was measured by comparing with reference 20% piperidine.
5. The average value of Fmoc amino acid loading into resin obtained using standard reference table 3.1 given below. Based on these values coupling efficiency was calculated

Table 3.1: Amino acid loading efficiency on the resins in terms of Fmoc absorbance 290nm after piperidine treatment.

Fmoc (μM)	0.1	0.2	0.3	0.4	0.5	0.6	0.7	0.8	0.9	1.0
Absorbance	0.165	0.330	0.495	0.660	0.825	0.990	1.115	1.320	1.485	1.650

Fmoc loading efficiency was also calculated by formula:

mmol/g = μmol Fmoc/mg of resin

3.2.3 End capping of un-reacted ends of resin:

End capping of un-reacted functional group on Rink amide resin was done to avoid formation of truncated peptide fragments. About 500μl of end capping solution containing DMF: acetic anhydride: DIEA (193:6:1) was added to the above vessel and stirred at 25^{o}C for 15mins at 150rpm. The beads were washed 3times with DMF.

3.2.4 Deprotection of Fmoc from N-terminal:

For addition of subsequent amino acid, deprotection of amino group was done.

The Fmoc amino acid-Rink amide resin was treated twice with 20% piperidine in DMF (v/v) and agitated for 15min each at room temperature. The beads were washed 3times each with DMF and one time with DCM and again 2times with DMF. Subsequently next coupling reactions were done.

3.2.5 Successive coupling of amino acids:

1. Rink amide was taken in dry DMF.
2. Fmoc-aa (2^{nd} amino acid) was taken 3eq. amount and dissolved in dry DMF.
3. For activation of amino acid 3eq.HOBt and 2.9eq.HBTU were added and kept at 0^{o}C for 15min.
4. Then this solution was added to Rink amide resin in reaction vessel and stirred for 2hr at room temperature (25^{o}C) at 160rpm.
5. Un-reacted amino acids and other reagents washed off with 2times with DMF.
6. Coupling was checked using Kaiser test. Incase of negative reaction coupling procedure was repeated without removing Fmoc group from the amino acid on Rink amide resin.
7. After successful coupling and deprotection next amino acid was added by repeating all the steps of deprotection, coupling and end capping to get peptide of desired length.
8. Finally, excessive reagent was removed and resin was washed thoroughly with DMF and then dried by washing with dry methanol and stored in dried form in desiccators until further use.

Kaiser Test. The "Kaiser Test" is a colorimetric test for the presence of amino groups. It is used to make sure that each coupling step in peptide synthesis goes to completion. It is based on the reaction of ninhydrin with amino groups to form a blue product. Therefore, an incomplete coupling cycle will lead to a positive Kaiser test, demonstrated by the development of a blue color, while coupling to completion will yield a negative result with yellow color.

3.2.6 Labeling bead bound peptides with FITC:

1. Beads with bound peptides were treated with 20% piperidine in DMF to remove Fmoc group from N-terminal end.
2. Coupling of linker (6-Aminohexanoic acid) was done similar to other amino acids before FITC addition.
3. FITC slurry was prepared by adding 1%v/v of DIEA in DMF and equimolar concentration of FITC.
4. Swelled beads were resuspended in FITC slurry prepared. The mixture was kept on vertex or shaker incubator at 70-80rpm for 20hrs at 25^{o}C.

5. Completion of FITC labeling was checked by using ninhydrin test (incomplete coupling of FITC gives a blue color).
6. Resin was washed twice each with DMF, isopropanol and DCM. Final deprotection and cleavage of peptide/FITC labeled peptide from resin was done.

3.2.7 Final deprotection and cleavage of peptide from resin:

1. Cleavage solution containing TFA: Water: Thioanisol: phenol: EDT (92:2:2:2:2) was added upto100-200µl/ tube to submerge the peptide bound resin and kept on vortex for 4hrs.
2. The tubes were centrifuged at 10,000rpm at room temperature for 5 minutes and TFA extract containing cleaved peptide was collected and peptides were precipitated by pouring in dry and chilled diethyl ether in separate tubes and washed five times with diethyl ether, vacuum dried and the white powder obtained was stored under dry condition in desiccators until further use.

3.3 Purification of peptides using Reverse Phase HPLC (RP-HPLC):

1. Peptides were purified on semi-preparative RP-HPLC (Ultropac Column, TSK ODS, 120T, 10µm, 7.8X300mm) and analyzed for their purity on analytical RP-HPL C-18 column (Phenomenex, Luna, C18, 5µm, 150X4.6).
2. Different elution gradients of water (A) and acetonitrile (B) having 0.1% TFA (v/v) were used in semi-preparative and analytical RP-HPLC (Table 3.2).

Table 3.2: Elution gradient of water (A) and acetonitrile (B) for semi-preparative RP-HPLC (I) and analytical RP-HPLC (II).

I. Semi-preparative RP-HPLC

Time (mins)	Solution A (%)	Solution B(%)
0.1	99.0	01.0
5	75.0	25.0
10	50.0	50.0
20	30.0	70.0
25	20.0	80.0
30	10.0	90.0
35	0.00	100.0
34	20.0	80.0
37	90.0	10.0
39	99.0	1.0
40	stop	

II. Analytical RP-HPLC

Time(mins)	Solution A (%)	Solution B(%)
0.1	99.0	01.0
7	70.0	30.0
10	50.0	50.0
13	30.0	70.0
16	0.00	100.0
18	30.0	70.0
20	99.0	01.0
21	stop	

The flow rate was kept 1ml/min for preparative purifications and 0.8 ml/min for analytical HPLC. Chromatograms were monitored at 220nm and 280nm using PDA as detector.

3.4 Virus binding ELISA for peptides:

To study the interactions between the RV and AChRα-subunit peptides of different species, virus binding ELISA for peptides was done. The steps involved in the protocol were given below.

1. Microtitre plates were coated with 100µg/ml peptide at 4°C overnight.
2. Plates were washed and blocked with 1% BSA in TBS for 1hr at room temperature.
3. Added inactivated RV 10µg/ml and incubated for 2hrs at room temperature. Plates were extensively washed with PBST (8times).
4. Plates were probed with primary antibody 1:1000 dilution of monoclonal mouse anti-RV (Rab-SC57994) and incubated for 1hr at 37°C.
5. Plates were washed (5times) and probed with 1:1000 dilution of secondary anti-mouse HRP-Mab for 1hr at 37°C.
6. Plates were washed (5times) and developed with 100µl of TMB substrate for 10mins.
7. Reaction stopped with 3M H_2SO_4 and read at 450nm.

3.5 Synthesis of gold nanoparticles (AuNP) using citrate reduction method:

Prior to colloidal preparation all glasswares were treated with aquaregia. Citrate stabilized gold nanoparticles were prepared using standard protocol with minor modifications. Briefly, 1mM hydrogen tetrachloroaurate ($HAuCl_4$) was dissolved in 50ml of double distilled water and solution was heated on hot plate with magnetic stirrer till boiling point. A volume of 5ml of 38.8mM of trisodium citrate was added rapidly to the boiling solution and further heated with constant stirring for 10min. The solution was stirred for another 15min without heating till brick red color appears in the solution. The nanoparticles were then cooled and stored at 4°C till further use.

3.6 Activation MAP (Multiple antigenic peptides) format on gold nanoparticles

For surface modification, different concentrations of MAP from 1 to 10μM were added to 1mL aliquots of AuNP suspension pretreated for 1hrs with 0.1% Tween20. The solution was stirred for overnight, washed and resuspended in distil water.

3.7 Synthesis of cysteamine stabilized gold nanoparticles (AuNP-Cys):

Gold nanoparticles stabilized with cysteamine (AuNPs-Cys) were synthesized according to a previous literature procedure (Niidome *et al*., 2004). Briefly, 40ml of 1.4mM $HAuCl_4$ solution was mixed with 400µl 0.213M cysteamine solution. The mixture was stirred for 20 min in room temperature in the dark. Subsequently 10µl of freshly prepared 10mM $NaBH_4$ solution was added. The reaction mixture was stirred for additional 30min. The brick red color of the resulting mixture indicates AuNP-Cys formation. The AuNPs-Cys were stored in the fridge (4°C) for further use.

3.8 Covalent immobilization of IgGanti-rabies on AuNPs-Cys:

Anti-rabies immunoglobulin G (IgGanti-rabies) was immobilized on AuNPs-Cys surface according to a modified literature procedure (Lesniewski *et al*., 2014). Breifly 0.5ml of synthesized AuNPs-Cys was mixed with 5µl 1.0mg/ml IgGanti-T7. Subsequently 5µl 0.2M EDC and 10µl 0.2M NHS was added to the reaction mixture to activate the carboxylic groups of the antibody. The mixture was stirred for 1hr at room temperature. Activated carboxylic groups react with amino groups present on the AuNPs-Cys surface forming amide bonds. As a result gold nanoparticles modified with covalently attached antibodies (AuNPs-Cys-IgGanti-rab) were obtained. The resulting particle suspension was diluted four times and used for further experiments without additional purification.

3.9 Transmission electron microscopy (TEM) characterization of AuNP-Cys and AuNP-Cys-peptide/IgG–RV complex:

Citrate stabilized AuNP and AuNP-Cys were suspended in DD H_2O. A drop of suspension was then deposited on carbon coated copper grid (200 mesh Cu, 01810 C-B, TED PELLA Inc, USA) and gently applied at the edge of the grid with fresh filter paper to adsorb excess solution and form a uniform layer. Negative staining was done for viruses. 1% uranyl acetate was briefly added over a dry layer of viruses on the grid and washed with ultrapure water. The grids were allowed to dry at room temperature and shifted to grid box. The TEM images were taken on TECNAI, G2-S, 20 Twin transmission (Philips/FEI, Hillsboro, Oregon, USA) electron microscope.

3.10 Particle size analysis:

Particle size for AuNP-peptide/IgG conjugates alone and after addition of virus were taken zetasizer (Nano S, Melvern, UK). Briefly after adjusting the concentration of the AuNPs conjugates, the solutions were taken in a sample holding curettes. Three 30s measurements were averaged for particle size determination.

3.11 Colorimetric assay AuNP-Cys-Peptide & AuNPs-Cys-IgGanti-RV conjugate:

Different dilutions of BPL inactivated RV stock suspension were added to each 100µl of AuNP-peptide conjugate. To check the selectivity of the test controls were included; plain DMEM + 10%FCS and PBS alone. The visible color change was observed. Further, the solutions were subjected to UV-Visible spectrometer and the absorption spectra were recorded for the range of 400nm to 700nm.

3.12 Culture of mice neuroblastoma (N2A) cells:

N2A cells procured from National Centre for Cell Sciences (NCCS), Pune. The cells were grown in Dulbecco's modified Eagle's medium (DMEM) with 5% fetal calf serum (FCS), incubated at 37°C with 5% CO_2. The cells were passaged every 3days after reaching the confluency. Briefly, the confluent monolayer of N2A cells in 25cm^2 flask was washed with sterile PBS. 1ml of Trypsin Versin Glucose (TVG) was added and incubated for 10min at 37^oC to detach the cells from the surface. The cells were gently pippetted and growth medium (DMEM added with 10% FBS) was added to stop the action of trypsin. Later the cells suspension was made in appropriate volume of medium and seeded to the new flask.

3.13 Counting of N2A cells:

Cells were counted using Neubaeur's counting chamber, briefly the cell suspension was stained with 1% of trypan blue and gently added below the coverslip placed on the counting chamber. The cells were counted in all the four squares of the slide and mean of the count was used for finding the number of cells per ml of suspension using standard formula.

Number of cells/ml=mean number of cells per counting field X 10^4X dilution factor.

Appropriate numbers of cells were seeded into the 24 well and 96 well culture plates for further experiments.

3.14 Growth of RV (CVS-18) in N2A cells:

RV, Challenge Virus Standard-18 (CVS-18) earlier used for mice inoculation test was taken for the propagation in N2A cells. 10% of brain suspension was prepared in PBS. Briefly, 0.5gm of brain sample was taken, triturated with wooden tongue depressor in a tissue paper towel and transferred to 15ml tube. 5ml of PBS with antibiotics (Streptopenicillin, 2mg/ml) added and vortexed vigorously. Sample was allowed to settle at $4^{o}C$ for 1hr. The upper clarified supernatant was taken and diluted 10fold to obtain 1% brain suspension.

3.15 RV tissue culture infection test (RTCIT) in N2A Cells

STEPS:

1. A complete monolayer of N2A cells from $25cm^2$ was trypsinized to make cell suspension.
2. Cells were counted and diluted appropriately to adjust $2X10^5$cells/ml.
3. Added 100µl of cells to each well of 96well plate.
4. Added 200µl of 1% brain suspension to each of the well.
5. Mixed the cells with brain suspension and incubated at $36^{o}C$ with 5% CO_2.
6. Cells were observed intermittently for any contaminations.
7. Separate plates with positive and negative control wells were also included.
8. After 72hrs of incubation, cell monolayer was washed.
9. RV growth and multiplication was detected using direct fluorescent antibody test.

3.16 *In vitro* detection of RV by immunofluorescence:

With the RV-specific labeled polyclonal antibodies (BioRad, USA) which are targeted against the ribonucleoprotein complex of the RV, growth and multiplication of RV can be detected by direct immune-fluorescence test (IFT). Polyclonal antibodies, which were produced by the means of the Pasteur Virus strain (PV) and known for their good specificity. The conjugate diluted in a phosphate buffer at pH 7.2. Prior to use, the appropriate working dilution were established by titrating the anti-rabies nucleocapsid conjugate. A dilution of 1/20 dilution had shown to be sufficient.

STEPS:

1. Washed the cells once with phosphate buffer saline (PBS).
2. Fixed the cells in 80% acetone at - 20°C.
3. Rapidly air dried the cells.
4. Added enough diluted conjugate to cover the slide.
5. Incubated at 37°C for 30mins in a moist chamber.
6. Washed the wells with PBS.
7. Applied a few drops of glycerin buffer as a mounting fluid.
8. DAPI (4',6-diamidino-2-phenylindole) staining done to visualize the nucleus.
9. The wells were observed for specific viral foci under inverted fluorescent microscope for green and blue filters and images were merged.

3.17 Propagation of RV in N2A cells:

N2A cells were seeded in 25cm^2 flask to grow a confluent monolayer on the day of infection. Medium was gently removed. 10% brain suspension was diluted to 1% in maintenance medium and 1ml of the inoculum was used for infecting the N2A cells. Cells incubated at 36^{o}C for 1hr with gentle intermittent rocking of the flask. After 1hr, the inoculum was removed and replaced and 5ml of maintenance medium was added and further cells were incubated at 36^{o}C at 5%CO_2 incubator for 48hrs. After the incubation, the flask was subjected to three cycles of rapid freeze-thaw and stored in -80 freezer. The inoculum from the flask was used for the subsequent infection and passage in the N2A cells. The titration of the virus was done to quantify the amount of virus (FFU/ml) following standard protocol.

3.18 Titration of RV in N2A cells:

1. Cell suspension: On the day of titration, a cell suspension containing 2X10^{5}cells/ml was prepared in cell culture medium containing 10% heat-inactivated FCS and distributed 100µl per well into 96-well microtitre plates.
2. Dilution of the virus: the serial dilutions are performed in 1.5ml tubes using a cell culture medium without FCS as diluent. Ten-fold dilutions from 10^{-1} to 10^{-10} are prepared (0.9 ml of diluent with 0.1 ml of the previous dilution).
3. Infection of the cells: 100µl of each virus dilution is distributed per well. Six replicates are used per dilution.
4. Incubation: The microtitre plate was incubated for 48hrs at 37°C in 5% CO_2.

5. Staining of infected cells: The cells are stained using the FAT as described in the section 3.16.
6. Calculation of the titre: The highest dilution of the virus showing the specific characteristic foci were counted and expressed as FFU/ml.

3.19 Staining of RV infected N2A cells with FITC labeled peptides:

N2A cells were seeded in 24 well tissue culture plates on the previous day to reach a semi confluent layer on the day of infections. RV stock diluted and added to the wells at 0.5moi and incubated for adsorption for 1hr at 37^{o}C with intermittent gentle rocking. The inoculum was removed and replaced with maintenance medium. The plates were incubated for 48hrs at 36°C in 5% CO_2 incubator. The medium was removed and monolayer was gently washed with the PBS once. Cells were fixed with 80% acetone at -20^{o}C for 30mins. The fixed cells were stained with 10µg/ml of FITC labeled peptides. Mock infected wells included as control. The cells were washed with PBS and DAPI stained for the nucleus. Observations were made under inverted fluorescent microscope.

3.20 Cytotoxicity test for peptides in N2A cells:

Cytotoxicity test for nAChRα-subunit peptides was performed with MTT method. The steps involved in the procedure are given below.

1. Equal number of cells ($2.5X10^4$) were seeded in each well of 96 culture plate.
2. 50µl of different concentration of peptides (6.25, 12.5, 25, 50, 100& 150µM) diluted in DMEM were added to the cells.
3. Positive control of cytotoxicity: 20% DMSO.
4. Negative control of cytotoxicity: DMEM alone.
5. Plates incubated for 24hrs at 37°C, under a humidified 5% CO_2 atmosphere.
6. The medium was removed and 50µL of MTT solution was added to each well and incubated for 4hrs.
7. 100µl of DMSO was added to the well and gently rocked to solubalize formazan.
8. Absorbances were measured using spectrophotometer at 540nm.

The CC_{50} was calculated as the concentration of the peptide that reduced the absorbance of treated cells to 50% when compared to the control.

3.21 Fluorescent Focus Inhibition Test (FFIT):

To determine the antiviral effect peptides against RV *in vitro* N2A cells, FFIT-was employed. The steps involved were given below.

1. Different concentrations of peptides (5µM to 50µM) were incubated with RV (50µl of 1:10 diluted $5X10^5$ FFU/ml) at 37°C for 1hr.
2. Peptide-Virus mixture was added to 100µl of N2A cells suspension ($2.5X10^4$ cells) in 96 well culture plate.
3. The cells were incubated at 37°C in a humidified chamber with 5% CO_2 culture incubator.
4. After 48hpi, medium was removed and washed with PBS twice.
5. Infected cells were stained with rabies anti-nucleocapsid antibody-FITC Conjugate (Bio-Rad^R)
6. The microtitre plates reading was performed in inverted fluorescence microscope (Nikon, 200× magnification).
7. Five random fields were counted for fluorescent foci showing cells.

The IC_{50} was calculated as the concentration of peptide that reduced the number of fields with fluorescent foci to 50%when compared with the negative control with plain medium.

3.22 Viral RNA isolation:

To determine the viral gene copy number in the peptide treated and control experiments viral RNA was isolated. Viral RNA mini kit (QlAmp Viral RNA, QIAGEN, Germany) was used following the steps mentioned by the manufacturers.

Briefly, carrier RNA provided in the kit was dissolved in the AVE buffer and mixed with the AVL buffer in appropriate volume. The remaining steps are as given below.

1. 200µl of culture supernatant was taken and 560µl of AVL buffer was added in 1.5ml sterile tubes.
2. The solution was vortex for 15secs and incubated at room temperature for 10mins.
3. To the above solution, 560µl of absolute ethanol was added and vortex mixed.
4. The total mixture was loaded into the column and spin to remove the filtrate.
5. Washing of the column was done with buffers provided (AW1& AW2) at 8000rpm for 1min each.

6. The RNA was eluted in the fresh tube with 30µl of elution buffer.
7. RNA aliquots were stored -80^{o}C.

3.23 Viral cDNA synthesis:

From viral RNA, cDNA was synthesized using Revert Aid first strand cDNA Synthesis Kit (Thermo Scientific). Equal quantity (500ng) of the RNA for each of the control and treated groups were taken using spectrophotometer (NanoDrop, Thermo Scientific) readings followed by appropriated dilution of the samples. cDNA was synthesized in two steps as mentioned below following manufacturers instructions.

First step:

Viral RNA =500ng+Random primer=20pmol+Nuclease free water=up to 12µl

Mixed gently and incubated at 65°C for 5 min, spin down and placed the vial back on ice.

Second step:

5X Reaction Buffer 4 µL + RiboLock RNase Inhibitor (20U/µL)1 µL + 10 mM dNTP Mix 2 µL + RevertAid M-MuLV RT (200 U/µL) 1 µL = Total volume 20µL

Mixed gently and incubate 5 min at 25°C followed for 60min at 42°C. Reaction was terminated by heating at 70°C for 5min. Resulting cDNA was stored in -20^{o}C for further use. cDNA synthesized was checked by performing a test PCR for the amplification of viral gene.

3.24 Quantitative Real time PCR:

Quantitative RT-PCR (qPCR) was performed using SYBR Green Master Mix (Fermentas, Life Sciences) in BI 7500 machine (Applied Biosystems, Foster City, CA). Triplicate reactions were performed for each sample and a no template control (NTC) was included as a negative control. The following reaction set up was used.

Maxima SYBR Green qPCR master mix (2X) =12.5µL

Forward primer=10pmol

Reverse primer=10pmol

Template DNA=10ng

Nuclease free water to make volume 25µL

The reaction conditions were used according to the manufacturers instructions after standardization of annealing temperature for the gene of interest.

3.25 Standard curve for viral copy numbers:

Absolute quantification was performed for viral gene copy numbers. Briefly RV polymerase (L) partial gene segment (184bp) was amplified and gel purified and quantified the amount using spectrophotometer (NanoDrop, Thermoscientific).

Known copies of the template were made into serial 10 fold dilutions and were used to perform the qPCR in triplicates. The mean Ct values obtained were plotted against the copy numbers of template used for performing the real time PCR experiments. The linear curve was obtained with optimum correlation coefficient. Thus the relationship between the Ct value and copy number was extrapolated by drawing the standard curve. Viral copy number of treated and untreated cells was determined based on the standard curve equation. The percentage of viral inhibition (%) was calculated as follows:

Percent viral inhibition= 100 – (viral copy number of treated cells/viral copy number of untreated cells) × 100.

3.26 Viral attachment study:

Virus attachment was studied with the help of virus adsorption ELISA. The steps followed in the method are as follows.

1. RV was incubated with different concentrations of the peptides in triplicates at 37^{o}C for 1hr and then immediately chilled.
2. The virus and virus–peptide solutions were plated on the N2A cells in 96-well plates (50µl per well at an moi of 6) for 1hr at 4^{o}C.
3. The cells were washed with cold PBS and fixed with 4% paraformaldehyde at room temperature for 30mins then washed with cold PBS and stored overnight at 4^{o}C.
4. Plates were blocked with 3%BSA in Tris-buffered saline (TBS) for 1hr at room temperature and then washed once with PBS.
5. Wells were probed with 1:2000 dilutions of mouse anti-RV glycoprotein IgG monoclonal (sc-57994, Santa Cruz) for 1hr at 37^{o}C and then washed five times with PBS.
6. Wells were probed with 1:2000 dilutions of secondary antibody chicken anti-mouse IgG-HRPO conjugate for1hr at 37^{o}C and then washed five times with PBS.

7. The TMB substrate (Amresco) was used (100µl per well) for 10mins incubation at room temperature to develop the color.
8. The reaction was stopped by adding 1M H_2SO_4 (100µl per well).
9. The absorbance readings were taken at 450nm. The average values for the triplicates were used for plotting the results.

3.27 Mice inoculation test:

All the animals experiments were duly approved by the Institute's Animal Ethics Committee [(No.F.1-53/2004-J.D.(Res)]. 2-3 week old Swiss albino mice were procured and maintained in the lab animal house with standard protocols of shelter, feeding and watering schedules.

Each experimental group had eight animals. Mice were inoculated by intracerebral route. 100µM of peptides were treated with $100LD_{50}$/0.03ml of RV (CVS-18) for 1hr at 37^{o}C and the PBS treated RV ($100LD_{50}$/0.03ml) was used as positive control and PBS alone is included as a negative control.

1. Mice were observed three times daily and assessed for visual signs of clinical disease including inactivity, ruffled fur and labored breathing. The observations were recorded in the lab registers.
2. Normal feeding and watering schedules were maintained during the experimental period after inoculation.
3. Deaths in the first 4days of inoculation were considered as nonspecific.
4. Survivability details were noted daily in the lab records.
5. The animals were maintained and observed for total 28days from the beginning of the experiments.

Results

4.1 Physical and chemical properties of nAChRα-subunit peptides and their analogues:

In the present study, nAChRα-subunit peptides of different species origin (torpedo-electric ray fish, bovine/calf, human and rat) were synthesized. These peptides sequences characteristically fall between 174aa to 203aa region of α subunit of the receptor. nAChR is a ion channel present at the synaptic neuronal junctions.

Neurotoxins like bungarotoxin, snake venom toxins were found to interact with α - subunit of this receptor to exert their effects. nAChRα-subunit also considered as receptor for RV. The same region or domain of nAChRα-subunit is involved in binding of neurotoxins and RV. This region of the receptor protein is highly conserved across the species as distant as electric ray fish (torpedo) to human beings. However, variations in amino acids at different positions (highlighted in table 4.1) were observed. These changes play significant role in their binding ability to different ligands. In addition, Lpep-13 and DDD-14 which were earlier found to mimic α subunit of the nAChR and showed specific binding to the neurotoxins (α-bungarotoxin) were also included in the present study.

The peptides were known to interact with RV, as RV glycoprotein has neurotoxin loop (similar to α-bungarotoxin) within its sequence. Using ExPASy (the Expert Protein Analysis System) provided by the Swiss Institute of Bioinformatics (SIB), the ProtParam algorithm was applied to determine different physical and chemical attributes of these peptides. The results obtained are represented in the table 4.1.

TABLE 4.1. Physical and chemical properties of peptides.

PEPTIDES	SEQUENCE	M.Wt g/mol	pI	GRAVY	t1/2 h	Stability
Torpedo-32 (T-32)	SGEWVMKDYRGWKHWVYYTCCPDTPYLDITYH	4014	7.1	-0.787	2	-5.9 (S)
Calf-32 (C-32)	SGEWV**I**K**ES**RGWKHWV**F**Y**A**CCP**S**TPYLDITYH	3859	8.2	-0.400	2	-5.9 (S)
Human-32 (H-32)	SGEWV**I**K**ES**RGWKH**S**V**T**Y**S**CCPDTPYLDITYH	3758	7.1	-0.672	2	20.9 (S)
Torpedo-20 (T-20)	KDYRGWKHWVYYTCCPDTPY	2581	8.8	-1.265	1.3	-6.2 (S)
Calf-20 (C-20)	K**ES**RGWKHWV**F**Y**A**CCP**S**TPY	2445	9.5	-0.775	1.3	94.3 (U)
Rat-14 (R-14)	K**ES**RGWKHWV**F**Y**A**C	1796	10.1	-0.857	1.3	103.0(U)
Lpep-13 (L-13)	MRYYESSLKSYPD	1637	9.3	-1.354	30	28.1 (S)
DDD-14 (D-14)	FRYYESSLEPWDDD	1820	3.8	-1.579	1.1	46.5 (U)

(Where pI-the theoretical isoelectric point; GRAVY-grand average of hydropathicity, positive values are hydrophobic; t1/2-estimated half-life in mammalian reticulocytes, *in vitro*; U-unstable; S-stable)

4.2 Synthesis and purification of linear and multiple antigenic peptides (MAPs):

The sequences mentioned in the table 4.1 are synthesized using solid phase peptide synthesis method using Rink amide MBHA resin. Four armed MAP formats were synthesized for T-20 and C-20 using lysine mosaic with cysteine at the c-terminal end. Cleaved peptides were subjected to semi-preparative RP-HPLC. The chromatograms were monitored with absorbance at 220nm and 280nm.

The results for each of these peptides showed a major peak along with some minor peaks. The major peak (with 280nm) in each of the chromatogram (Figure 4.1) represented the peptide of interest. The sequences of these peptides had tyrosine and tryptophan. The aromatic rings of these amino acids gave specific and maximum absorbance at 280nm. The minor peaks indicated the presence of salt impurities which also had some absorbance.

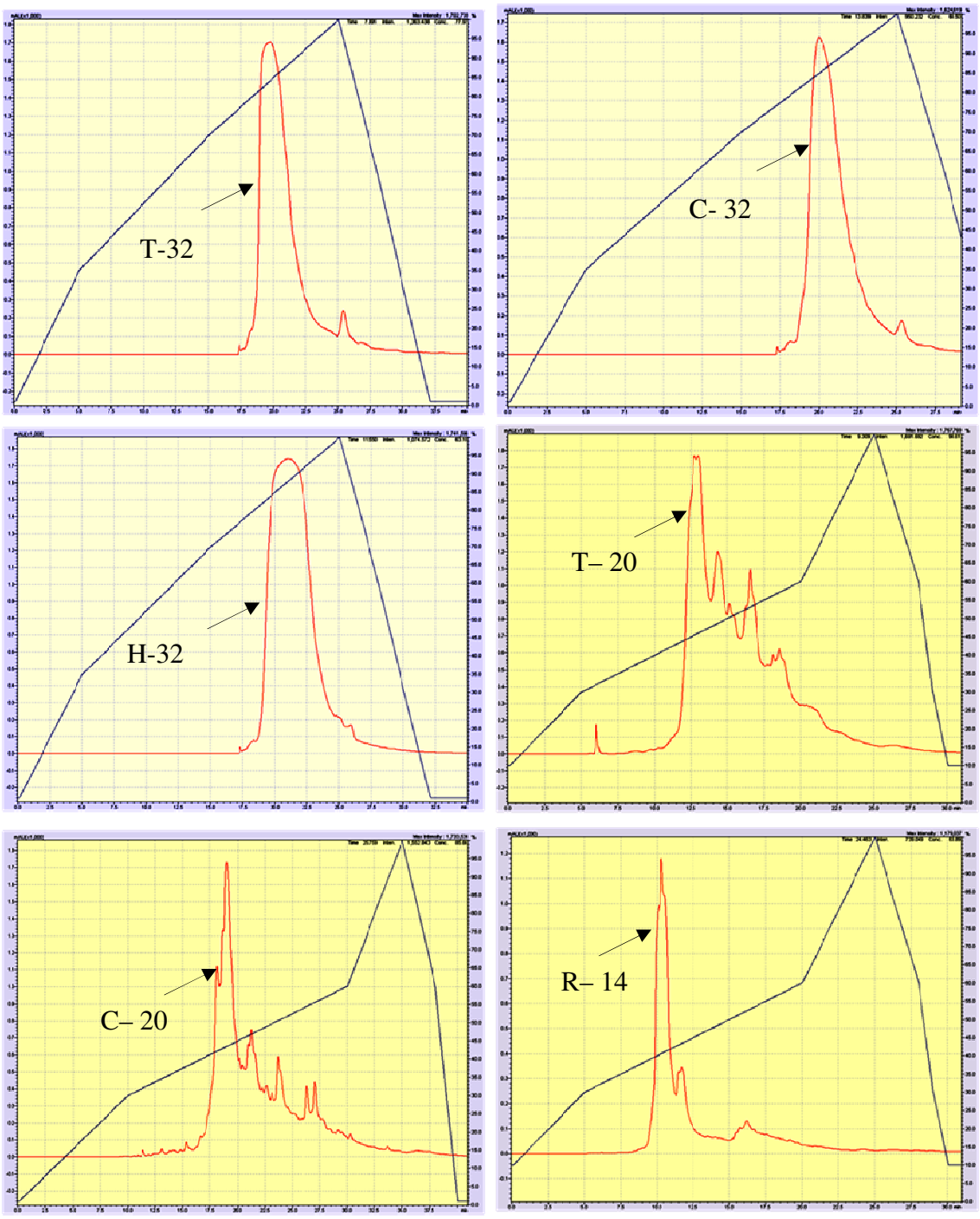

Figure 4.1: RP-HPLC chromatograms (red) of chemically synthesized crude peptides in semi-preparative column (Ultropac Column, TSK ODS, 120T, 10µm,7.8X300mm) The tented line (black) indicates the gradient profile of solution B (ACN with 0.1% TFA v/v) in solvent A (H_2O with 0.1% TFA v/v). The arrows indicate major peaks of peptides collected.

The major peaks of the chromatogram for each of these peptides were carefully collected and subsequently dried in the vacuum concentrator. The dried purified peptides were used for further experiments.

4.3 Analysis and characterization of purified peptides:

The semi-preparative RP-HPLC purified peptides were re-dissolved and subjected to analytical RP-HPLC. The results showed, single major sharp peaks for each peptide tested. The characteristics of the chromatograms indicated the purity of the peptides (Figure 4.2). Based on the area under curve calculations, the chemically synthesized peptides were more than 95% pure. The level of purity observed was optimum for antiviral experiments of the peptides.

The concentration of the purified peptides was determined based on absorbance of the diluted peptides at 280nm using spectrophotometer. The values of molar extinction coefficient at 280nm for each peptides depend on the number of aromatic amino acids and their extinction coefficient. The values were (represented in table 4.1) used to calculate the concentration of each of the peptides.

The purified peptides were further characterized for their mass using MALDI-TOF. The results indicated the experimentally determined mass for the peptides in daltons (Figure 4.3). The tested peptides showed similar mass compared to the expected theoretical mass (Table 4.1).

4.4 Elucidation of secondary structures of peptides using CD-spectroscopy:

To elucidate the structural conformation of the peptides, CD spectra of peptides were recorded in water, 10% TFE, 25% TFE, 50% TFE and 75% TFE. CD spectra in solutions for T-32, C-32, H-32, T-20, C-20 and R-14 were depicted in figure 4.4 and 4.5. The quantitation of different secondary structure conformations was carried out using CD structure quantitation software. The percentages of different secondary structures for the peptides are given table 4. 2 and table 4. 3.

The CD spectrum of T-32 peptide (0.1mg/ml) in water shows a dominant negative minimum at 198nm with cross over to have positive band around 225nm. Addition of 10% TFE (decrease in dielectric constant) there was a negative band at 200nm where as positive band was still observed at 225 nm.

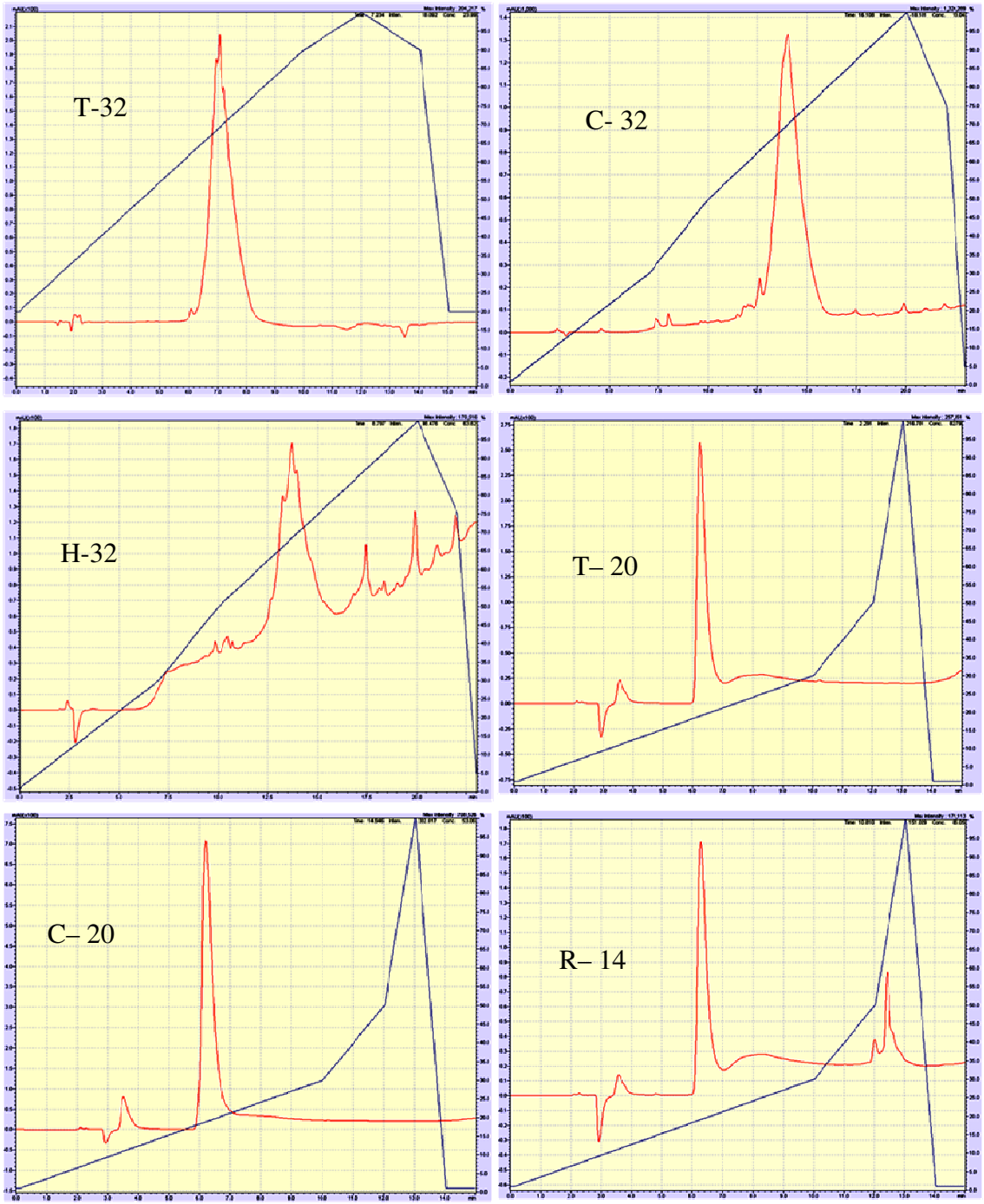

Figure 4.2: RP-HPLC chromatograms (red) of peptides in analytical column (Phenomenex, Luna, C18, 5µm, 150X4.6mm). The tented line (black) indicates the gradient profile of solution B (ACN with 0.1% TFA v/v) in solvent A (H_2O with 0.1% TFA v/v).

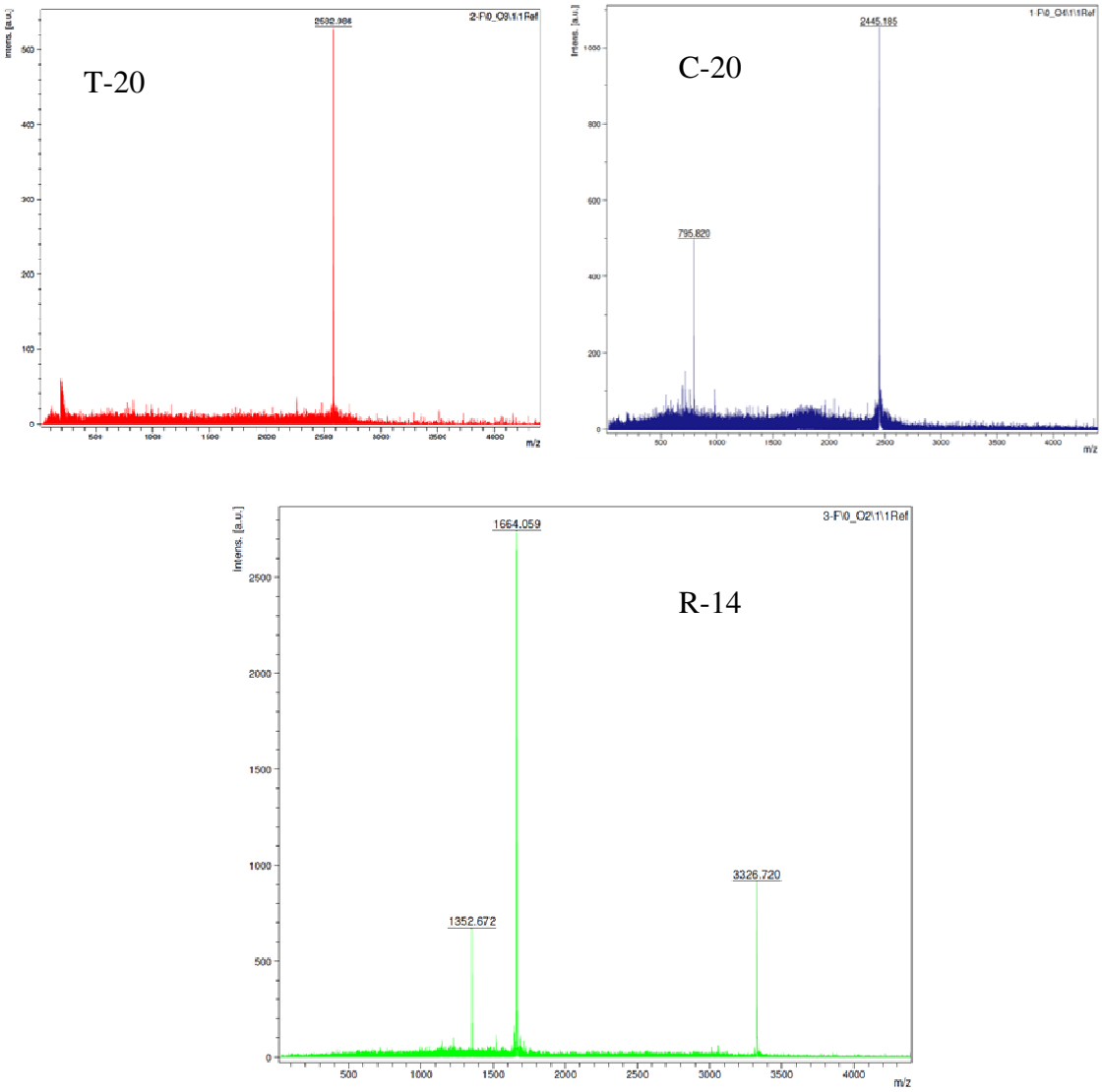

Figure 4.3: MALDI-TOF of peptides showing different charged fragments with average mass in dalton.

Table 4.2: Elucidation of secondary conformations of peptides (T-32, C-32 & H-32) using CD spectroscopy.

T-32 (SGEWVMKDYRGWKHWVYYTCCPDTPYLDITYH) M.wt 4014 g/mol

	Water	10% TFE	25% TFE	50% TFE	75% TFE
Alpha helix%	0.0	0.0	0.0	25.3	83.1
Beta sheet%	0.0	0.0	0.0	0.0	0.0
Turn%	0.0	0.0	0.0	0.0	0.0
Random%	100. 0	100. 0	100. 0	74.7	16.9

C-32 (SGEWVIKESRGWKHWVFYACCPSTPYLDITYH) M.wt- 3859 g/mol

	Water	10% TFE	25% TFE	50% TFE	75% TFE
Alpha helix%	0.0	0.0	67.1	100. 0	100. 0
Beta sheet%	0.0	0.0	0.0	0.0	0.0
Turn%	0.0	0.0	0.0	0.0	0.0
Random%	100. 0	100. 0	32.9	0.0	0.0

H-32 (SGEWVIKESRGWKHSVTYSCCPDTPYLDITYH) M.wt 3758 g/mol

	Water	10% TFE	25% TFE	50% TFE	75% TFE
Alpha helix%	0.0	0.0	0.0	20.3	76.2
Beta sheet%	0.0	0.0	0.0	0.0	0.0
Turn%	70.4	48.5	0.0	0.0%	0.0
Random%	29.6	51.5	100. 0	79.7	23.8

Further increased concentration of TFE resulted into incremental increase in positive and negative wavelengths bands. In 75% TFE, there was a marked increase in the molar ellipiticity indicating increase in ordered conformations having maximum positive band at 193nm and two minimum positive bands at 207 and 218nm as expected. These results were further corroborated by quantitative estimates of secondary structures (Table 4. 2) obtained using spectra manager software. Initially the peptide had random coil structure in aqueous, 10% and 25% TFE, but further increased concentration of TFE (50% and 75%) largely induced alpha helix conformation.

C-32 peptide (0.1mg/ml) mostly adopts random coil structure in water. As the apolar environment was created by increasing concentration of TFE, the peptide adopted largely alpha helix conformation. Beta sheet and turn structures are absent even in 75% TFE. In water, the CD spectrum shows a dominant negative minimum at 193nm with a cross over to have a positive band around 220nm. Addition of TFE concomitantly decreased the 197nm band and progressive red shift in minima up to 230nm was seen. In 75% TFE, there was marked increase in molar ellipticity indicating increase in ordered conformations having maximum positive band at 191nm and minima at 210nm. The secondary structure estimation showed 100% helix conformation in 75% TFE solution.

The CD spectra recorded for H-32 peptide in water and different concentration of TFE is shown in figure 4.4. The secondary structures quantified are given in table 4.2. The spectra of the peptide (0.1mg/ml) in water shows prominent negative band at 195nm with positive band cross over at 220nm. The secondary structure quantification shows maximum 'turn' conformation (70.4%) and rest random coil. As the concentration of TFE was increased, there was a decrease in the 195nm band and a progressive shift in minima up to 210nm was seen. In 75% TFE solution, the peptide had alpha helix conformation up to 76%. Most of the 'turn' structure was converted to alpha helix conformation.

The T-20 peptide (0.1mg/ml) was studied for its secondary structure conformation. The CD spectrum recorded in water and in different concentration of TFE is shown in figure 4.5. The secondary structures quantified are given in the table 4.3. In water the spectrum shows negative band around 195nm with no positive band cross over observed even above 250nm.

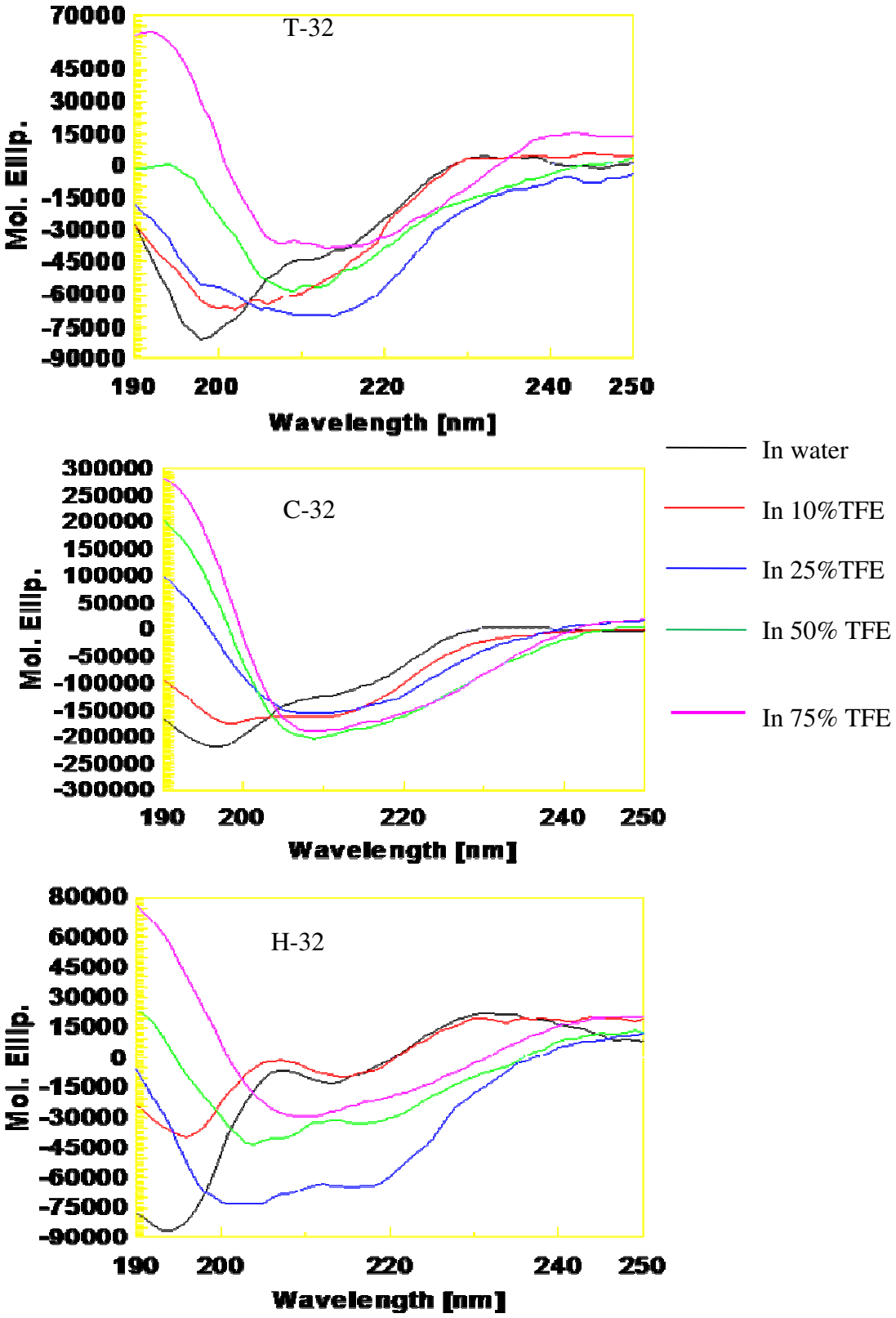

Figure 4.4: CD spectra of nAChRα-subunit peptides in different polar and aploar environments; in water, 10% TFE, 25% TFE, 50%TFE, 75% TFE.

Table 4.3: Elucidation of secondary conformation of peptides (T-20, C-20 & R-14) using CD spectroscopy.

T-20 (KDYRGWKHWVYYTCCPDTPY) M.wt 2581g/mol					
	Water	10% TFE	25% TFE	50% TFE	75% TFE
Alpha helix%	2.7	4.6	6.9	5.6	9.7
Beta sheet%	50.1	48.7	55.2	73.5	58.0
Turn%	12.5	13.5	10.6	2.7	11.3
Random%	34.6	33.1	27.2	18.2	21.1

C-20 (KESRGWKHWVFYACCPSTPY) M.wt 2445g/mol					
	Water	10% TFE	25% TFE	50% TFE	75% TFE
Alpha helix%	0.0	0.0	3.8	1.6	5.8
Beta sheet%	67.1	68.7	61.8	78.8	44.5
Turn%	6.5	4.8	6.5	0.0	17.5
Random%	26.4	26.6	28.0	19.6	32.2

R-14 (KESRGWKHWVFYAC) M.wt 1796 g/mol					
	Water	10% TFE	25% TFE	50% TFE	75% TFE
Alpha helix%	0.0	0.0	0.0	0.0	0.0
Beta sheet%	65.2	55.9	62.4	71.0	66.1
Turn%	8.7	10.2	7.4	3.8	8.2
Random%	26.2	33.9	30.1	25.2	25.7

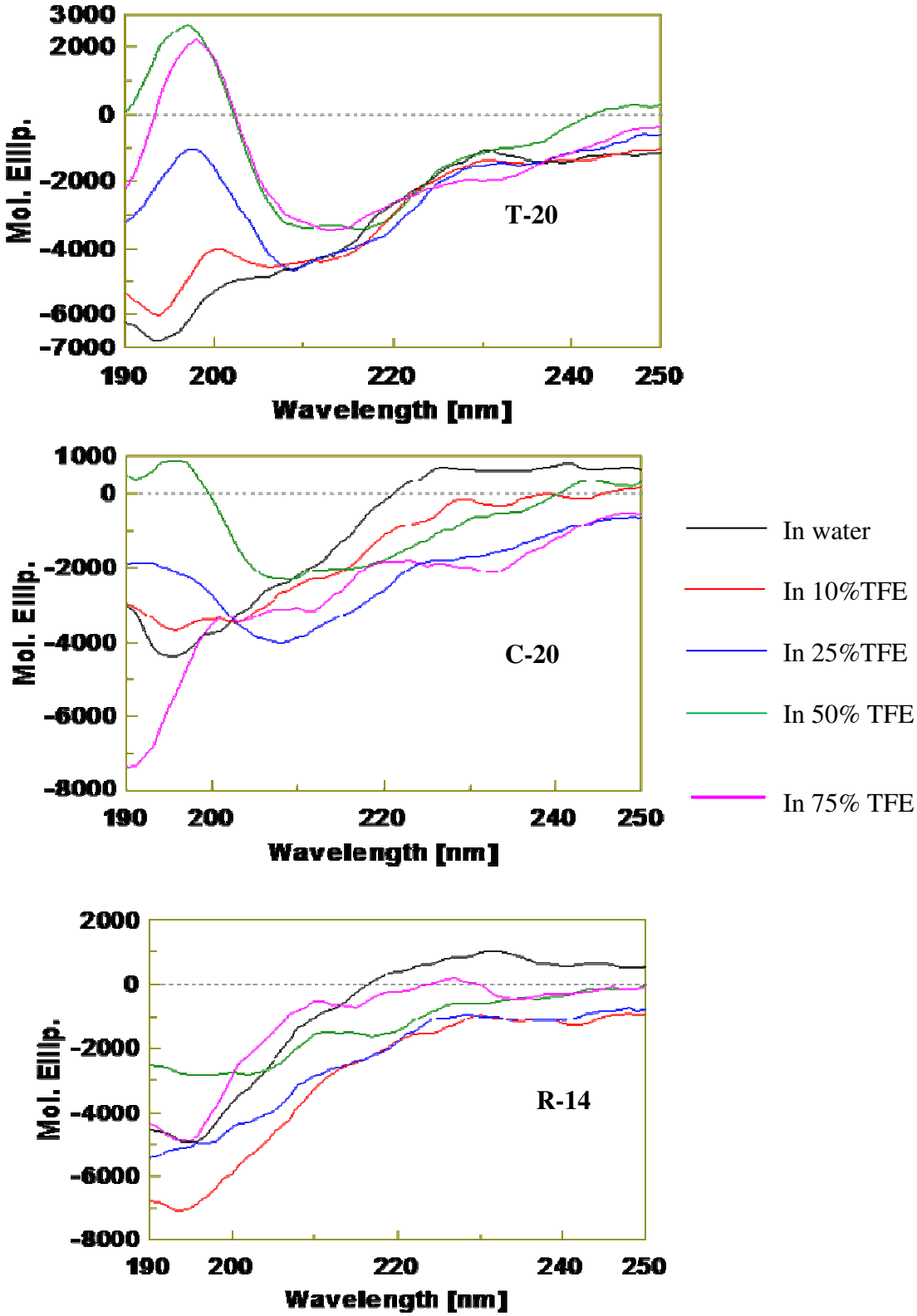

Figure 4.5: CD spectra of nAChRα-subunit peptides in different polar and aploar environments; in water, 10% TFE, 25% TFE, 50%TFE, 75% TFE.

With increase in TFE concentration, a progressive red shift was observed reaching up to 210 nm. The peptide had mainly Beta sheet conformation in water which got little increased in higher TFE concentration. In 75% TFE, there was around 10% helix conformation of the peptide at the expense random coil structure of the peptide in water solution.

The CD spectra of C-20 peptide recorded in water and different concentration of TFE is shown in Figure 4.5. In water the spectrum shows negative band around 195nm with no positive band cross over observed even above 250nm. With increase in TFE concentration, progressive red shift was observed reaching up to 210nm. In water the peptide had mostly Beta sheet conformation and rondom coil which got reduced with progressive increase in TFE concentration with small increase (6%) in the helix conformation.

R-14 peptide was similarly studied for secondary conformation in water and with increase in TFE concentration. The quantified different conformation components of the peptide in different aqueous and apolar environments are given in table 4.3. The CD spectrum of the peptide in water showed negative band at 195nm with positive band cross over at 218nm. In water the peptide had predominant beta sheet and random coil structures.

4.5 Interaction of nAChRα-subunit peptides & their analogues with RV:

nAChRα-subunit is a receptor for RV. Interaction with the receptor molecule is essential for attachment and entry of the virus into the host cells for productive infections. Virus capturing/binding enzyme linked immunosorbant assay (ELISA) was done to determine the interaction of α subunit peptides with the RV.

Virus captured by the equal quantity of the peptides was detected by indirect ELISA method. Primary mouse monoclonal anti-RV glycoprotein antibody was used followed by anti-mouse HRPO conjugate and developed with TMB substrate. Absorbance for each of these peptides coated wells were taken after subtracting values of the BSA coated well. The results of the experiments are depicted in figure 4.6.

It was found that nAChRα-subunit peptides of different species origin were able interact and capture the inactivated RV. However, the binding efficiency was different for each of these peptides. Peptide of torpedo origin (T-32 & T-20) had higher binding ability to capture the virus when compared to the other peptides.

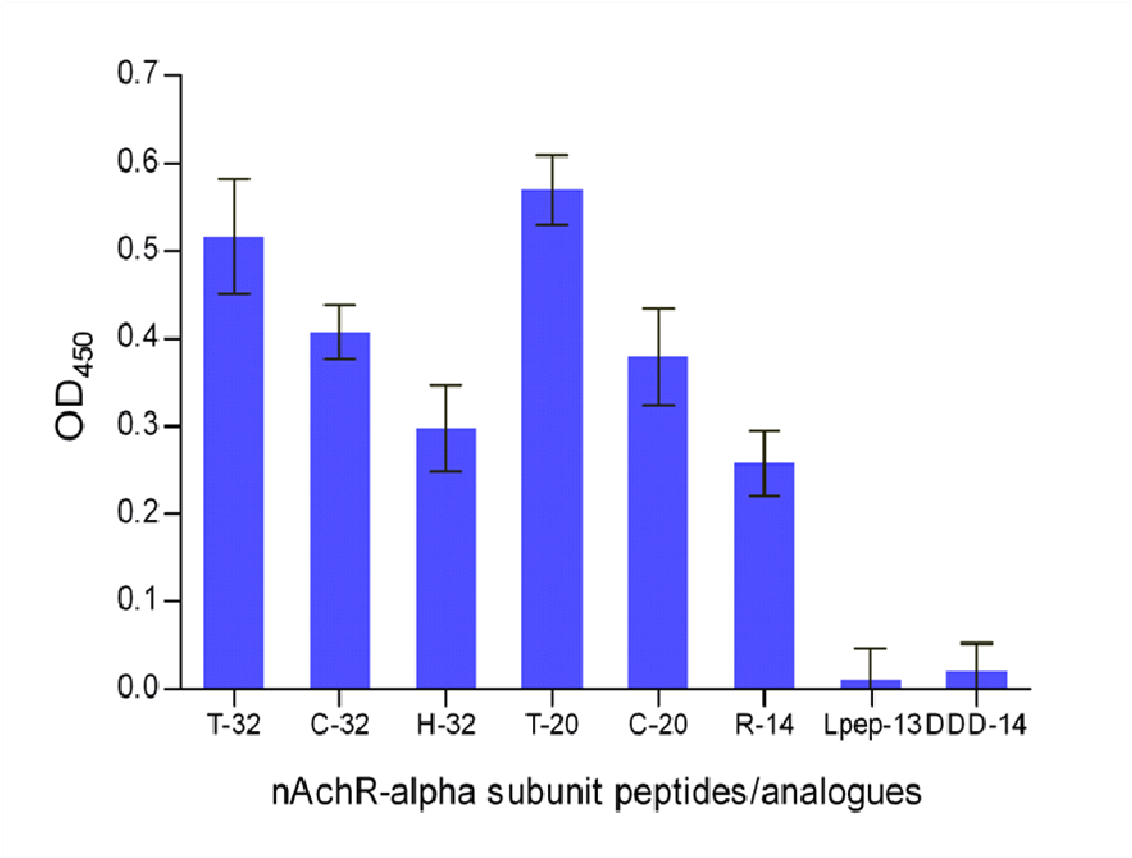

Figure 4.6: Interactions of nAChRα-subunit peptides with RV. Absorbance values for each peptide were taken after subtracting the values of the BSA coated control well. Triplicates of two independent experiments were used for plotting the results (values represent Mean ±SD).

The bovine/calf origin peptides (C-32 &C-20) had comparatively lower ability to capture the virus. The human (H-32) and rat origin peptide (R-14) had shown least efficiency in binding to the virus. The two neurotoxin binding peptides (Lpep-13 & DDD-14) which were earlier shown to mimic α subunit of nAChR and interacted with the bungarotoxins however showed little or no binding to the RV.

Among all the peptides tested, the mean values representing the interaction and capturing of the RV indicated that T-20 had highest RV binding efficiency when compared to other peptides (Figure 4.6).

4.6 Synthesis and characterization of AuNPs:

AuNPs synthesized using citrate reduction of auric chloride ($HAuCl4.3H_2O$). At high temperature (80-100^oC), citrate helps in reduction and stabilization of gold particles. The color of the solution changed from yellow to brick red as the reaction proceeded to completion. Citrate stabilized AuNP were characterized by UV-Vis spectrophotometer and TEM. The solution exhibited characteristic absorbance maxima at 519nm. The sharpness of the peak and wavelength of absorbance indicates fairly mono -dispersed uniform particles . The TEM images indicated the synthesized AuNP were of the sizes 12.88 ± .50 nm (Figure 4.7A & 4.7B)

4.7 Conjugation of MAP with AuNP:

The synthesized AuNPs were used for covalent activation with peptides. MAP formats were designed using the sequences of T-20. These branched peptides were synthesized with lysine mosaic and cysteine at the c-terminal end. Sulfar in the terminal cysteine was used for conjugating the MAP peptides. The schematic representation of functionalization of peptides on the AuNP is given in figure 4.8A. Strong sulfar–gold interaction involving simple thiol-gold chemistry successfully functionalized the peptides on AuNP. The presence of the peptides on the AuNP surface was observed using UV-Visible spectrophotometer. The results indicated the red shift in the absorbance spectra of functionalized AuNP compared with the plain AuNP (Figure 4.8B).

4.8 RV interaction with MAP functionalized AuNPs:

T-20 had better RV binding efficiency to compared to other nAChRα-subunit peptides as previously observed in virus binding ELISA. Similarly, T-20 MAP format was likely to interact with RV in solution. The MAP formats were decorated on the surface of AuNP.

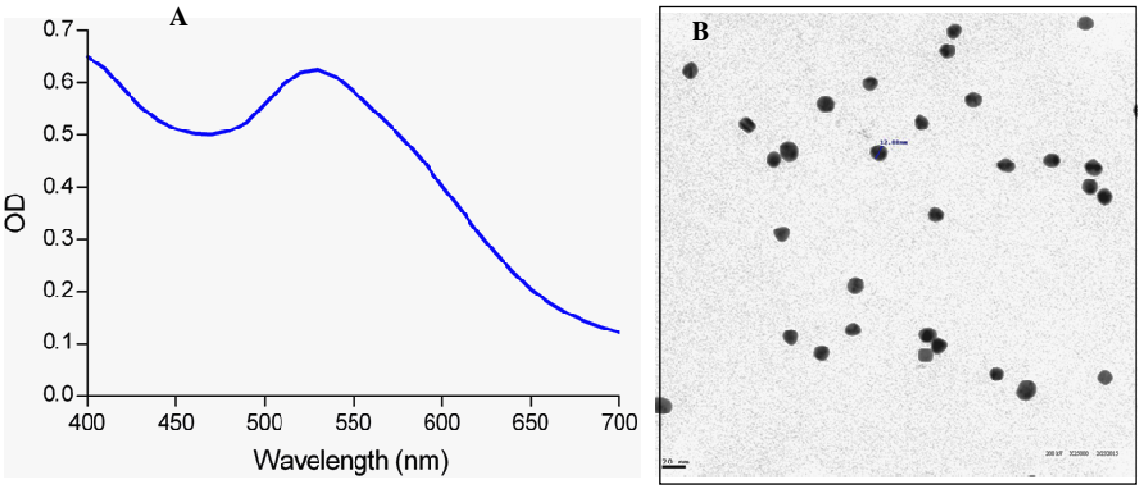

Figure 4.7: Characterization of AuNP using UV-Vis spectrophotometer (A) and TEM (B)

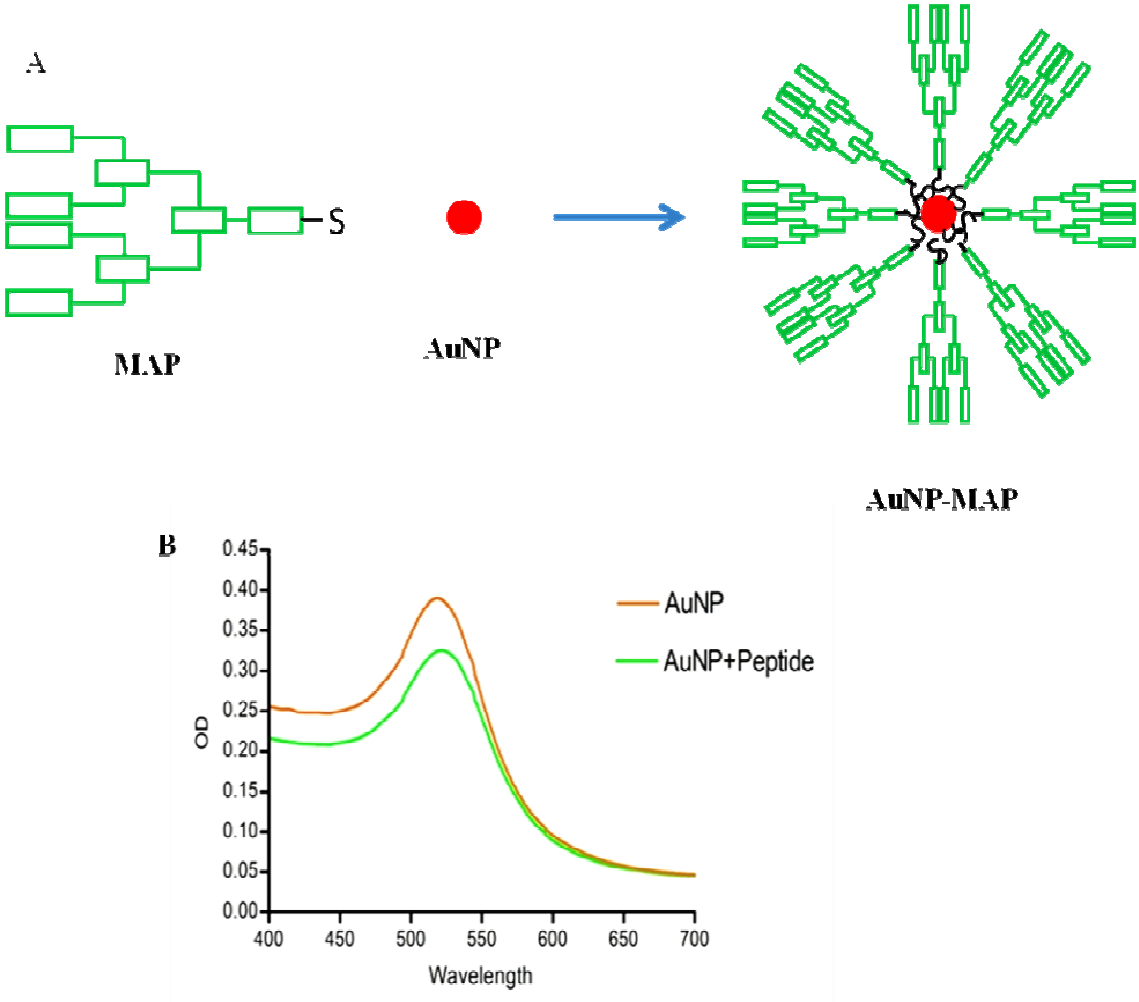

Figure 4.8: Schematic representation of conjugating MAP to citrate stabilized AuNP using strong gold-sulfur interface (A). UV-Vis spectra of AuNP and AuNP-MAP (B).

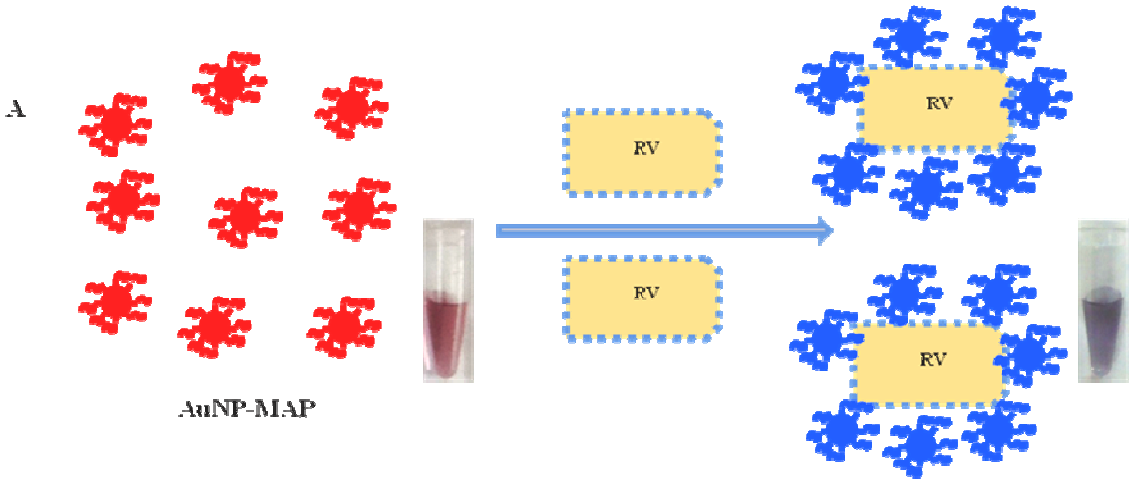

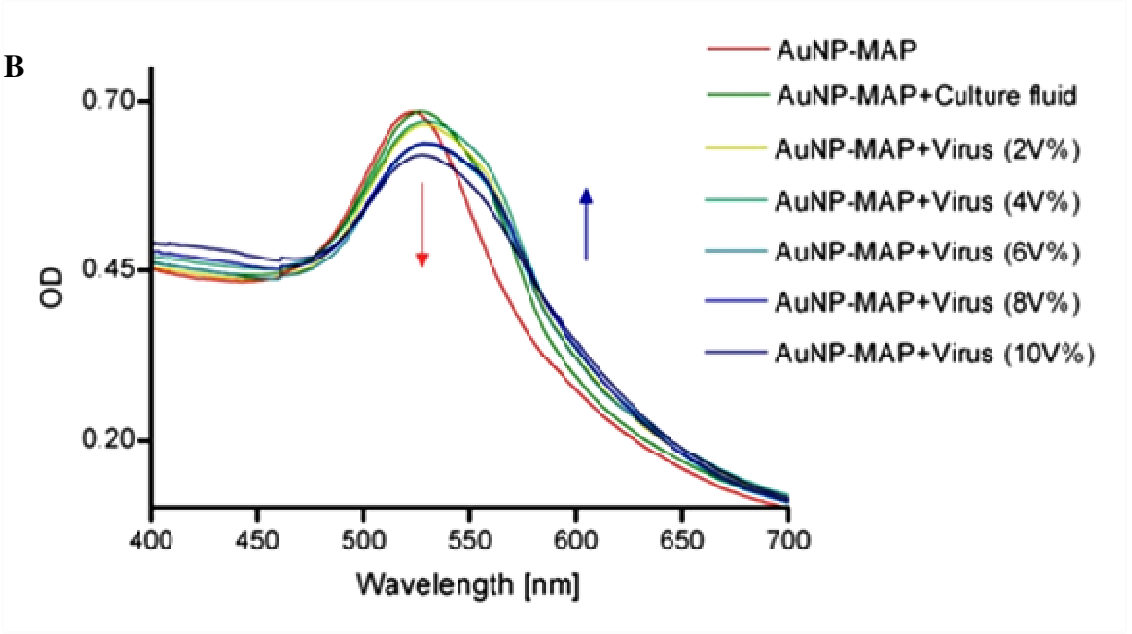

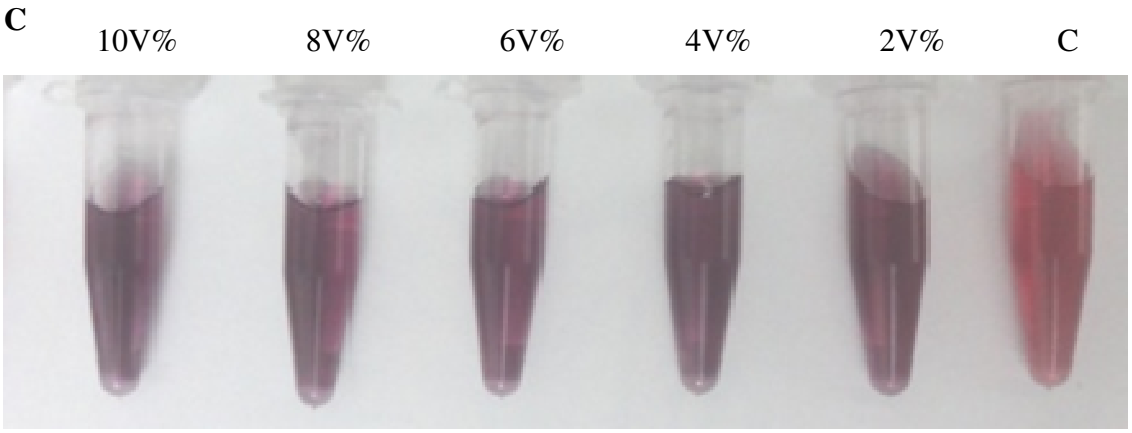

Figure 4.9: Schematic representation of AuNP-MAP visual plasmon change on addition of inactivated RV(A); UV-Vis spectra changes on showing decrease at A_{520} and increase at A_{610}nm (B); Visual color change from red to purple/blue after addition of inactivated RV(C).

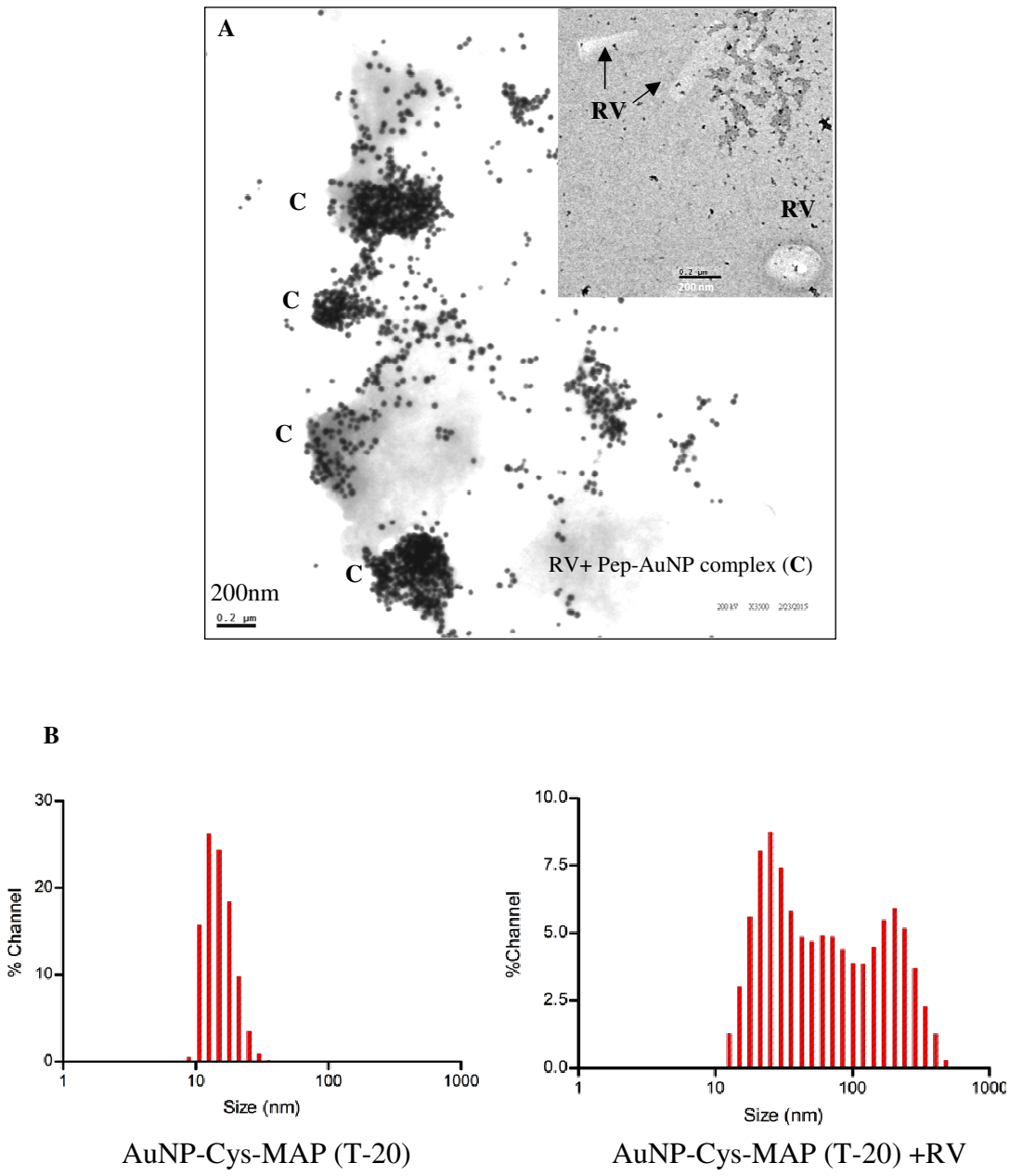

Figure 4.10: Interaction of AuNP-Cys-MAP (T-20) and inactivated RV observed under TEM (A) and DLS particle size analysis by zetasizer (B).

The functionalization process did not alter the Surface Plasmon of individual gold colloid. RV may bind to the individual AuNPs via the conjugated peptide. The interaction between each virus particles with large number of AuNP will reduce the distance between individual AuNPs. The change in the inter-particle distance results in altered Plasmon leading to change in the visible color change in the colloid. The schematic diagram of the concept is shown in figure 4.9A. In our experiment, the addition of inactivated RV to peptide-AuNPs solution resulted in change of original brick red to purple/blue color. The results indicated the presence of RV in a given solution.

Different concentrations of virus (v%) were added in the AuNP-MAP conjugates. For spectroscopic detection of the change, absorption spectra (400-700nm) were recorded every minute after the addition of 10v% of inactivated RV suspension to 1nM peptide-AuNP. Over a period of time, OD at 610nm increases while that at 510nm decreases. The increased absorbance at 610nm indicates that AuNP aggregates have formed, thus decreasing the population of single AuNPs as they were converted into AuNP aggregate on the viral particle surface (Figure 4.9B). Different volumes of virus suspensions were added to the peptide-AuNP. The results indicated direct correlation of color change with the amount of virus added (Figure 4.9C).

The interactions of AuNP-MAP conjugates with the inactivated RV was also studied with the help of TEM and DLS zetasizer. The results of the interaction are presented in figure 4.10A and 4.10B respectively. The specific binding of the AuNP-MAP on the virus particle leading to aggregation of AuNPs was observed. The size of aggregates were well comparable with the combined size of virus particle and the AuNPs (~200nm). Both individual AuNP-MAPs and clustered particles were observed in the TEM images (Figure 4.10A). The results indicated that specific interactions were mediated by the T-20 peptides (MAPs) coated on the AuNPs. Similarly DLS particle size analysis showed a hydrodynamic diameters of individual AuNP-conjugates as 40-50nm. However the addition of RV (inactivated) dramatically increased the sizes present in suspension to 200-250nm (Figure 4.10B). The results of both TEM and DLS further established the binding specificity of nAChRα-subunit peptides to the RV.

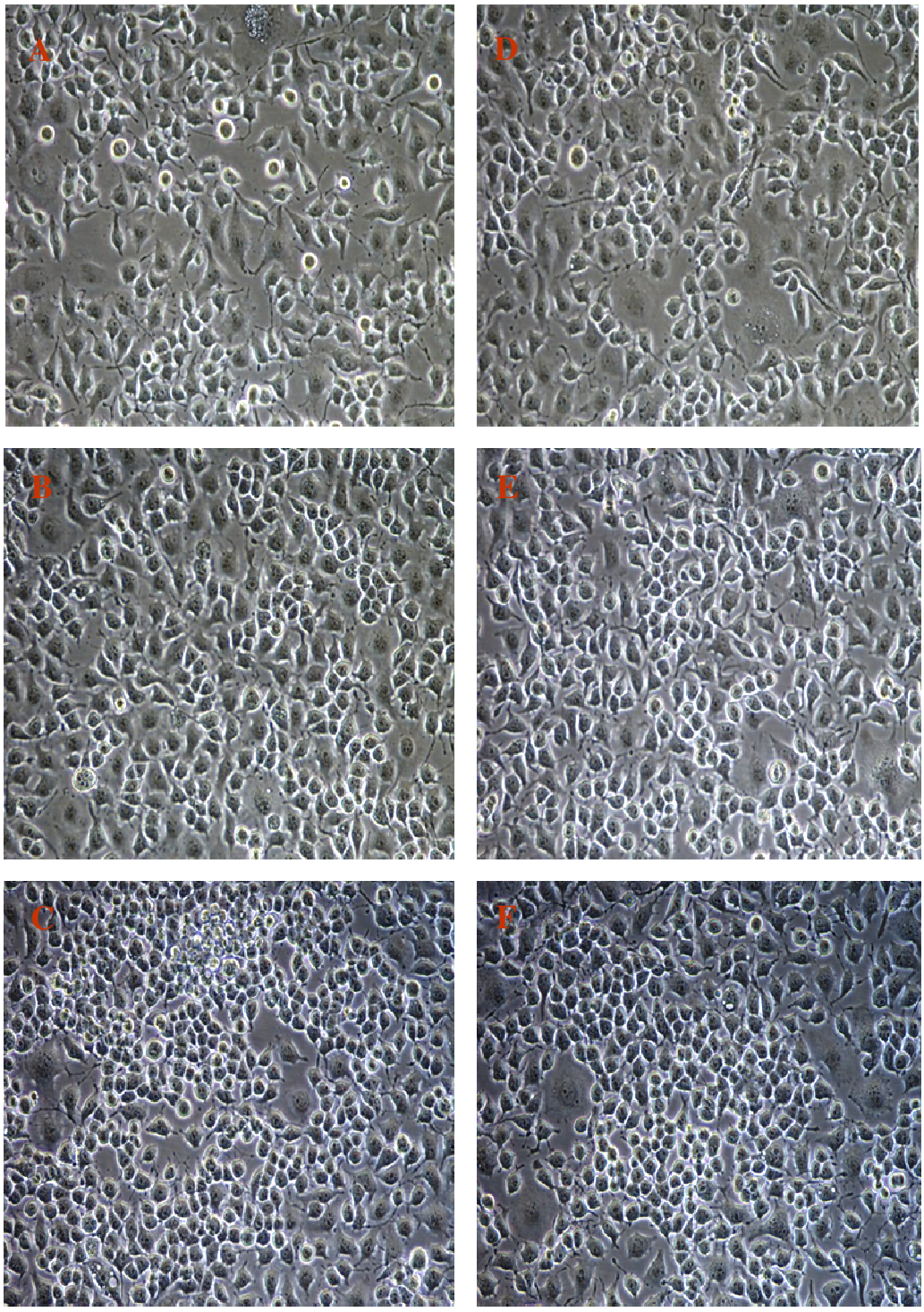

Figure 4.11: RV (CVS-18) propagation in N2A cells. Infected cultures were incubated in CO_2 incubator at 37°C and observed at regular intervals (A, B, C were RV infected cells observed at 24hpi, 48hpi and 72hpi; D, E, F were mock infected controls observed at 24hpi, 48hpi and 72hpi). Images at 200X. No morphological differences (CPE) were observed between RV infected and mock control cells.

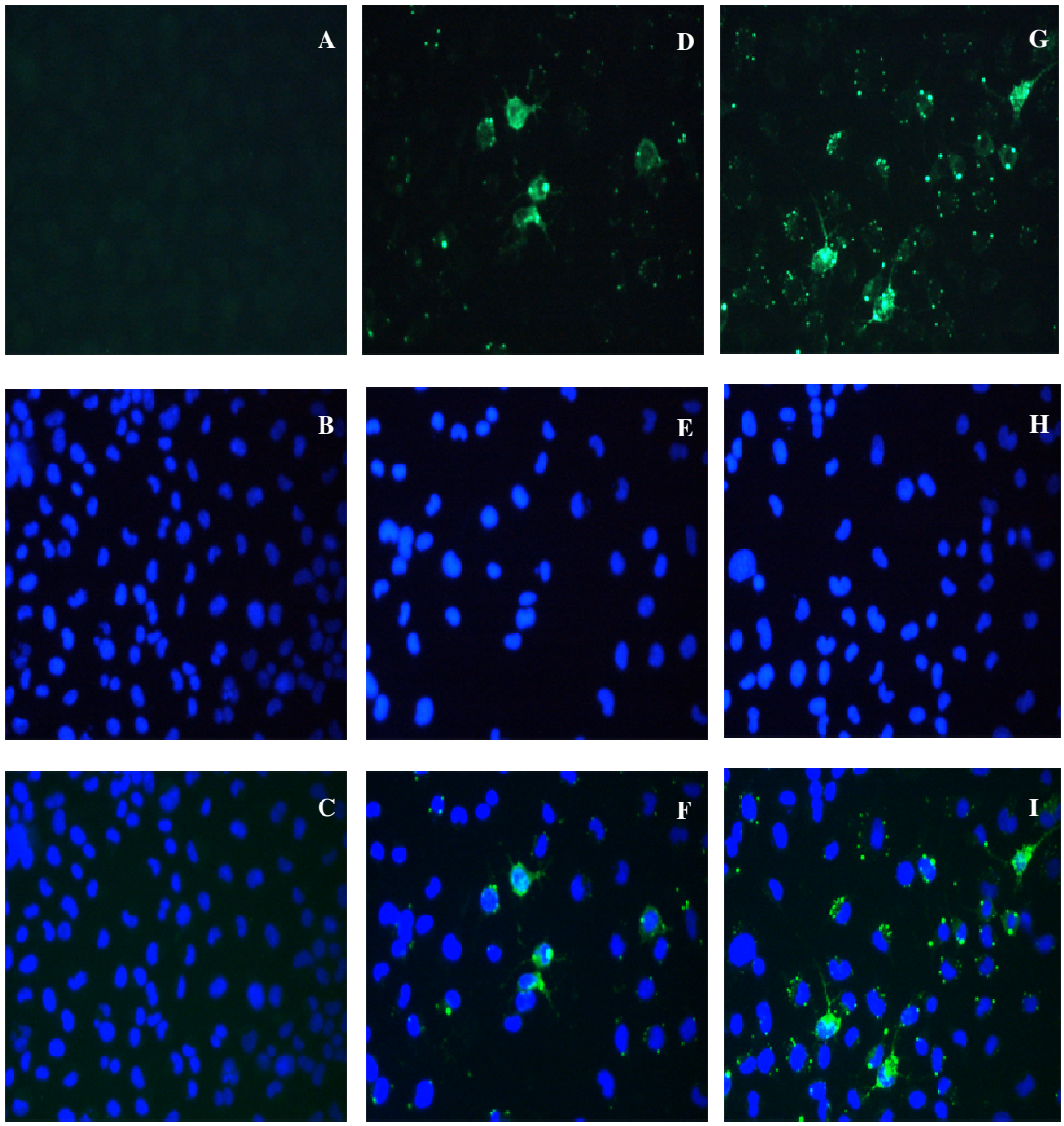

Figure 4.12: RV detection in N2A cells using direct immunofluorescence test. RV infected N2A cells were stained with anti nucleocapsid antibody FITC conjugate (A, B & C- mock infected; D, E & F-24hpi; G, H & I-48hpi) (A, D, G -Green; B, E, H -Blue/ DAPI; C, F, I–Merge; images at 400x).

4.9 Propagation of RV in neuroblastoma cells (N2A):

Mice brain adapted CVS-18 was used in the present study. 1% brain suspension was used as a inoculum in semi-confluent monolayer of N2A cells. The inoculum was replaced with maintenance medium and incubated up to 72hrs at $36^{o}C$ in 5% CO_2 in-culture incubator. Any changes in the morphologies of the cells were recorded at regular intervals of 24, 48 & 72hrs post infection (hpi).

The observations of infected N2A cells indicated that RV did not produce any morphological cytopathic changes (CPE) in the N2A cells compared to the mock control flask. Further no CPE was observed even after 72hpi (figure 4.11). In the absence of cytopathic effect, RV multiplication in the N2A cells can only be detected by other methods like immunofluorescense technique using specific FITC labeled antibodies.

4.10 Detection of RV in infected N2A cells by immunofluorescence:

For detection of RV multiplication, N2A cells were infected in 24well culture plates. Cells were washed with PBS and fixed with 80% acetone for 30min at $-20^{o}C$ and probed with anti-rabies nucleocapsid monoclonal FITC conjugate. The cells observed under inverted fluorescent microscope.

The results showed specific fluorescent foci present in the cytoplasm of infected N2A cells. The fluorescent foci indicated the RV presence and multiplication (figure 4.12). Wells incubated for different time intervals (24, 48 and 72hpi) were included in the experiment. The number of cells infected with the virus were lesser in 24hr compared to 48 and 72hpi. There is no significant difference in the number of foci observed between 48hpi and 72hpi. The mock infected cells showed no specific fluorescence confirming the specificity of the immunofluorescence test.

4.11 Titration of the RV in N2A Cells:

Serial passages of RV was done to increase the titre of the virus. Lesser inoculums were used in subsequent passages. Culture fluids from different passage numbers were titrated using standard FFU/ml protocol in N2A cells. After 24hpi, the cells were stained with rabies anti-nucleocapsid FITC conjugate. The wells of highest virus dilutions showing specific intracytoplasmic fluorescent foci were counted. The results indicated gradual increase in the titre values of RV ranging from $3X10^{2}$ FFU/ml in the beginning however the same was increased to $1X10^{5}$FFU/ml in the 5^{th} passage.

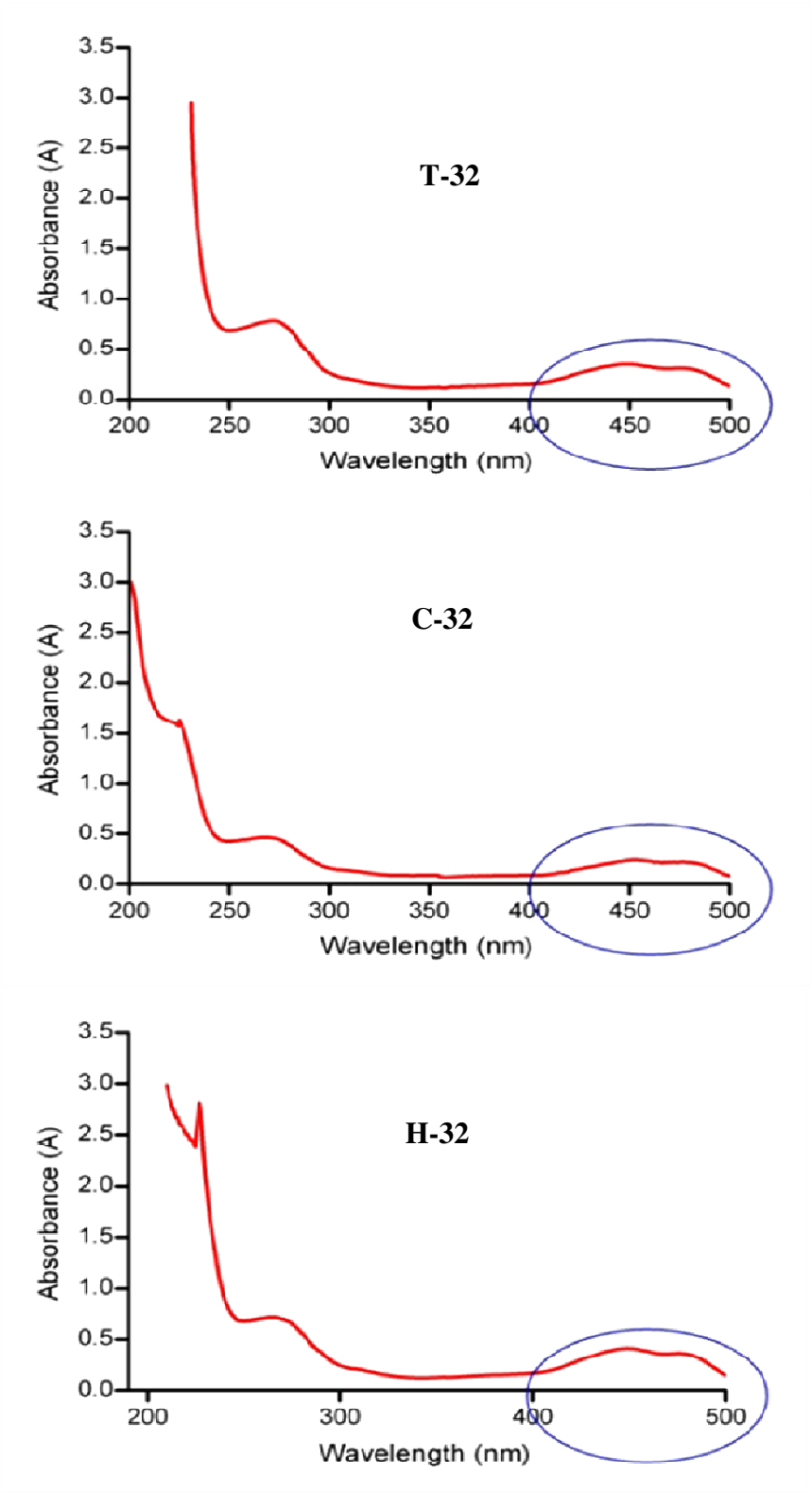

Figure 4.13: UV-Vis spectra of FITC labeled nAChRα-subunit peptides showing characteristic absorbance between 420-490nm ranges.

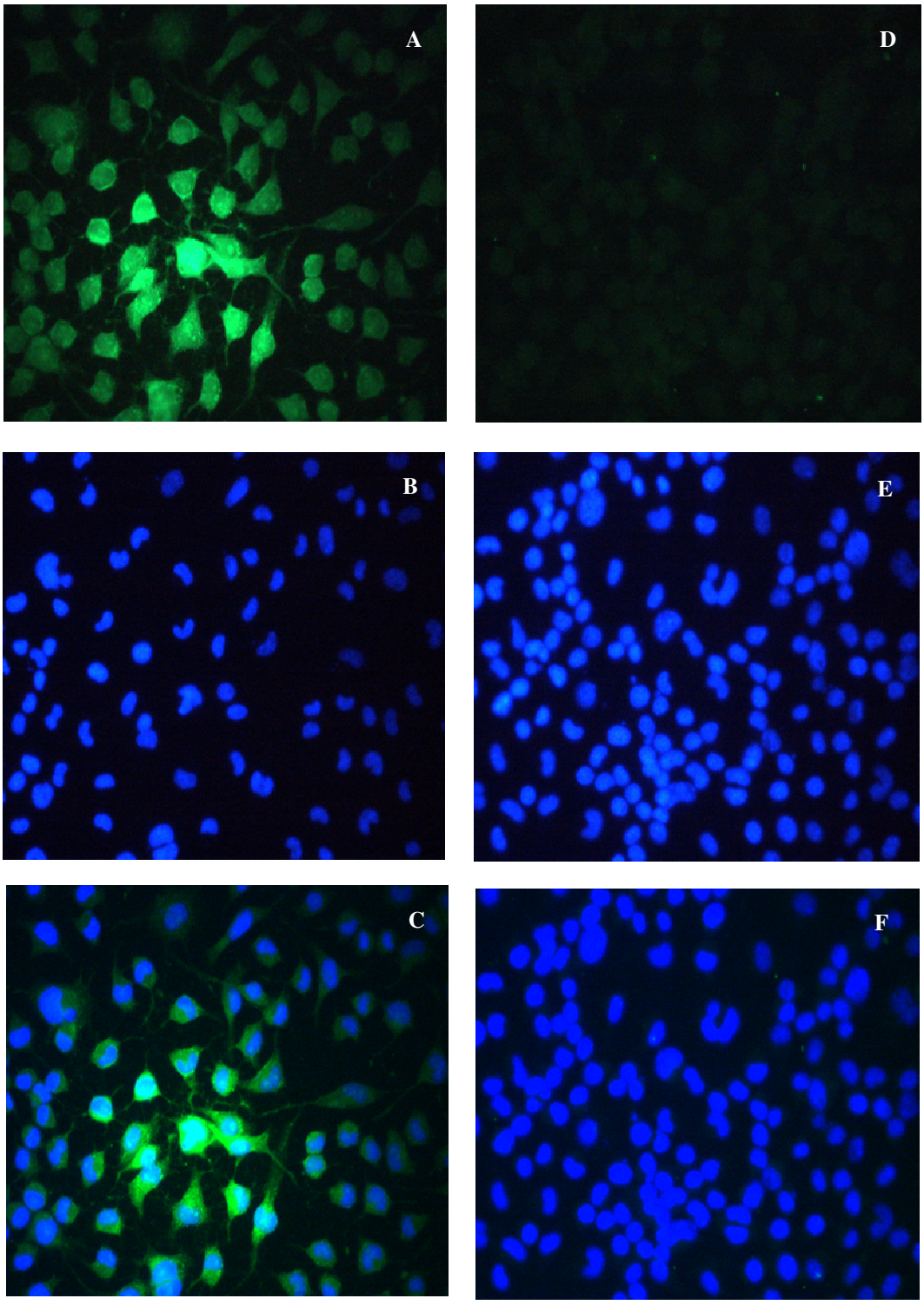

Figure 4.14: RV infected N2A cells stained with FITC labeled T-32 peptide showing interaction of peptide with the RV glycoprotein expressed on the infected cell membranes. (A, B & C-RV infected N2A cells; D, E & F- Mock infected N2A cells; A & D - Green; B & E-Blue nuclear DAPI; C & F- Merge)

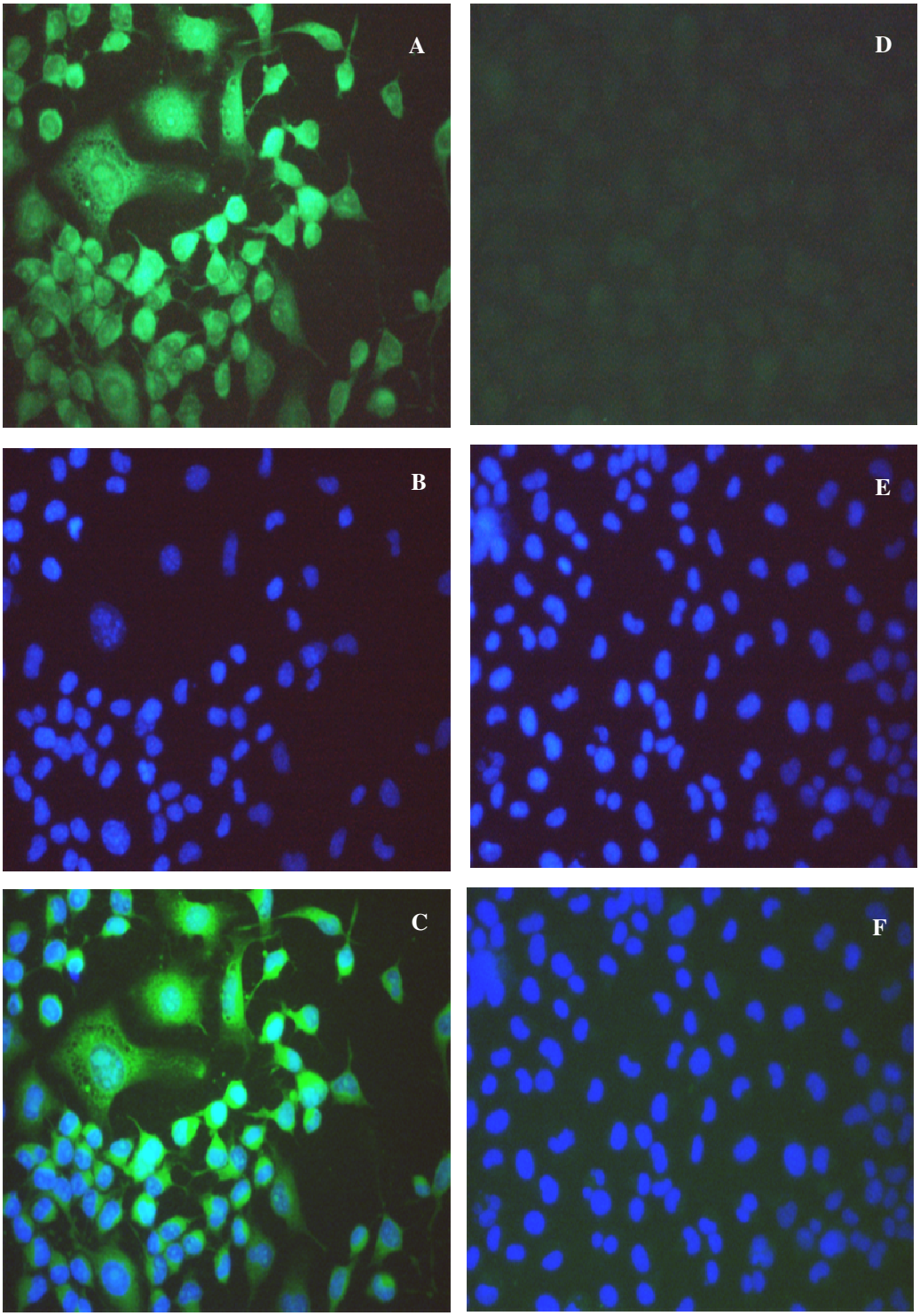

Figure 4.15: RV infected N2Acells stained with FITC labeled C-32 peptide showing interaction of peptide with the RV glycoprotein expressed on the infected cell membranes. (A, B & C-RV infected N2A cells; D, E & F- Mock infected N2A cells; A & D - Green; B & E-Blue nuclear DAPI; C & F- Merge).

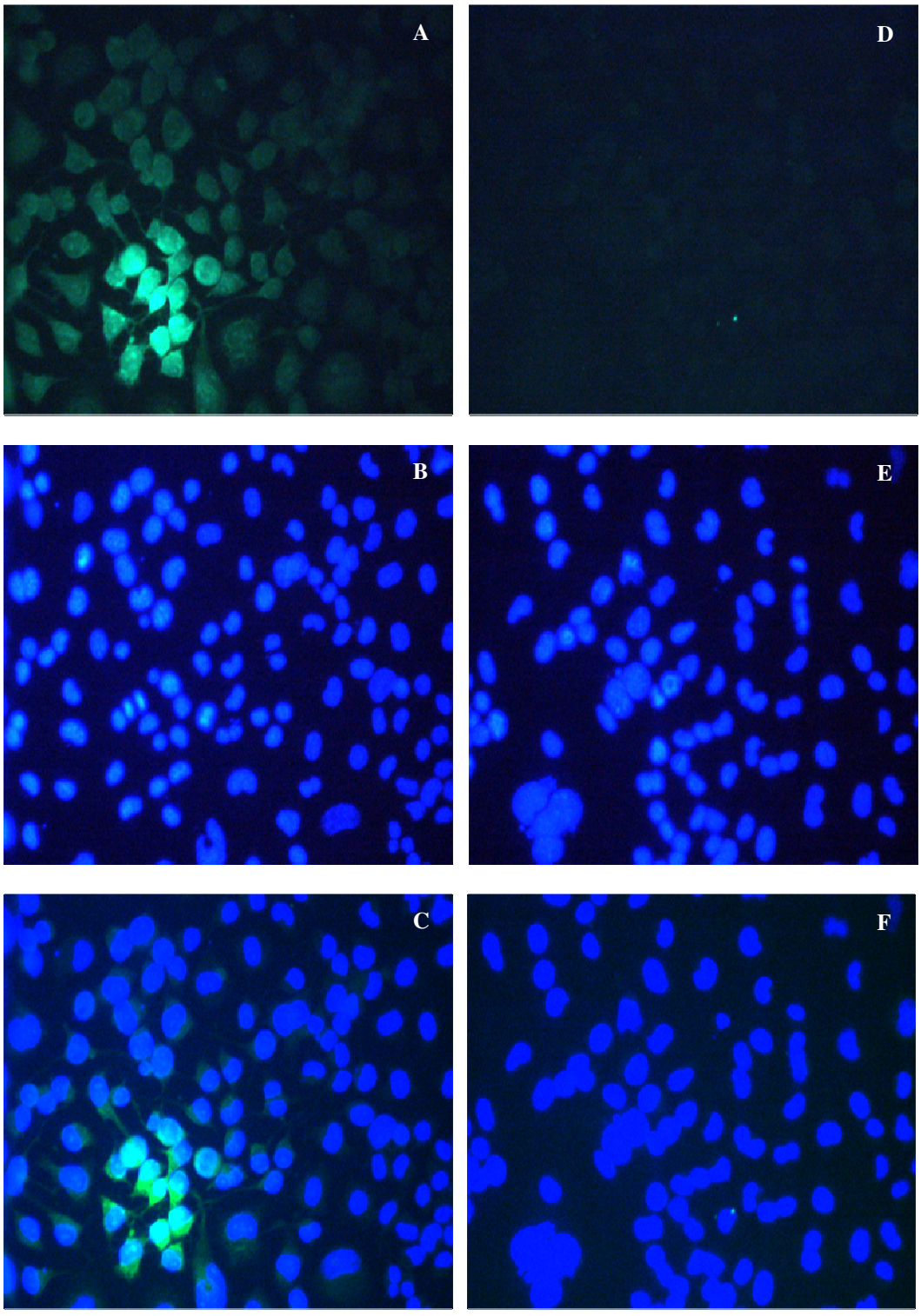

Figure 4.16:RV infected N2Acells stained with FITC labeled H-32 peptide showing interaction of peptide with the RV glycoprotein expressed on the infected cell membranes. (A, B & C-RV infected N2A cells; D, E & F- Mock infected N2A cells; A & D - Green; B & E-Blue nuclear DAPI; C & F- Merge)

4.12 Interaction of FITC labeled peptides with RV infected N2A cells:

32mer nAChRα-subunit peptides were labeled with FITC after addition of linker to the original sequence at amino terminal end. The linker reduced the adverse effect of dye (hydrophobicity) on the specific binding ability of the peptide to their ligands. The labeled peptides were evaluated using UV-Vis spectrophotometer. The results are presented in the figure 4.13. The absorbance spectra of the peptides showed marked peaks between 420 to 490nm which is the characteristic FITC dye. The absorbance spectra clearly indicated the successful labeling of the peptides with the FITC.

The labeled peptides were tested for their ability to interact with the RV infected N2A cells. The results observed in the fluorescent microscope indicated specific fluorescence. The peptide bound cells were in the form of clusters showing fluorescence, where as surrounding cells were not fluorescent. RV glycoprotein expressed in the infected cells and is located on the cell membranes which ultimately contribute to the viral envelope as the progeny virus bud from the infected cells. The cell surface fluorescence observed confirms the binding of the peptides to the viral glycoproteins. T-32 -FITC and C-32-FITC showed enhanced fluorescence where as H-32-FITC showed weak fluorescence in the RV infected N2A cells surface (Figure 4.14, 4.15 and 14.16).

4.13 Cytotoxicity of nAChRα-subunit peptides in N2A cells:

Before *in vitro* testing of peptides for antiviral effect against RV, their cytotoxicity was evaluated. Increasing concentrations of peptides were incubated with N2A cells and percentage viability of cells was calculated based on the reduction of the MTT dye. Absorbance values at 540nm by the peptide treated and control wells were plotted against the concentration of the peptides used. These values were also converted to percentage cell survivability and plotted against concentration of the peptides. The results are presented in figure 4.17 and 4.18.

The concentrations of the peptides at which the 50 percent of the cells are viable (CC_{50}) was calculated for the peptides and compared. The results indicated that the 32 mer peptides (T-32, C-32 & H-32) show comparatively similar level of cytotoxicity in terms of percentage of viable cells. The CC_{50} values were found to be more than 100μM for each of the tested peptide (Figure 4.17A and 4.17B).

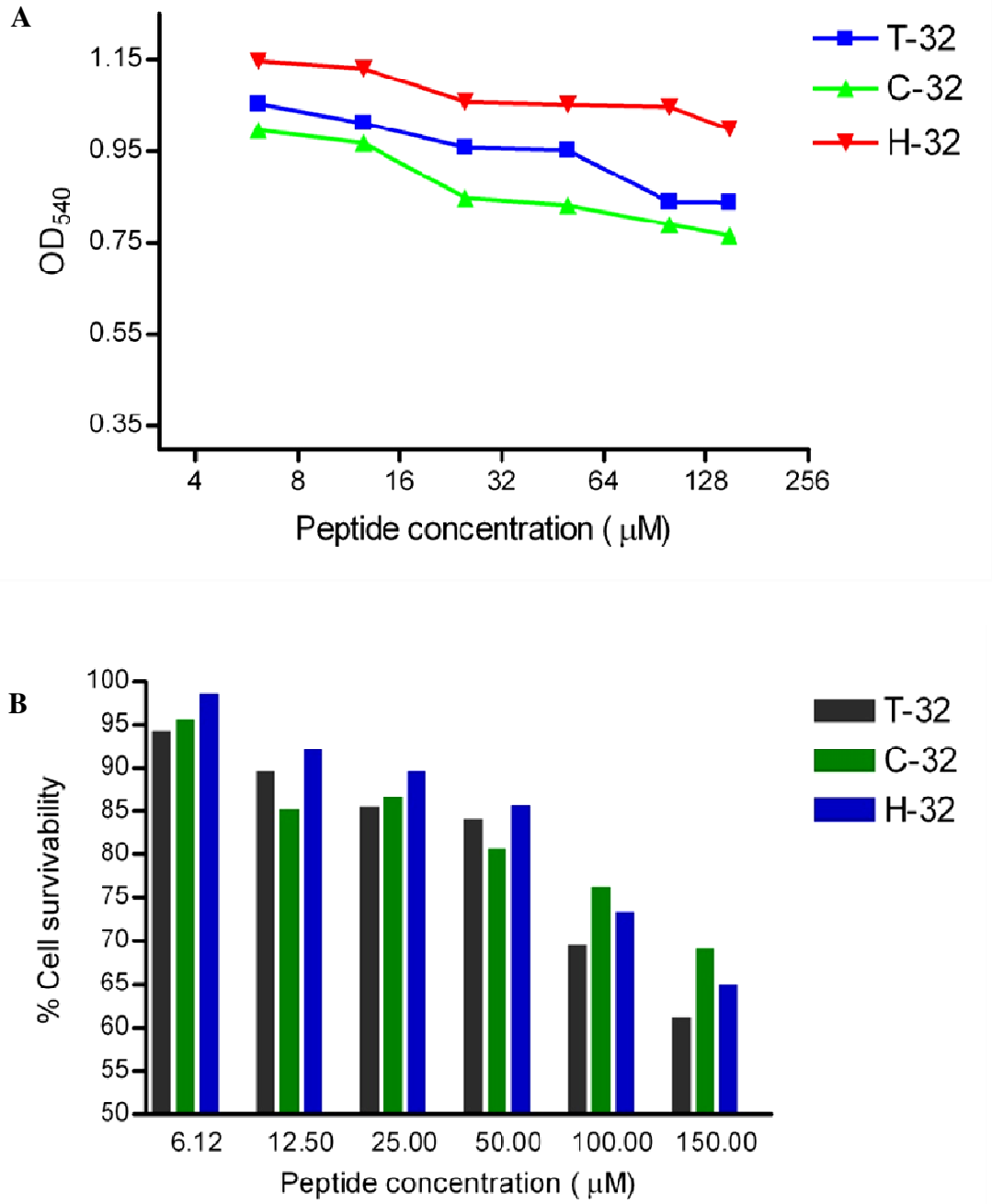

Figure 4.17: Cytotoxic effects of 32mer nAChRα-subunit peptides in N2A cells. The absorbance in the DMEM alone is considered as 100% cell survivability. Values represent mean of triplicates. Cytotoxic concentration 50 (CC_{50}) for peptides was more than 100μM.

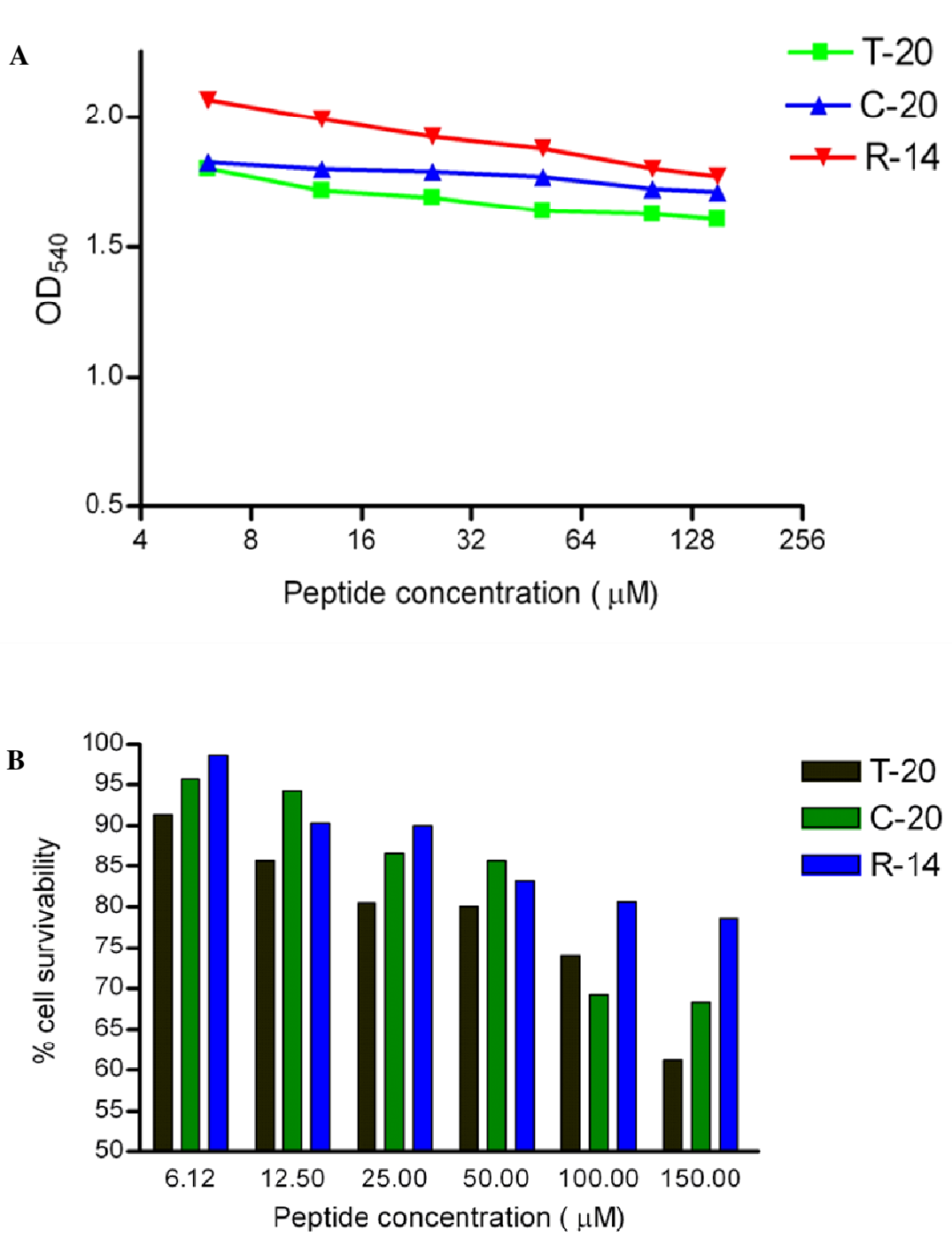

Figure 4.18: Cytotoxic effects of 20mer and 14mer nAChRα-subunit peptides in N2A cells. The absorbance in the DMEM alone is considered as 100% cell survivability. Values represent mean of triplicates. Cytotoxic concentration 50 (CC_{50}) for peptides was more than 100μM.

The smaller length peptides (T-20, C-20 & R-14) were also evaluated for their CC_{50} values in N2A cells. They were also found comparatively less cytotoxic with CC_{50} values more than 100 μM (Figure 4.18A and 4.18B).

4.14 Antiviral effect of nAChRα-subunit peptides against RV in N2A cells:

To determine the antiviral effect of nAChRα-subunit peptides against RV in N2A cells, fluorescent focus inhibition test (FFIT) was used. Increasing concentrations of the peptides were incubated with the virus and the peptide-virus mixture was used for infecting the N2A cells. After 24hpi, the cells were stained and observed for the reduction in the fluorescent foci.

In the T-32 peptide treated wells, the number of infected cells gradually reduced as the concentration of the peptide increased. The results of the experiment were presented in the figure 4.19. At 20μM concentration of the peptide, there was significant decrease in the number of infected cells. Complete inhibition of the virus was observed at 50μM concentration of the peptide (Figure 4.19). The IC_{50} value, the concentration which showed 50% reduction in the virus infection was calculated and found to be 14 ± 3.015μM.

Similarly the C-32 peptide had inhibitory effect on the RV infection in N2A cells as represented in the figure 4.20. The antiviral effect of C-32 was comparatively lesser as the infected foci were significantly visible even at 30μM concentration of the peptide (Figure 4.20). The IC_{50} value for C-32 peptide was found to of 24 ± 2.6μM.

H-32 peptide when evaluated for the antiviral effect against RV in N2A cells did not show inhibition and most of the cells featured virus specific foci similar to the control wells. Even at higher concentration of the peptide (50 μM) there was no significant decrease in the number of infected cells (Figure 4.21).

The 32mer peptides of different species origin (T-32, C-32 and H-32) were compared for their antiviral efficacy with the help of peptide dose response curves. The values were compared and depicted in figure 4.22. The results showed that T-32 was more effective in preventing the RV infection compared to the other two peptides.

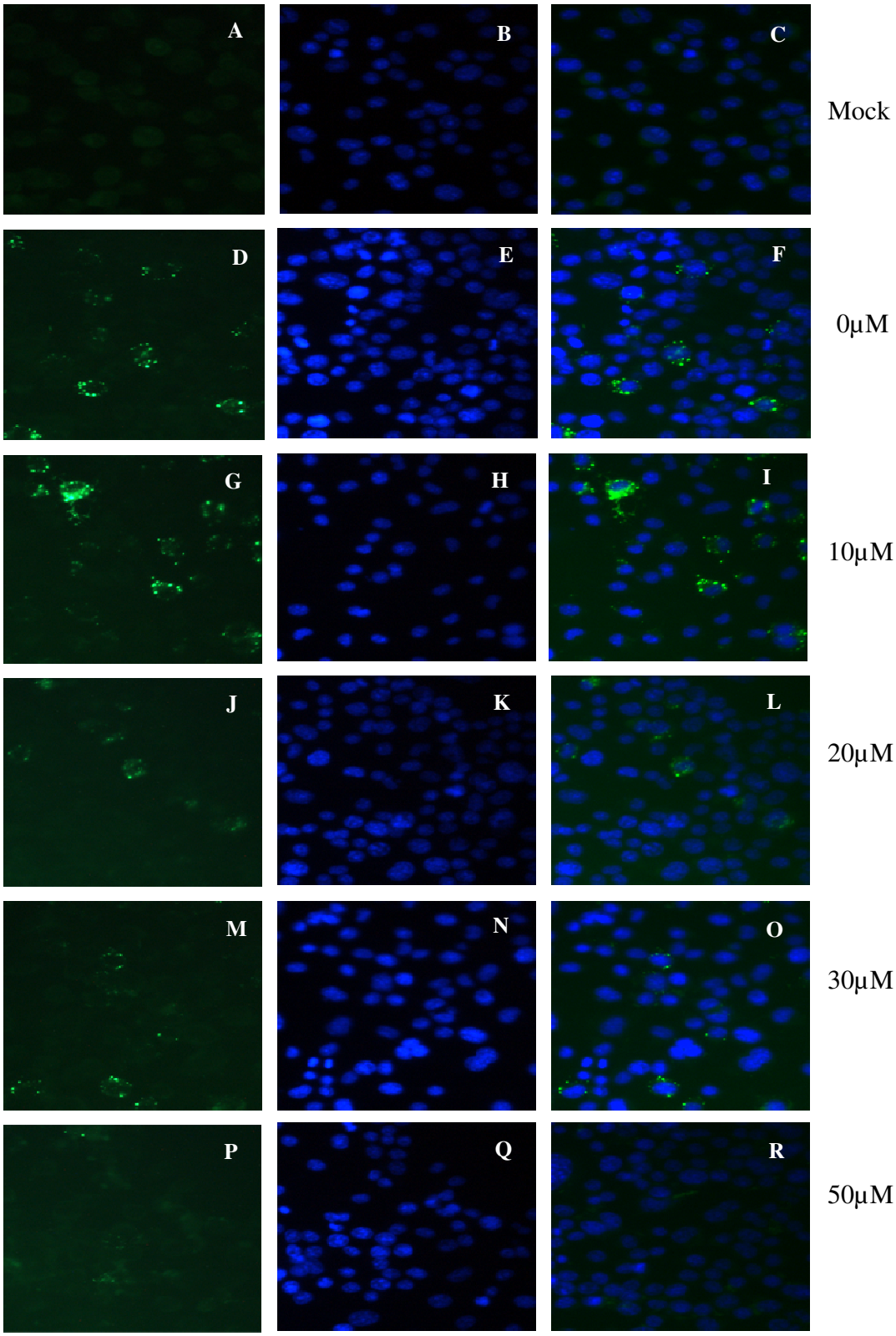

Figure 4.19: Antiviral effect of T-32 in different concentrations (µM) in RV infected-N2A cells by FFIT method. Images taken under fluorescent microscope (200X) (A, D, G, J, M, P- Green; B, E, H, K, N, Q- Blue; C, F, I, L, O, R- Merge).

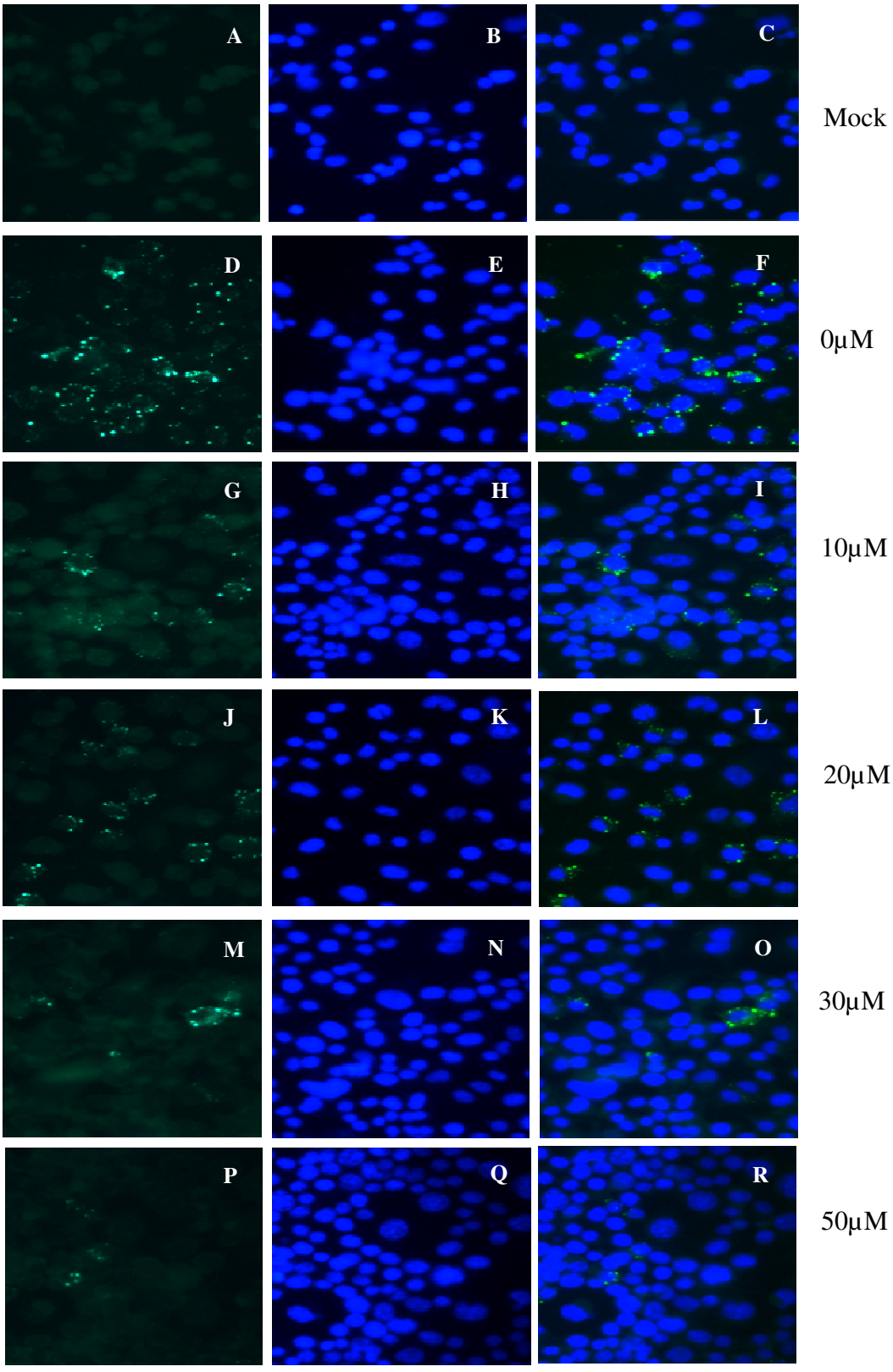

Figure 4.20: Antiviral effect of C-32 in different concentrations (µM) in RV infected N2A cells by FFIT method. Images taken under fluorescent microscope (200X) (A, D, G, J, M, P- Green; B, E, H, K, N, Q- Blue; C, F, I, L, O, R- Merge).

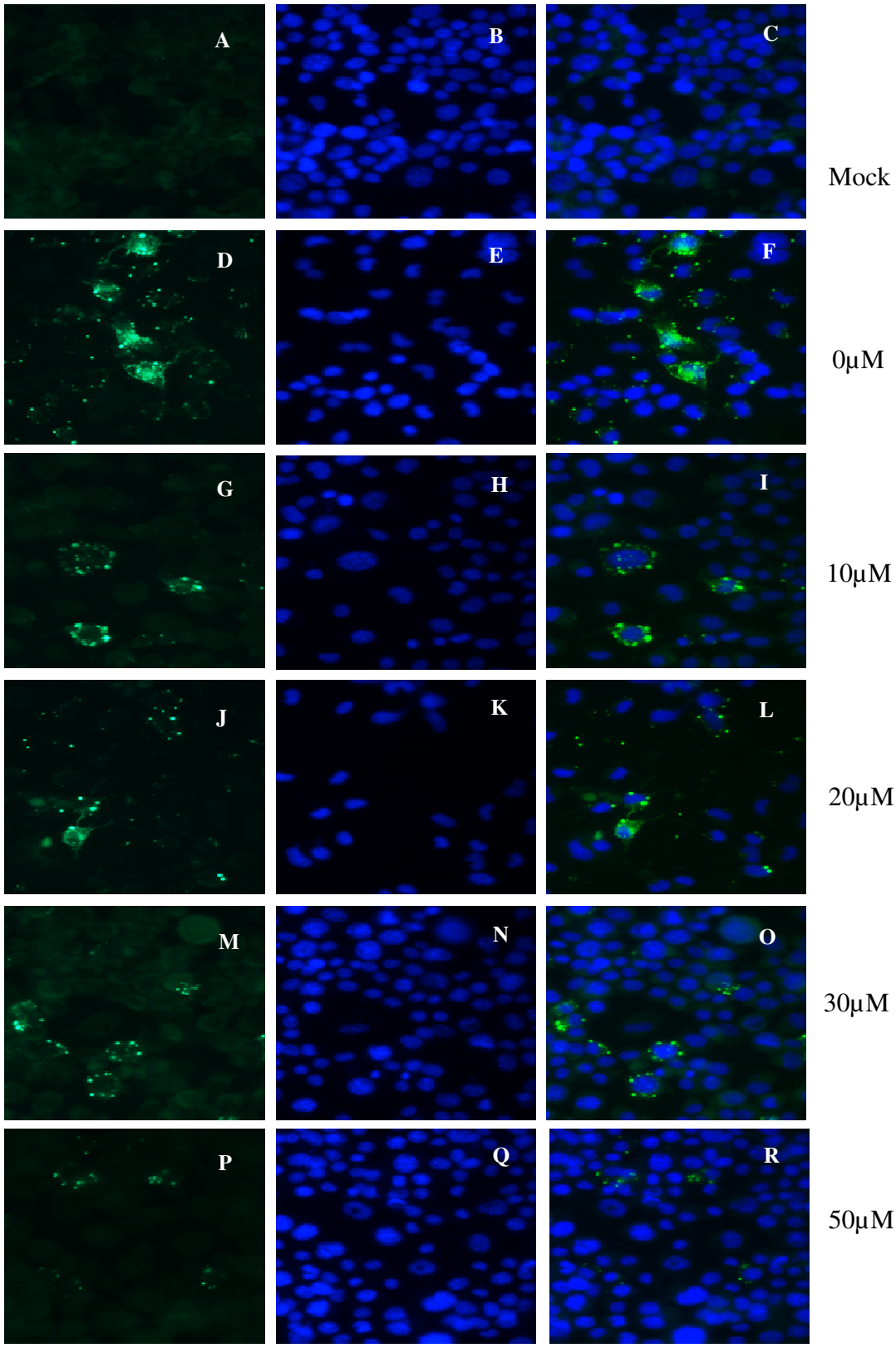

Figure 4.21: Antiviral effect of H-32 in different concentrations (µM) in RV infected N2A cells by FFIT method. Images taken under fluorescent microscope (200X) (A, D, G, J, M, P- Green; B, E, H, K, N, Q- Blue; C, F, I, L, O, R- Merge).

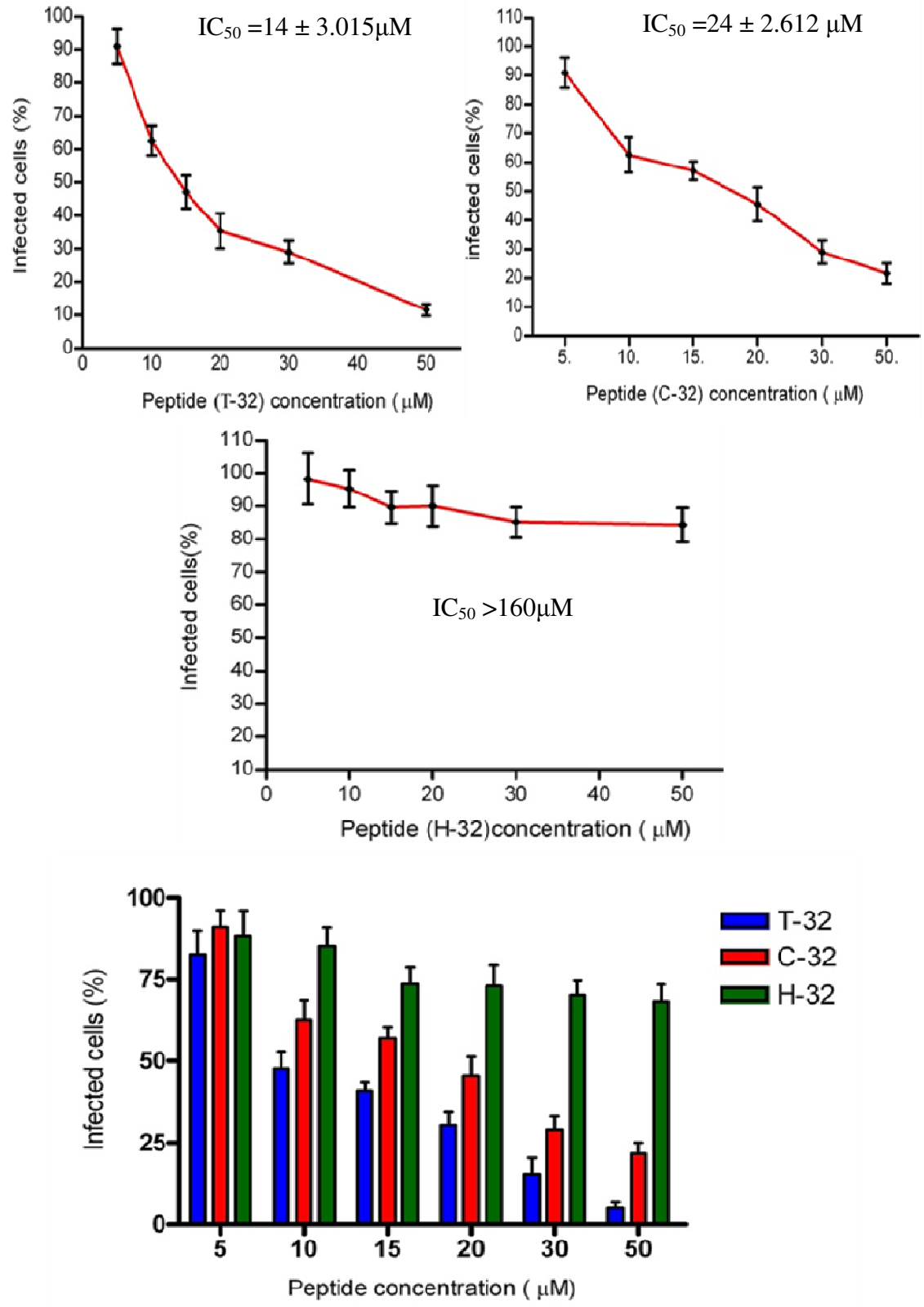

Figure 4.22: Comparison of antiviral effect of 32 mer nAChRα-subunit peptides in RV infected N2A cells.

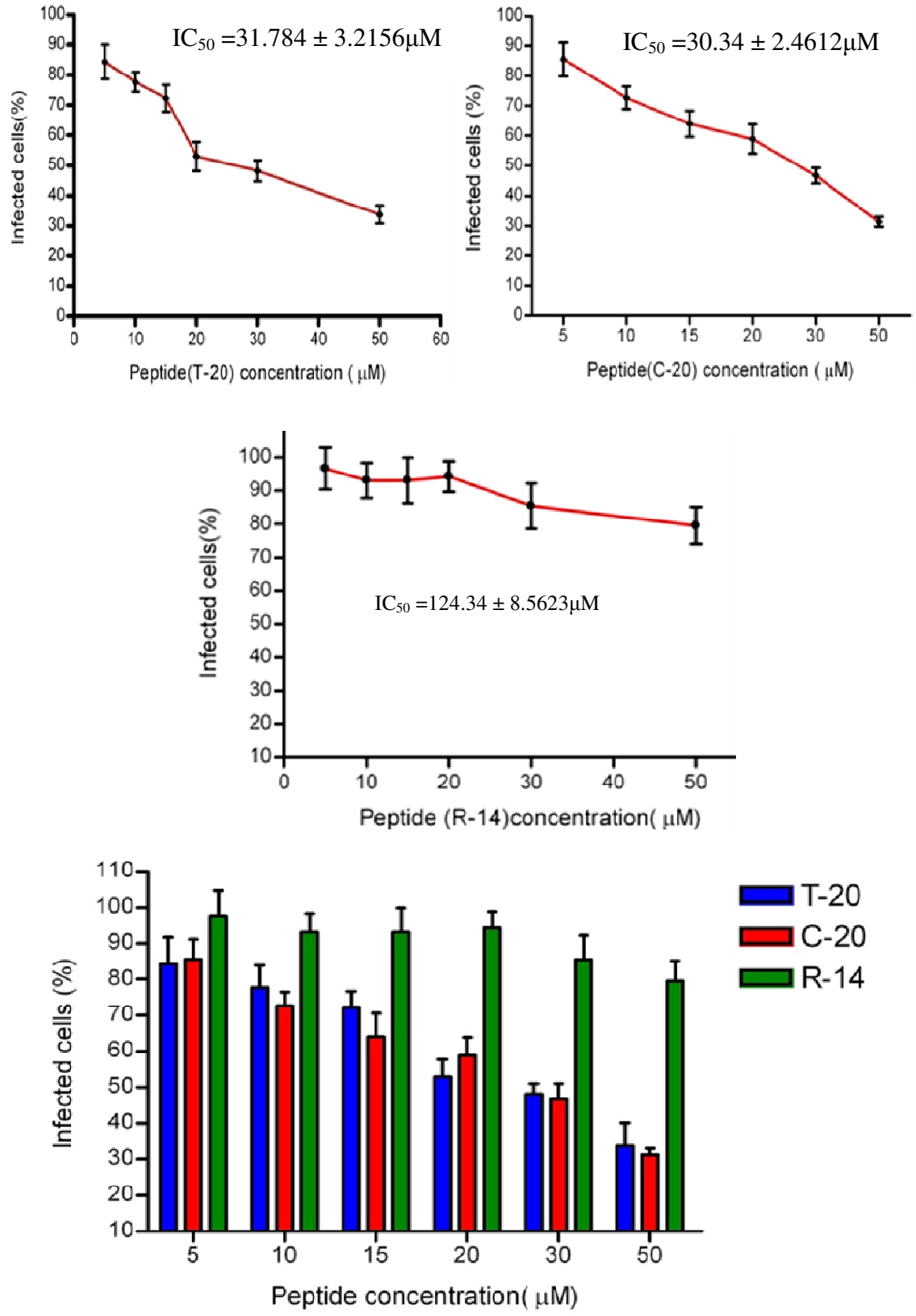

Figure 4.23: Comparison of antiviral effect of 20mer and 14mer nAChRα-subunit peptides in RV infected N2Acells.

Similarly the 20mer and 14mer peptides were evaluated for the antiviral effect. The results of T-20 peptide showed considerable decrease in the number of infected cells as the peptide concentration was increased. The IC_{50} value of the T-20 was found to be 31 ± 3.21μM. The C-20 peptide also decreased the number of virus infected cells as the concentration of the peptide increased with IC_{50} value 30 ± 2.46μM. Rat origin peptide (R-14) had less antiviral effect as there was no reduction in the number of virus infected cells even the virus was treated with higher concentration of R-14 peptide. The IC_{50} value for R-14 peptide was 124± 8.5μM.

All these three smaller length peptides (T-20, C-20 and R-14) were compared for their antiviral efficacy based on the percentage of infected cells in the presence increasing concentration of the peptides (figure 4.23). The results indicated that T-20 peptide had higher inhibitory effect on the multiplication of RV compared to the C-20 and R-14 peptides. Among all the peptides tested the torpedo origin (T-32 &T-20) indicated higher antiviral effect against RV compared to the peptides of bovine/calf, human and rat origin peptides.

4.15 Effect of peptide treatment on viral gene expression by quantitative real time PCR:

The effect of peptides treatment on the viral gene expression was determined by the qPCR. The level of RV L gene (RNA dependent RNA polymerase, RdRP) expression in the infected N2A was used in the experiments.

Standard curve for Real time PCR

For copy number determination, partial L gene segment of 184bp was amplified by conventional PCR. The result of specific amplification is depicted in figure 4.24. The PCR product was gel purified and the amount of DNA was quantified. Based on the amount of specific DNA, the numbers of template copies were calculated. The serial 10 fold dilutions of the template copies were included in the quantitative real time PCR for determining the respective threshold (Ct) values.

The results of the qPCR are depicted in the table 4.4. The same was used to derive bivariate fit of Ct value against copy numbers. The result of the standard curve generated is depicted in the figure 4.25.

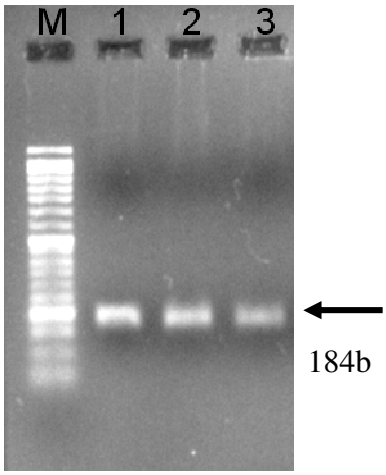

Figure 4.24: Amplification and Gel purification of rabies polymerase (L) partial gene fragment (184bp).

Amount (ng)	Log copy no	Ct value	Mean Ct
1ng	9	8.22	8.41
1ng	9	8.44	
1ng	9	8.57	
0.1ng	8	12.0	12.16
0.1ng	8	12.13	
0.1ng	8	12.37	
0.01ng	7	15.44	15.54
0.01ng	7	15.69	
0.01ng	7	15.49	
0.001ng	6	18.83	18.86
0.001ng	6	18.91	
0.001ng	6	18.85	
0.0001ng	5	21.65	21.86
0.0001ng	5	22.04	
0.0001ng	5	21.9	
0.00001ng	4	23.96	23.58
0.00001ng	4	23.91	
0.00001ng	4	22.87	

Table 4.4: Standard curve Results of qPCR (Ct values)

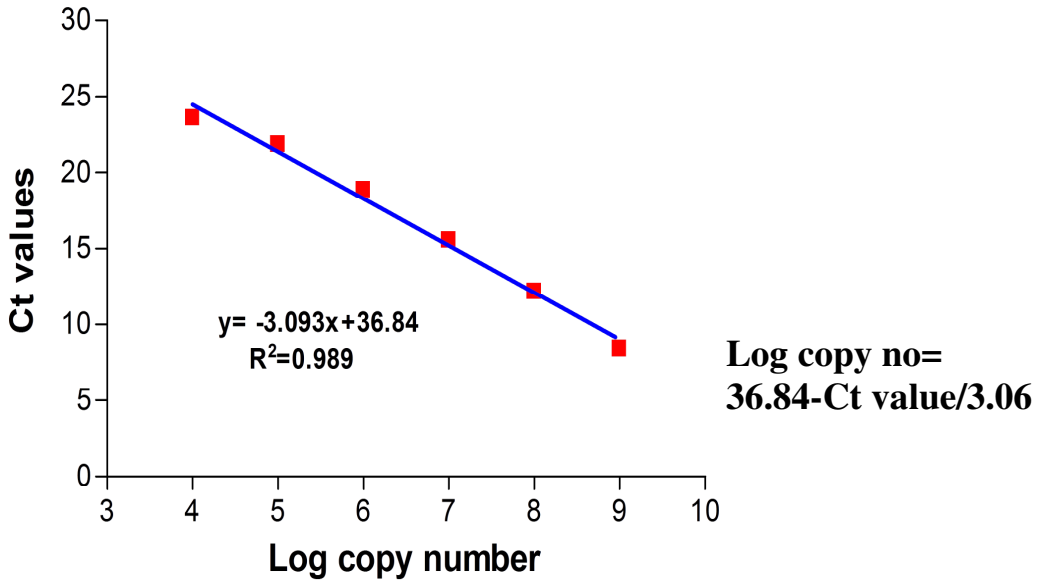

Figure 4.25: Standard curve for RV L gene copy number using quantitative real time PCR. Equations to calculate viral gene copy number.

The optimum correlation was observed between the log copy numbers to the Ct values with R^2 value 0.989. Based on the results of the standard curve, the equations for calculation of viral copy numbers in experimental group and control group was derived. The equations are depicted in the figure 4.25.

Effect of peptides on viral gene expression:

For viral gene expression studies, N2A cells grown in 24 well culture plate infected with 0.5moi of RV after treatment with different peptides (25µM each). Viral RNA was isolated and cDNA synthesized from each group including mock infected and control wells (No peptide). Viral copy number of treated and untreated cells was determined based on the standard curve equations. Percent viral inhibition was calculated using control well values. The results of viral gene expression are depicted in figure 4.26. The results showed decrease in the viral gene expression in the peptide treated virus group compared to the control. The T-32 peptide treated cells showed 55.89% of reduced gene expression in terms of viral inhibition. The C-32 peptide treated groups indicated viral inhibition up to 35.13%. The human origin (H-32) peptide could not significantly inhibit viral gene expression. Similarly T-20 peptide had comparatively higher effect on viral gene expression. It inhibited the virus to the extent of 40.30% where as the C-20 peptide reduced the viral infection by 25.13%. The R-14 peptide showed less effect on the viral gene expression (5%) compared to other peptides.

4.16 Determination of virus attachment on host cells:

Virus attachment to the neuronal cells was studied using virus adsorption ELISA. Different concentrations of the peptides were mixed with the virus (moi 6) and incubated for 1hr at 37^{o}C followed by infection on cell monolayer. The adsorbed virus was probed using primary and secondary antibodies. The results indicated that the peptide at higher concentration were able to inhibit the adsorption of the virus to the N2A cells (Figure 4.27). Without peptides virus adsorption was highest where as it decreased as the peptide concentration was increased. At 100µM concentration of the peptide, the adsorption was least. These results further indicates that peptides may be interfering the attachment of the virus on the neuronal entry hence prevent the viral infection in the cultured cells.

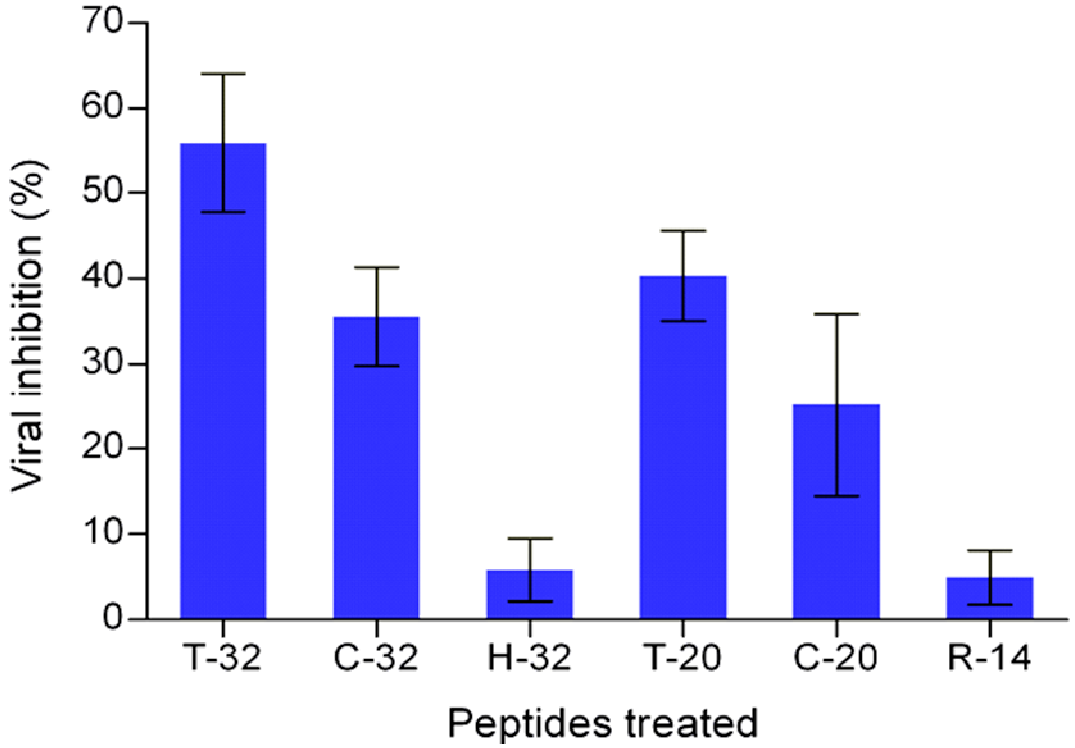

Figure 4.26: Inhibition of RV infection in N2A cells by nAChRα-subunit peptides and reduction in viral gene expression determined by quantitative real time PCR.

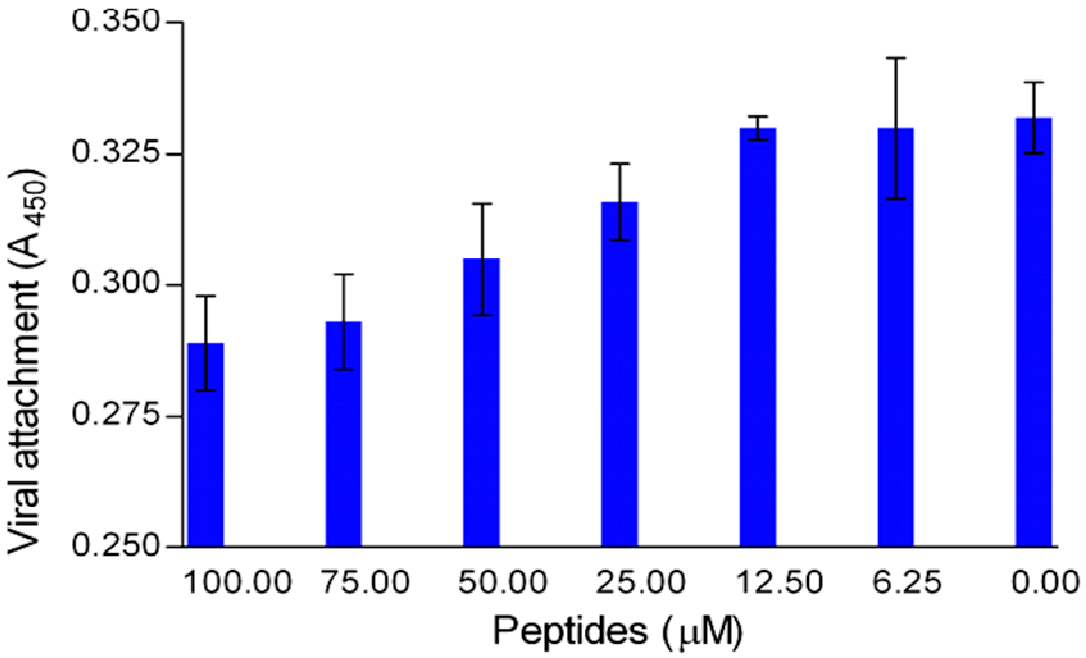

Figure 4.27: Peptide mediated inhibition of virus adsorption on N2A cells. Chilled N2A cells were adsorbed with CVS18 previously treated with increasing concentration of T-32 peptide. Cell associated virus was detected with indirect ELISA. The values represent mean ± SEM for triplicates and representative of two independent experiments.

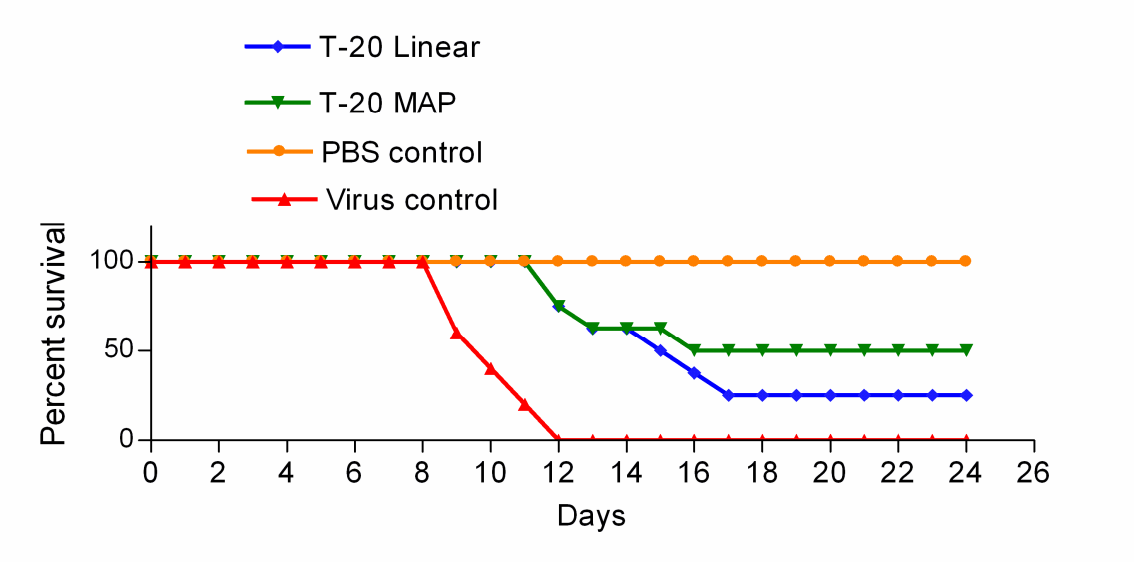

Figure 4.28: Evaluation of anti-RV effect ofT-20 linear and T-20 MAP format peptides by mice inoculation test.

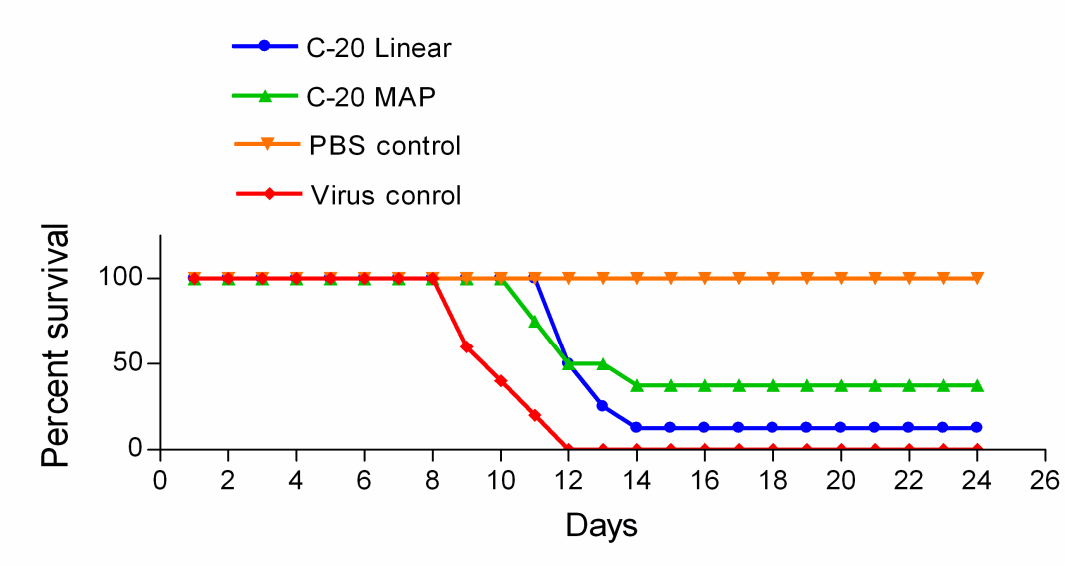

Figure 4.29: Evaluation of anti-RV effect of C-20 linear and C-20MAP format peptides by mice inoculation test.

4.17 *In vivo* efficacy of peptides against RV infection in mice:

Based on the results of the *in vitro* experiments, multiple antigenic peptide (MAP) format of T-20 and C-20 peptides were synthesized for *in vivo* experiments. 100μM of each of the linear and MAP format peptides were mixed with $100LD_{50}$ of the virus incubated for 1hr at 37°C and inoculated intra-cerebrally in 2-3 week old mice. Positive control (untreated virus) and negative control (PBS without virus) included. The results of the *in vivo* studies were recorded in terms of percent survivability on daily basis up to 28days. The results were represented in the form of survivability graph and depicted in figure 4.28 & 4.29. In the positive control, clinical signs started appearing on 7^{th}day and animals showed ruffled feathers, changed gait. Between 9^{th} and 10^{th} day, affected animals showed in-coordination, recumbancy, paralysis and deaths were observed. In treatment group, the affected animals also showed similar signs. In the positive control, all the animals were dead by the 12^{th} day after inoculations. In most of the peptide treated groups, there was a delay of two days in the appearance of clinical signs. This indicates peptides were successful in preventing some of the inoculated viruses from infecting the cells.

Among the different peptide treated groups, T-20 MAP format group had highest survival effect. In this group 50% animals were remained alive even after 28 days of observation. Similarly C-20 MAP treated group was also found effective in protecting the mice but there was lesser survival rate (37.5%) compared to the T-20 MAP. Compared to the MAP formats, the linear versions of these peptides showed lesser effect in preventing viral infection in the mice. In the T-20 linear peptide treated group, clinical signs appeared earlier than its MAP format treated group. At the end of observation period (28 days), T-20 linear peptide treated group indicated the survival rate of 25%. Similarly C-20 linear peptide treated group showed lesser survival rate (12.5%) compared to its MAP format. MAP formats are the branched peptides having higher avidity than their linear counterparts.

The results of the *in vivo* mice inoculation tests indicated that the nAchRα subunit of torpedo and calf origin peptides inhibited intra-cerebrally injected RV infection. It was also found that the branched MAP format peptides had higher inhibitory survival effect in virus infected mice compared to the linear versions of RV receptor peptides.

5 Discussion

In the present study, the nAChRα-subunit peptides were tested for their effect on the RV infection by both *in vitro* N2A cells and mice inoculation test. The peptide sequences were selected from different species; torpedo (electric ray fish), bovine, human and rat. The peptides were synthesized using solid phase peptide synthesis chemistry using Rink amide MBHA resins. The synthesized peptides were subjected semi-preparative RP-HPLC and characterized with the help of analytical RP-HPLC and MALDI-TOF. The results confirmed the purity and the observed mass were similar to the theoretical M.wts of the peptides.

Initially the peptides were characterized for their interaction with the RV using virus capture ELISA. The results indicated binding of nAChRα-subunit peptides with RV. T-20 interacted with RV strongly compared to other peptides. In another method to confirm the interactions, 32mer nAChRα-subunit peptides were FITC labeled and used to stain RV infected cells. The fluorescent images indicated the binding of peptides on the surface of infected cells.

Earlier peptides binding to the whole viruses or viral proteins were analyzed using different immunoassay methods. The anti-influenza peptides were found to interact with HA protein of the virus as determined by the ELISA, where the peptide coated wells were probed for binding to the viral HA protein (Jones *et al*., 2006). Similarly, in a study on antiviral peptide against dengue virus, Rothan et al (2014) had used a method to determine binding affinity of Ltc1 to dengue NS2B-NS3pro. They had used fluorescent labeled peptides for binding to the coated virus. The fluorescence spectrophotometer readings had confirmed the binding of the peptides to the viral proteins.

The antiviral peptides against West Nile Virus (WNV) identified with the help of random peptide phage display library were analyzed for their binding to the virus envelope protein using a biosensor surface plasmon resonance (SPR) assay. These peptides were found to interact with viral surface protein (Bai *et al*., 2007). In our experiments, the nAChRα-subunit peptides were able to interact with RV in both virus capture ELISA and peptide immunofluorescense tests. For the first time Lentz (1990) had given the evidence of purified torpedo nAChRα-subunits interacting with the labeled RV. Later in a solid phase radioassay, torpedo AChRα-subunit peptide was found to interact with RV (Gastka *et al*., 1996). The results in the present study also clearly indicated the binding of peptides from different species including torpedo, bovine, human and rat. Additionally it was also found that among the peptides studied, torpedo (T -20) sequence had highest binding affinity compared to other sequences.

The strong binding of T-20 peptide to RV was utilized to develop novel method of RV detection based on the nanoparticles. In the recent years nanotechnology, with the application of metallic nanoparticles has expedited the diagnostic procedures with improved sensitivity and specificity. Size, shape and inter-particle distance governs plasmon resonance of nanoparticles. Hence, by changing the inter-particle distance, the plasmon resonance of metallic nanoparticles can be tuned across the visible spectrum into near–infrared (West and Halas 2000; Jin *et al*., 2001). This makes multicolor assay possible with single source even under white-light illumination without need for filters.

Among the known metallic nanoparticles, gold nanoparticles (AuNP) are preferred most for designing theronostics, because of facile synthesis and versatile activation with proteins, nucleic acids, carbohydrates and drugs. Interactions between the target analyte and activated AuNP results in specific visible plasmon change and has been well adopted for various detection schemes including heavy metals, cells, polynucleotides and bacteriophages (Darbha *et al*., 2008; Medley *et al*., 2008; Joshi *et al*., 2013; Lesniewski *et al*., 2014). In the present study, the RV binding peptide sequence (T-20) were synthesized in the branched format using cysteine core and lysine mosaic as multiple antigenic peptides (MAPs).

The cysteine at the core with sulfahydryl (SH) group enables strong gold-sulfar interaction for proper functionalization without affecting much of the native structure of the peptides. The peptide MAP decorated AuNP were analyzed using UV-Vis spectrophotometer showing red shift in the spectra which confirmed the conjugation process. It is well known that AuNPs are popularly functionalized with strong sulfur-gold interface for wide ranging applications including site-specific bioconjugate labeling, drug delivery and medical therapy (Häkkinen, 2012).

In a colorimetric test for visual detection of the RV, the surface glycoproteins of RV may bind to the individual AuNP via the conjugated MAP sequences. The interaction between each virus particles with large number of AuNP will reduce the distance between individual AuNP turning original brick red color of AuNP to purple color. In the present visual viral detection assay, addition of RV to AuNP-MAPs solution resulted in change of original brick red to purple/blue color which indicated the presence of viral particles in the solution.

Different concentrations of virus (v%) were added to the AuNP-MAP conjugates, which showed incremental visual Plasmon change. For spectroscopic detection, absorption spectra (400-700nm) were recorded after the addition of RV suspension to 1nM peptide-AuNP. Spectra changes after addition of the virus, indicated the aggregation of AuNPs. The OD at 610nm increases while that at OD at 520nm decreases over time. The increased absorbance at 610nm indicates that AuNP aggregates have formed, thus decreasing the population of single AuNPs as they are converted into AuNP aggregate on the viral particle surface. These characteristic observations were found in other studies where specific analyte-target interactions involved functionalized AuNP. For example Lee et al (2013) observed similar characteristic color change in detection of influenza virus using sialic acid stabilized AuNP. This method of visual plasmon changes were also formed the basis for the detection of T7 bacteriophages developed by Lesniewski et al (2014).

Virus infections can be inhibited by interference to any of the steps in productive virus life cycle. Attachment and entry into the host cells is the first and critical step for establishing virus infection. Blocking this first step in the virus life cycle is a well known strategy of overcoming viral diseases. Targeting cell entry of enveloped viruses as an antiviral method is recently reviewed (Teissier *et al*., 2011).

The virus binding peptides may compete along with native host receptor for interacting with the virus (Lentz, 1990). For example, in CD4 receptor based therapies for HIV, soluble CD4 (sCD4) or recombinant truncated CD4 (rsCD4) tested to compete with the binding of the virus to CD4 at the cell surface. It was found that both of these molecules were able to efficiently block the infection of human cells by the laboratory strains of HIV *in vitro* (Daar *et al*., 1990). Further, truncated CD4 virus binding domain inhibited HIV infection in chimpanzee (Ward *et al*., 1991).

In the present study, receptor (nAChRα-subunit) peptides were evaluated against RV infection in N2A cells. Before *in vitro* tests in N2A cells, the peptide cytotoxicity was determined using MTT assay. In the presence of increasing concentration of peptides, reduction of MTT dye by mitochondrial dehydrogenases indicated the metabolic activity of the cells. Based on the specific absorbance, the degree of cytotoxicity in terms of percent survivability indicated that the tested peptides had less cytotoxicity even at higher concentrations. The CC_{50} values for these peptides were found to be more than 100µM. MTT dye reduction based methods were earlier used for evaluating the cytotoxicity of peptides. In the previous study on antiviral peptides against influenza virus H9N2, peptides were analyzed for cytotoxicity using MTT assay. It was found that the peptides showed no significant cytotoxicity at the concentration of 100µM (Rajik *et al*., 2009). Similarly phage display derived peptides against porcine reproductive and respiratory syndrome virus (PRRSV) were studied for cytotoxicity in MARC-145 cells. Peptides were used in increasing concentration from 1µM to 500µM to determine CC_{50} values which was more than 500µM (Liu *et al*., 2012). The peptides used in the present study were derived from the host cell receptors that are native domains of nAChRα-subunits present in the neuronal cells hence may probably show comparatively low cytotoxicity with higher CC_{50} values.

Earlier it was found that nAChR as one of the receptor molecules for the RV (Lentz *et al*., 1982). The same findings were confirmed by anti-idiotypic network study that nAChR acts as receptor for RV (Hanham *et al*., 1993). Later other two potential receptors; Neuronal Cell Adhesion Molecule-1 (NCAM-1) and and low- affinity p75 neurotropin receptor ($p75^{NTR}$) were identified (Etessami *et al*., 2000; Lafon, 2005; Tuffereau *et al*., 2007). However, mice in which the gene that encodes NCAM-1 was deleted were still susceptible to infection with the virus, although the disease was delayed. This indicated that although the receptor might not be essential for infection, it has a role in the infection process. The function of p75NTR is also less clear indicating the mystery of RV entry receptors (Schnell *et al*., 2010).

nAChRs are a critical component of the brain's cholinergic neurotransmission system that modulates important physiological processes. nAChRs are a heterogeneous family of receptor subtypes consisting of pentameric combinations of α and β subunits, and these receptors are widely expressed in neuronal and non-neuronal tissues (Gotti & Clementi, 2004; Albuquerque et al., 2009). The domain sequences of the nAChR protein particularly involved in interacting with the RV was identified as α subunit (Lentz, 1990). Further with the help of virus overlay protein binding assay (VOPBA), it was shown that radio-labeled (^{125}I) RV was bound to 40kDa purified α subunit of nAChR protein (Gastka *et al*., 1996).

Mouse neuroblastoma cells (N2A) with neurotic processes were used in the present study. N2A cells were originated from post ganglionic symphathetic neuroblasts of embryonic neuronal crest. These cells express most of the neuronal and neuroendocrine properties including neurofilaments, muscarinic and nichotinic types (Thiele, 1998). The unique neurotropism of the RV and its ability to move towardscentral nervous system ultimately reaching the brain indicates the role of virus receptors and binding molecules which are widely distributed in the mammalian body system.

Binding of the RV to nAChRα-subunit occurs via its glycoprotein. RV glycoprotein resembles neurotoxins like α-bungarotoxin (Btx) and king cobra toxins (Kcx). The segment of the virus glycoprotein (residues 175-203) bears a structural similarity to loop 2 of the neurotoxins (Lentz *et al*., 1984, 1988). These neurotoxins also bind to the same region of α-subunit nAChR. Hence monoclonal antibodies raised against a rabies glycoprotein peptide (residues 190-203) inhibited binding of RV glycoprotein and α-Btx to the nAChR (Bracci *et al*., 1988).

The modeling of RV glycoprotein indicated that a tetra peptide (Asn194-Ser195-Arg196-Gly197) as a essential part of the binding site of the RV glycoprotein (RVG), indicated that the side chains of Asn and Arg could also mimic the acetylcholine structure. Hence RVG binds similar to acetyl choline at nAChR (Rustici et al., 1993). These findings predicted that the synthetic α-subunit peptides of nAChR may inhibit binding of the RV to the native AChR present on the host cells.

Results of our study revealed that α-subunit peptides of nAChR of different species were able to inhibit RV infection in N2A cells. The T-32 and C-32 peptides were considerably more effective than the H-32 peptides. Sequence comparison between these three different species peptides (torpedo, bovine/calf and human) shows changes in 6 residues. Between T-32 and C-32 there are two non-conservative changes (Tyr-181 to Ser and Asp-195 to Ser) where as between T-32 and H-32 there are three non-conservative changes (Tyr-181 to Ser, Trp-187 to Ser, and Tyr-189 to Thr). In the human peptide, all the three changes involve the replacement of an aromatic residue with a polar residue. Considerably less affinity of the H-32 to RV observed in our study (ELISA and Immunofluorescence) indicates the importance of aromatic residues within these sequences.

In the antiviral experiments, there was a inhibition of RV multiplication in N2A cells. Among 32mer peptides T-32 and C-32 peptides had antiviral effect where as H-32 peptide did not show any inhibition even used at higher concentration (50μM). Similarly the T-20 and C-20 had shown inhibition of RV multiplication in N2A cells. However R-14 peptide was not effective against RV.

The results of the viral gene expression also showed similar trends showing decrease in the viral copy numbers in peptide treated groups. In the present study, the results of the virus adsorption tests showed that peptides inhibited the viral attachment to the neuronal cells. The inhibition of attachment and entry of the virus, a critical step was used in different studies to develop peptides against different viruses. A peptide derived from the signal sequence of the fibroblast growth factor was evaluated against vaccinia virus. This peptide blocked the entry of the virus into the host cells and had shown the antiviral effect with IC_{50} of 15µM in Hela cells (Altmann *et al*., 2009).

A cytokine protein mimetic peptide was found to have antiviral property against influenza virus. Different sequence analogues of these peptides are tested for inhibiting influenza infection. The virus adsorption ELISA indicated that the peptide blocked the attachment and entry of the virus into the host cells (Nicol *et al*., 2012). In a similar study an antimicrobial peptide, latarcin (Ltc1) was found significantly effective against dengue virus multiplication in mosquito cells (HepG2) (Rothan *et al*., 2014).

In a recent study on hepatitis C Virus (HCV), host cell receptor subunit peptide was used to inhibit the attachment and entry of the virus. HCV entry requires multiple host cell receptor molecules including the subunit of claudin 1 (CLD1). An 18–amino acid peptide that was derived from the CLDN1 intracellular and first transmembrane region inhibited both *de novo* and established HCV infection *in vitro* (Si *et al*., 2012).

Against RV there are no still therapeutic drugs and death can only be averted by prompt post-exposure prophylaxis (PEP). However, if PEP is delayed and clinical symptoms develop, the mortality rate is almost 100%. There are only countable cases reported to have survived after the onset of clinical disease (Nigg and Walker, 2009). In one such case, the patient had survived rabies encephalitis without PEP, after treatment including induction of coma and administration of an antiviral drug (Willoughby *et al*., 2005). This method when employed in other cases had shown only few successes (Hemachudha *et al*., 2013). Hence the efficacy of this method is still controversial.

To establish more stable and successful therapy, novel approaches based on specific anti-rabies agents are required. Peptides targeting replication of RV were identified which are derived from the amino terminal end of the RV phosphoprotein. These peptides were found to inhibit RV multiplication in both in BHK-21 and neuronal cells (Castel *et al*., 2009). In other study, antiviral peptides targeting the phosphoprotein (P) of the RV was recently shown to have reduced the virus multiplication in N2A cells. The mechanism of these peptides was to target polymerase complexes by binding to P protein and preventing replication of the viral genome (Real *et al*., 2004).

There are no reports of antiviral peptides against the rabies that inhibit the attachment and entry of the RV. However in one of the study, intracellular immunization using single-chain variable fragments (scFvs) against RABV phosphoprotein (RABV-P) had been tried. One of the scFV clone had highest transfection efficiency in neuronal cells and inhibited the RV titer 3 days after infection up to 98.6% and 99.9% (Kaku *et al*., 2011). Recently an alternative and novel approach of virus host protein-protein interaction screening was used to determine druggable antiviral targets. This approach had identified some of the compounds which are having antiviral effciancy against RV *in vitro* cell culture (Lingappa *et al*., 2013).

In our study, the *in vitro* effective peptides namely T-20 and C-20 were used both in linear and multivalent antigenic peptide (MAP)/ branched format of peptides for mice inoculation test. MAP format peptides are well defined molecules offering highly efficient means of presenting multiple ligands. With more binding elements they have greater avidity. For example a peptide mimotypes of nicotinic receptor inhibited α-bungarotoxin and neutralized its toxicity. However, when presented in tetra-arm branched format it had significantly higher protection in mice experiments (Bracci *et al*., 2002).

Earlier studies showed that branched multiple ligand molecules have higher inhibitory effect than the linear ligands with increased resistance to protease activity in *in vivo* (Pini *et al*., 2005). In another work, phage display cyclic nonamer peptides screening was done against Sin Nombre viruses (SNV, New World hantavirus that causes cardiopulmonary syndrome in human) to identify peptides that inhibited the entry of the viruses. The identified peptides in linear format had less antiviral effect compared to the branched format where their activity was increased (Hall *et al*., 2008).

6 Summary & Conclusions

Viruses are obligate intracellular parasites; they must bind and enter host cells to exploit cellular biosynthetic machinery required for their replication. Antivirals are the agents that obstruct one or more steps in the virus life cycle. Molecular details of virus host interactions may help to design and develop novel agents to fight viral infections in both humans and animals.

Rabies is the oldest and devastating disease and remains as a huge burden for the developing countries. In case of rabies infection death can only be averted by prompt post-exposure prophylaxis (PEP). However, if PEP is delayed and clinical symptoms develop, the mortality rate is almost 100%. Till now there are no therapeutic drugs against rabies. To establish more stable and successful therapy, novel approaches based on specific anti-rabies agents are required.

To produce infection, RV must bind to the specific host cell receptors. nAChR α subunits were identified as one of the such receptor molecules. These receptor proteins are richly distributed in post synaptic membranes as well as both in central and peripheral nervous system. The α-subunit peptides may act as receptor decoy molecules and prevent the entry and spread of the RV preventing the viral infection.

In the present study, nAChRα-subunit sequences from four different species (torpedo/electric ray fish, calf/bovine, human and rat) and two neurotoxin binding peptides were evaluated. Protparam algorithm under ExPASy platform was used to determine the physic-chemical properities of these peptides. The amino acid sequence variations among the receptor peptides and other attributes were recorded. The solid phase peptide synthesis protocol was employed to synthesize these peptides. The peptides were purified using semi-preparative RP-HPLC.

The purified peptides were characterized with analytical RP-HPLC and mass determination using MALDI-TOF. The results indicated the formation of desired specific peptides with the level purity required for further experiments. The secondary structures of the peptides were determined using CD-spectroscopy in aqueous and apolar environments using different concentration of TFE. It was found that the peptides had particular conformations within aqueous solutions. However the characteristic alpha helices were induced in higher TFE concentration mimicking the environment of membranes. Since these peptides are parts of the receptor on cell membranes, the apolar solution represents close to native environment.

In the present study mice brain adapted RV was initially propagated in the N2A cells. Serial blind passages were given with reduced inoculums at each passage. The observations at regular intervals revealed the absence of any cytopathic effects (CPE) in the infected flask compared to the mock infected flask. The virus multiplication was confirmed by direct immunofluorescence test using rabies anti-nucleocapisd conjugate staining. It was observed that at 24hpi, the virus was able to multiply and produce characteristic fluorescent foci. After 5^{th} passage, virus stock had a titer of $1X\ 10^5$ FFU/ml.

To determine interactions between peptides and RV, different tests were done. The results of the virus capture ELISA experiment indicated that the nAChRα-subunit peptides interact with RV. Different species origin nAChRα-subunit peptides were analyzed. It was found that torpedo origin peptides (T-32 & T-20) had higher interaction compared to calf (C-32 & C-20), human (H-32) and rat (R-14) peptides. Among all the peptides tested T-20 had better interaction with highest binding ability to RV.

The AChRα-subunit peptides were FITC labeled at the amino-terminal end after including the linker (6-Amino hexanoic acid) in their sequences. The FITC labeled peptides were evaluated for their binding to the RV infected N2A cells. The images under fluorescent microscope indicated the binding of peptides to the cluster of infected N2A cells. Some of the infected cells showed surface fluorescence after staining with the FITC labeled peptides indicating the interaction of the peptides with RV glycoprotein which is expressed on the infected host cell membranes.

AuNP-MAP conjugates were prepared for visual detection of the RV. T-20 peptide was synthesized in four arm MAP format with lysine mosaic and cysteine at c-terminal end. The MAP format was decorated on the citrate stabilized AuNP. The interaction of the AuNP-MAP with the RV reduced the distance individual AuNP leading to the change in Plasmon. This change was confirmed by the visual color change from brick red to purple/blue. The results of absorbance spectra indicated a decrease at 520nm and simultaneous increase at 610nm which is characteristic of specific interactions.

The cytotoxicity studies were done for the nAChR α-subunit peptides using MTT dye reduction assay in N2A cells. Increasing concentrations of the peptides were tested in the cells. The CC_{50} determination indicated that the tested peptides had relative less cytotoxicity in N2A cells with CC_{50} values more than 100µM.

Anti-RV effects of peptides were determined by using fluorescent focus inhibiton test (FFIT) *in vitro* N2A cells. There were less number of infected foci in the peptide treated group compared to the non-treated control group. These observations indicate that nAChRα-subunit peptides had anti-RV effect. Torpedo origin (T-32 and T-20) peptides and calf origin peptides (C-32 and C-20) had shown anti-RV effect. However human (H-32) and rat (R-14) origin peptides could not prevent the infection even at 50µM concentration. Based on the IC_{50} value determination, T-32 had higher antiviral effect compared to the C-32. Similarly the T-20 peptide had higher antiviral effect compared to the C-20 peptide.

The receptor subunit peptides also found to reduce viral gene expression in N2A cells. The L gene of RV was used to generate a standard curve for viral gene copy number using quantitative real time PCR. Based on the standard curve, the peptide treated RV infected in N2A cells showed decrease in viral gene copy number compared to the non treated group. The percent viral inhibition calculated with the results of viral copy number indicated that T-32 and T-20 peptides had higher viral inhibition compared to the C-32 and C-20 peptides. There was no significant reduction in the viral gene expression by human and rat origin (H-32 and R-14) receptor peptides.

Virus adsorption assay was done to determine the nAChRα-subunit peptide's likely mechanism of RV inhibition in N2A cells. Concentrated RV (moi 6) was incubated with the peptides followed by adsorption on chilled N2A cells at 4^{o}C. The results revealed that peptide treated group had reduced adsorption of the virus compared to the control group. At higher concentration increased inhibition was observed. These results confirmed that peptides act by preventing the attachment of virus on to the cells.

Mice inoculation test was used to determine the *in vivo* efficacy of nAChRα-subunit peptides against RV infection. The linear and MAP format peptides of T-20 and C-20 were selected for *in vivo* study based on results of the *in vitro* tests. The results of experiments indicated that the clinical signs in the affected mice appeared 1-2 days late in peptide treated groups compared to the non-treated control group. The delay in appearance of clinical signs is significant especially it may provide much needed winning time to the host to drive the immune response against RV. In the tested peptides, both linear and MAP formats of receptor peptides protected the infected mice. In the T-20 MAP treated group, 50% of the animals were survived where as the survival rate in C-20 MAP was 37.5%. Similarly in linear monovalent peptides, T-20 and C-20 had shown 25% and 12.5% protection respectively.

In conclusion, the results of the *in vivo* mice inoculation tests indicated that the nAchRα-subunit of torpedo and calf origin peptides(T-20 and C-20) inhibited intracerebrally injected RV infection. It was also found that the branched MAP formats had higher survival effect in virus infected mice compared to the linear monovalent peptides.

7 Mini Abstract

Rabies is a zoonotic disease and remains an important public health problem especially in developing countries. Upon onset of symptoms, the disease has nearly 100% case fatality rate and no effective therapeutics has been found previously. nAChR is one of the recognized receptor of RV. Receptor decoy molecules can be used to prevent the viral entry and hence may prevent the infection. In the present study, nAChR α subunit peptides of four different species (torpedo-electric ray fish, calf-bovine, human and rat) synthesized and analyzed with RP-HPLC, Mass spectroscopy and CD spectroscopy. The interaction of the receptor peptides with RV was studied with virus capture ELISA, immunofluorescence and by specific Plasmon changes in gold nanoparticles peptide conjugates. The results indicated that the receptor peptides specifically interact with the RV albeit with different binding efficiency. The torpedo peptide (T-32 &T-20) had highest efficiency of binding to the RV compared to the other peptides (C-32, C-20, H-32 & R-14). The RV (CVS-18) was propagated in mouse neuroblastoma (N2A) cells and it was found that RV did not produce any cytopathic changes during its multiplication. After the fifth passage, the titre of the virus was found $1X10^5$ FFU/ml. In the cytotoxicity tests, the peptides did not induce significant cell death even at higher concentration with CC_{50} values more than 100µM. In the fluorescent focus inhibition test (FFIT) in N2A cells, nAChRα-subunit peptides had shown antiviral properties. T-32 & T-20 peptides had higher antiviral effect followed by C-32 & C-20 peptides, where as H-32 and R-14 had no observable antiviral effects. These results were also corroborated by reduced expression of viral genes by the peptides treatment. Effective peptides selected from the *in vitro* tests were designed in multivalent MAP format and analyzed along with their linear monovalent counter parts in mice inoculation tests. The results indicated that the peptides delayed the appearance of clinical rabies in the infected mice by maximum two days and one of the peptide (T-20 MAP) protected up to 50% of infected animals. In conclusion, the present study shows that nAChRα-subunit sequences acted as receptor decoy and inhibited RV infection in both *in vitro* and *in vivo* experiments.

४ लघु सारांश

रेबीज एक जनोटिक बीमारी है और विषेश रूप से विकासषील देषों में एक महत्वपूर्ण सार्वजनिक स्वास्थ्य समस्या बनी हुई है। लक्षणों के प्रकट होने पर यह रोग पूर्णरूप से घातक हो जाता है। और मृत्यु निश्ष्ति है और इस रोग की रोकथाम व निदान हेतु अभी तक कोई भी प्रभावषाली औशधी उपलब्ध नहीं है। nAChR अणु रेबीज वायरस का प्रमाणित रिसेप्टर है। रिसेप्टर मिमिक (कृतिम) अणु वायरस के कोषिका में प्रवेष पर रोक लगा सकता है और इनफैक्षन को अवरुद्ध कर सकता है इस षोध कार्य में nAChR रिसेप्टर मालूक्यूल के, जो चार विभिन्न प्रजातियों–तारपीडो मछली, पषु, मानव व चूहा में पाये जाते है, के पैप्टाइड लैब में बताये गये और उनका परीक्षण व चरित्र विष्लेशण रिवर्स–फेज–एच पीएलसी एवं डी स्पैक्ट्रोस्कोपी से किया गया।

रिसेप्टर पैपटाइड तथा रैबीज वाइरस की परस्पर क्रिया का अध्ययन कैप्चर एलिजा, इम्यूनोफ्लोरीसेन्स व स्वर्णकणों के पेप्टाइड सयुग्मों के प्ला. जमान–कलर के परिवर्तन के आधार पर किया गया। टारपीडो पैप्टाइड T-32 व T-20 की कार्य की कार्य कुषलता अन्य पैप्टाइड C-32, C-20, H-32 व R-14 की तुलना में अधि ाक पायी गयी। रैबीज वायरस चूहा की न्यूरोब्लासटामा में प्रसारित गया तो रैबीज वायरस ने कोई भी कोषिका विकृति उत्पन्न नहीं की। पांचवें पसाज के बाद वायरस का टाइटर $1x10^5$ FFU/ml पाया गया। कोषिका विकृति के परीक्षण में पैप्टाइड नें 100 से अधिक मात्रा पर भी कोषिका मृत्यु को प्रेरित नहीं किया। nAChR अल्फा सबयूनिट पैप्टाइड की फलोरोसेन्स इनहिबिसन टैस्ट परीक्षण में वायरस प्रतिरोधी क्षमता पायी गयी। T-32 व T-20 पैप्टाइड में वायरस प्रतिरोधी क्षमता अधिक पायी गयी, सर्थक H-32 व R-14 को कोई भी वायरस प्रतिरोधी क्षमता नहीं पायी गयी। इन सभी परिणामों को पैप्टाइड उपचार से रिडयूस्ट एक्सप्रेषन के द्वारा स्थापित किया गया। प्रभाव कारी पैप्टाइड की मल्टीवैलेंट प्रारुप में डिजाइन किये गये और उनका परीक्षण माइस इनोकुलेषन टैस्ट में, लीनियर पैप्टाइड के साथ किया गया। परिणामों में पैप्टाइड के प्रयोग से रैबीज के लक्षणों के प्रकट होने में दो दिन की देरी पायी गयी और पैप्टाइड T-20 मैप ने सर्वाधिक 50% तक सुरक्षा बीमार चूहा में प्रदान की।

अन्ततः समग्र रुप से, इस अध्ययन ने nAChR पैप्टाइड ने एक रिसेप्टर (कृत्रिम रिसेप्लर) की तरफ कार्य किया और इन विट्रो तथा इन वायवो परीक्षणों में रैबीज वायरस के निशेध का प्रभावी कार्य किया है।

References

Albuquerque, E.X., Pereira, E.F., Alkondon, M. and Rogers, S.W. 2009. Mammalian nicotinic acetylcholine receptors: from structure to function. Physiol Rev. **89 (1)**:73-120.

Altmann, S. E., Jones, J. C., Schultz-Cherry, S. and Brandt, C. R. 2009. Inhibition of Vaccinia virus entry by a broad spectrum antiviral peptide. Virology. **388(2**): 248 -59

Baer, G. M. 2007. Rabies (eds Jackson AC & Wunner WH), Elsevier, London. 1–22

Bai, F., Town, T., Pradhan, D., Cox, J., Ashish, Ledizet, M., Anderson, J. F., Flavell, R. A., Krueger, J. K., Koski, R. A. and Fikrig, E. 2007. Antiviral peptides targeting the west nile virus envelope protein. J Virol. **81(4)**: 2047-2055.

Bo-Jian, Z., Yi, G., Ming-Liang, H., Hongzhe, S., Lanying, D., Ying, Z., Kin-Ling, W., Honglin, C., Ying, C., Linyu, L., Julian, A. T., Rory, M. W., Neri, N., Andrea, B., Ottavia, S., Patrick, C.Y., Hsiang-fu, K., Kwok-Yung, Y. and Jian-Dong H. 2005. Synthetic peptides outside the spike protein heptad repeat regions as potent inhibitors of SARS-associated coronavirus. Antiviral Therapy.**10**: 393–403

Bracci, L., Antoni, G., Cusi, M.G., Lozzi, L., Niccolai, N., Petreni, S., Rustici, M., Santucci, A., Soldani, P., Valensin, P.E. and Neri, P. 1988. Antipeptide monoclonal antibodies inhibit the binding of rabies virus glycoprotein and a- bungarotoxin to the nicotinic acetylcholine receptor. Mol. Immunol. **25**: 881 -888

Bracci, L., Lozzi, L., Pini, A., Lelli, B., Falciani, C., Niccolai, N., Bernini, A., Spreafico, A., Soldani, P. and Neri, P. A. 2002. Branched peptide mimotope of the nicotinic receptor binding site is a potent synthetic antidote against the snake neurotoxin alpha-bungarotoxin. Biochemistry. **41(32)**:10194-10199.

Bridge, T. P., Heseltine, P. N. R., Parker. E. S., Eaton E, Ingraham LJ, Gill M, Ruff, M., R and Pert, C. B. 1989. Improvement in AIDS patients on peptide T. Lancet. **2**: 226-227

Brochier, B., Kieny, M.P., Costy, F., Coppens, P., Bauduin, B., Lecocq, J.P., Languet, B., Chappuis, G., Desmettre, P. and Afiademanyo, K. 1991. Large scale eradication of rabies using recombinant vaccinia-rabies vaccine. Nature. **354**: 520-522.

Byrn, R. A., Mordenti, J., Lucas, C., Smith, D., Marsters, A., Johnson, J. S., Cossum, P., Chamow, S. M., Wurm, F. M., Gregory, M., Groopman, J. E. and Capon, D. J., 1990. Biological properties of a CD4 immunoadhesin. Nature. **344**: 667–670.

Capon, D. J., Chamow, S. M., Mordenti, J., Marsters, S. A., Gregory, T., Mitsuya, H., Byrn, R. A., Lucas, C., Wurm, F. M., Groopman, J. E. and Smith, D. H. 1989. Designing CD4 immunoadhesions for AIDS therapy. Nature. **337**: 525–531.

Castel, G., Chtéoui, M., Caignard, G., Préhaud, C., Méhouas, S., Réal, E., Jallet, C., Jacob, Y., Ruigrok, R. W. and Tordo, N. 2009. Peptides that mimic the amino-terminal end of the rabies virus phosphoprotein have antiviral activity. J Virol. **83** (**20**): 10808-10820.

Chan, D. C. and Kim, P. S. 1998. HIV entry and its inhibition. Cell. **93**: 681-684.

Chang, K. Y. and Yang, J. R. 2013. Analysis and prediction of highly effective antiviral peptides based on random forests. PLoS One.**5(8)**:e70166.

Chao, B. H., Costopoulos, D. S., Curie, T., Bertonis, J. M, Chisholm, P., Williams, C., Schooley, R. T., Rosa, J. J., Fisher, R. A. and Maraganore, J. M. 1989. A 113-amino acid fragment of CD4 produced in *E. coli* blocks human immunodeficiency virus- induced cell fusion. *J*. Biol.Chem. **264**: 5812-5817.

Cleaveland, S., Fevre, E. M., Kaare, M. and Coleman, P. G. 2002 Estimating human rabies mortality in the United Republic of Tanzania from dog bites injuries. Bull; World Health Organ. **80**: 304–310.

Cliquet, F. and Picard-Meyer, E. 2004. Rabies and rabies-related viruses: a modern perspective on an ancient disease. Rev Sci Tech. **23(2)**: 625-642.

Co, I. S., Gaulton, G. N., Tominaga, A., Homcy, C. J., Fields, B. N. and Greene, M. I. 1985. Structural similarities between the mammalian fl-adrenergic and reovirus type 3 receptors. PNAS. **82**: 5315-5318.

Conzelmann, K. K., Cox, J. H., Schneider, L. G. and Thiel, H. J 1990. Molecular cloning and complete nucleotide sequence of the attenuated rabies virus SAD B19. Virology. **175**: 485–499.

Daar, E. S., Li, X. L., Moudgil, T. and Ho, D. D. 1990. High concentrations of recombinant soluble CD4 are required to neutralize primary HIV1 isolates. Proc. Natl. Acad. Sci. **87**: 6574–6578.

Darbha, G. K., Singh, A. K., Rai, U. S., Yu, E., Yu, H. and Chandra Ray, P. 2008. Selective Detection of Mercury (II) Ion Using Nonlinear Optical Properties of Gold Nanoparticles. J Am Chem Soc. **130(25)**:8038-8043.

de Haan, C. A., Li, Z., te Lintelo, E., Bosch, B. J., Haijema, B. J. and Rottier, P. J. 2005. Murine coronavirus with an extended host range uses heparan sulfate as an entry receptor. J Virol. **79(22)**:14451-14456.

Dietzschold, B., Wiktor, T.J., Trojanowski, J. Q., Macfarlan, R. I., Wunner, W. H., Torres-Anjel, M. J. and Koprowsk, H. 1985. Differences in cell-to-cell spread of pathogenic and apathogenic rabies virus *in vivo* and *in vitro.* J Virol. **56(1)**:12–18.

Do-Hyoung, K., Yi, N., Si-Hyung, L., Stephan, U. and Kyou-Hoon, H. 2008. An antiviral peptide derived from the preS1 surface protein of hepatitis B virus. BMB reports. **41(9)**: 640-644.

Donalisio, M., Rusnati, M., Civra, A., Bugatti, A., Allemand, D., Pirri, G., Giuliani, A., Landolfo, S. and Lembo, D. 2010. Identification of a dendrimeric heparan sulfate-binding peptide that inhibits infectivity of genital types of human papillomaviruses. Antimicrob Agents Chemother. **54(10)**: 4290-4299.

Ele´onore, R., Jean-Christophe, R., Ve´ronique, B., Corinne, J., Pierre, P., Noe¨l, T., Peggy, C., Jacques, D., Pierre, L. and Yves, J. (2004). Antiviral drug discovery strategy using combinatorial libraries of structurally constrained peptides J. Virol, **78**: 7410-7417.

Engelke, M., Mills, K., Seitz, S., Simon, P., Gripon, P., Schnolzer, M. and Urban, S. 2006. Characterization of a hepatitis B and hepatitis delta virus receptor binding site. Hepatology. **43**: 750-760.

Eppstein, D.A., Marsh, Y.V., Schreiber, A.B., Newman, S. R., Todaro, G. J. and Nestor, J. J. 1985. Epidermal growth factor receptor occupancy inhibits vaccinia virus infection. Nature. **318**: 663-665

Erik, D. C. 2002. Strategies in the design of antiviral drugs. Nat Revi Drug Dis. **1**: 13-25

Etessami, R., Conzelmann. K. K., Fadai-Ghotbi, B., Natelson, B., Tsiang, H. and Ceccaldi, P. E. 2000. Spread and pathogenic characteristics of a G-deficient rabies virus recombinant: an *in vitro* and *in vivo* study. J. Gen. Virol. **81**: 2147–2153.

Expasy, ViralZone, *Cell receptor*, http://expasy.org/viralzone/all_by_protein/233.html.

Fengwei, B., Terrence, T., Deepti, P., Jonathan, C., Ashish., Michel, L., John, F. A, Richard, A. F., Joanna, K. K., Raymond, A. K. and Erol, F. 2007. Antiviral peptides targeting the West Nile Virus envelope protein. J.Virol. **81**: 2047-2055.

Gastka, M., Horvath, J. and Lentz, T. L. 1996. Rabies virus binding to the nicotinic acetylcholine receptor alpha subunit demonstrated by virus overlay protein binding assay. J Gen Virol. **77 (10)**: 2437-2440.

Gaudin, Y., Ruigrok, R. W., Tuffereau, C., Knossow, M. and Flamand, A. 1992. Rabies virus glycoprotein is a trimer. Virology. **187**: 627–632.

Gotti, C. and Clementi, F. 2004. Neuronal nicotinic receptors: from structure to pathology. Prog Neurobiol. **74(6)**: 363-396.

Greber, U. F. 2002. Signalling in viral entry. Cell Mol Life Sci. **59**: 608–626.

Greve, J. M., Davis, G., Meyer, A. M., Forte, C. P., Yost, S. C., Marlor, C. W., Kamarck M. E., McClelland, A. 1986. The major human rhinovirus receptor is ICAM-1. Cell. **56(5)**: 839-847.

Grove, J. and Marsh, M. 2011. The cell biology of receptor-mediated virus entry. J Cell Biol. **195(7)**:1071-1082.

Häkkinen, H. 2012. The gold-sulfur interface at the nanoscale. Nat Chem. **4(6)**:443-455.

Hall, P. R., Hjelle, B., Brown, D. C., Ye, C., Bondu-Hawkins, V., Kilpatrick, K. A. and Larson, R. S. 2008. Multivalent presentation of antihantavirus peptides on nanoparticles enhances infection blockade. Antimicrob Agents Chemother. **52 (6)**:2079-2088.

Hamzeh-Mivehroud, M., Alizadeh, A. A., Morris, M. B., Church, W.B. and Dastmalchi, S. 2013. Phage display as technology to deliver on the promise of peptide drug discovery. Drug Discov.Today. **18**: 1144-1157

Hanham, C. A., Zhao, F. and Tignor, G. H. 1993. Evidence from the anti-idiotypic network that the acetylcholine receptor is a rabies virus receptor. J Virol. **67(1)**:530-542.

Haywood, A. M. 1994. Virus receptors: binding, adhesion strengthening, and changes in viral structure. J. Virol. **68**, 1–5.

Hemachudha, T. and Mitrabhakdi. 2000. E. Rabies. In: Davis LE, Kennedy PGE, eds. Infectious diseases of the nervous system. Oxford: Butterworth & Heinemann, :401–444.

Hemachudha, T., Ugolini, G., Wacharapluesadee, S., Sungkarat, W., Shuangshoti, S. and Laothamatas. J. 2013. Human rabies: neuropathogenesis, diagnosis, and management. Lancet Neurol. **12(5)**: 498-513.

Huang, J.X., Bishop, H.S.L. and Cooper, M. H. 2012. Development of anti-infectives using phage display– biological agents against bacteria, viruses and parasites. Antimicrobial. Agents Chemo. **56**: 4569-4582.

Jacob, Y., Badrane, H., Ceccaldi, P. E. and Tordo, N. 2000. Cytoplasmic dynein LC8 interacts with lyssavirus phosphoprotein. J. Virol. **74**: 10217–10222.

Jameson, B. A., Rao, P. E., Kong,L. I., Hahn, B. H., Shaw, G. M., Hood, L. E. and Kent, S. B. 1988. Location and chemical synthesis of a binding site for HIV-1 on the CD4 protein. Science. **82**: 7053-7057.

Jeremy, C. J., Elizabeth, A. T., Hermann, B., Curtis, R. B. and Stacey, S.C. 2006. Inhibition of influenza virus Infection by a novel antiviral peptide that targets viral attachment to cells. J.Virol. **81**: 11960–11967.

Jin, R., Cao, Y., Mirkin, C. A., Kelly, K.L., Schatz, G. C. and Zheng, J. G. 2001. Photoinduced conversion of silver nanospheres to nanoprisms. Science. **294 (5548)**:1901-1903.

Jolly, C. L. and Sattentau, Q. J. 2011. Attachment factors: in Viral Entry into Host Cells edited by Stefan Pöhlmann and Graham Simmons. Landes Bioscience and Springer Science, 1-23.

Jones, J. C., Turpin, E. A., Bultmann, H., Brandt, C. R. and Schultz-Cherry, S. 2006. Inhibition of influenza virus infection by a novel antiviral peptide that targets viral attachment to cells. J Virol. **80(24)**:11960-11967.

Joshi, V. G., Chindera, K., Singh, A. K., Sahoo, A. P., Dighe, V. D., Thakuria, D., Tiwari, A. K. and Kumar, S. 2013. Rapid label-free visual assay for the detection and quantification of viral RNA using peptide nucleic acid (PNA) and gold nanoparticles (AuNPs). Anal Chim Acta. **795**:1-7.

Kaku, Y., Noguchi, A., Hotta, K., Yamada, A. and Inoue, S. 2011. Inhibition of rabies virus propagation in mouse neuroblastoma cells by an intrabody against the viral phosphoprotein. Antiviral Res. **91(1)**: 64-71.

Kalia, M. and Jameel, S. 2011.Virus entry paradigms. Amino Acids. **41(5)**:1147-1157.

Kelly, R. M. and Strick, P. L. 2000. Rabies as a transneuronal tracer of circuits in the central nervous system. J. Neurosci. Methods. **103**: 63–71.

Khawplod, P., Wilde, H., Chomchey, P., Benjavongkulchai, M., Yenmuang, W., Chaiyabutr, N. and Sitprija, V. 1996. What is an acceptable delay in rabies immune globulin administration when vaccine alone had been given previously? Vaccine. **14(5)**: 389-391.

Klingen, Y., Conzelmann, K. K. and Finke. 2008 Double labeled rabies virus: live tracking of enveloped virus transport. J. Virol. **82**: 237–245.

Knobel, D. L., Sarah, C., Coleman, P. G., Eric ,M. F., Martin, I. M., Elizabeth, G. M., Alexandra, S., Jacob, Z. and Francois, F. M. 2005. Re-evaluating the burden of rabies in Africa and Asia. Bull. World Health Organ. **83**: 360–368.

Lafon, M. 2005. Rabies virus receptors. J. Neurovirol. **11**: 82–87.

Lee, C., Gaston, M. A., Weiss, A. A. and Zhang. P. 2013. Colorimetric viral detection based on sialic acid stabilized gold nanoparticles. Biosens Bioelectron. **42**: 236-241.

Lentz, T. L., Burrage, T. G., Smith, A. L., Crick, J. and Tignor, G. H. 1982. Is the acetylcholine receptor a rabies virus receptor? Science. **215**: 182–184.

Lentz, T. L., Wilson, P. T., Hawrot, E. and Speicher, N. W. 1984. Amino acid sequence similarity between rabies virus glycoprotein and snake venom curaremimetic neurotoxins. Science. **226**: 847-848.

Lentz, T. L. 1988. Binding of viral attachment protein to host cell receptor: The Achilles heel of infectious viruses. Trends in Pharm. Sci. **9**: 247-252.

Lentz, T. L. 1990. The recognition event between virus and host cell receptor: a target for antiviral agents. J. Gen.Virol. **71**: 751-756.

Lentz, T. L., Yiguang, F. and Peter. L. 1997. Rabies virus infection of IMR-32 human neuroblastoma cells and effect of neurochemical and other agents. Antiviral Research. **35**: 29–39.

Lesniewski, A., Los, M., Jonsson-Niedziółka, M., Krajewska, A., Szot, K., Los, J. M. and Niedziolka-Jonsson, J. 2014. Antibody modified gold nanoparticles for fast and selective, colorimetric T7 bacteriophage detection. Bioconjug Chem. **25(4)**: 644-648.

Lifson, J. D., Hwang, K. M., Nara, P. L., Fraser, B., Padgett, M., Dunlop, N. M. and Eiden, L. E. 1988. Synthetic CD4 peptide derivatives that inhibit HIV infection and cytopathicity. Science. **241**: 712–716.

Lingappa, U. F., Wu, X., Macieik, A., Yu, S. F., Atuegbu, A., Corpuz, M., Francis, J., Nichols, C., Calayag, A., Shi, H., Ellison, J. A., Harrell, E. K., Asundi, V., Lingappa J. R., Prasad, M. D., Lipkin, W. I., Dey, D., Hurt, C. R., Lingappa, V. R., Hansen, W. J. and Rupprecht, C. E. 2013. Host-rabies virus protein-protein interactions as druggable antiviral targets. Proc Natl Acad Sci USA. **110(10)**: E861 -868.

Liu, C. K., Wei, G. and Atwood, W. J. 1998. Infection of glial cells by the human polyomavirus JC is mediated by an N-linked glycoprotein containing terminal alpha(2-6)-linked sialic acids. J Virol. **72(6)**: 4643-4649.

Liu, K., Feng, X., Ma, Z., Luo, C., Zhou, B., Cao, R., Huang, L., Miao, D., Pang, R., He, D., Lian, X. and Chen. P. 2012. Antiviral activity of phage display selected peptides against Porcine reproductive and respiratory syndrome virus in vitro. Virology. **432(1)**: 73-80.

Lonberg-Holm K. and Philipson, L. 1974. Early interaction between animal viruses and cells. Monographs in Virology. **9:** Edited: Melnick JL, Basel, Karger S

Lonberg-Holm, K. 1981. Attachment of animal viruses to cells: an introduction, p. 1–20. In K. Lonberg-Holm and L. Philipson (ed.), Virus receptors, part 2. Animal viruses. Chapman & Hall, Ltd., London.

Luganini, A., Giuliani, A., Pirri, G., Pizzuto, L., Landolfo, S. and Gribaudo, G. 2010. Peptide-derivatized dendrimers inhibit human cytomegalovirus infection by blocking virus binding to cell surface heparan sulfate. Antiviral Res. **85(3)**: 532-540.

Maddon, P. J., Dalgleish, A. G., McDougal, J. S., Clapham, P. R, Weiss, R. A and Axel, R. 1986. The T4 gene encodes the AIDS virus receptor and is expressed in the immune system and the brain. Cell. **47(3)**: 333-348.

Malgaroli, A., Vallar, L. and Zimarino, V. 2006. Protein homeostasis in neurons and its pathological alterations. Curr. Opin. Neurobiol. **16**: 270–274.

Maria, G., Joseph, H. and Lentz, T. L. 1996. Rabies virus binding to the nicotinic acetylcholine receptor subunit demonstrated by virus overlay protein binding assay. J.Gen.Virol. **77**: 2437-2440.

Marsh, M. and Helenius, A. 1989. Virus entry into animal cells. Adv Virus Res. **36**: 107-151

Marsh, M. and Helenius, A. 2006. Virus entry: Open sesame. Cell. **124**:729–740.

Mazarakis, N. D., Azzouz, M., Rohll, J. B., Ellard, F. M., Wilkes, F. J., Olsen, A. L., Carter, E. E., Barber, R. D., Baban, D. F., Kingsman, S. M., Kingsman, A. J., O'Malley, K. and Mitrophanous, K. A. 2001. Rabies virus glycoprotein pseudotyping of lentiviral vectors enables retrograde axonal transport and access to the nervous system after peripheral delivery. Hum Mol Genet. **15**: 2109-2121.

McGettigan, J. P., Foley, H. D., Belyakov, I. M., Berzofsky, J. A., Pomerantz, R. J. and Schnell, M. J. 2001. Rabies virus-based vectors expressing human immunodeficiency virus type 1 (HIV-1) envelope protein induce a strong, cross-reactive cytotoxic T-lymphocyte response against envelope proteins from different HIV-1 isolates. J Virol. **75(9)**: 4430-4434.

Mebatsion, T., Weiland, F. and Conzelmann, K. K. 1999. Matrix protein of rabies virus is responsible for the assembly and budding of bullet-shaped particles and interacts with the transmembrane spike glycoprotein. J. Virol. **73**: 242–250.

Medley, C. D., Smith, J. E., Tang, Z., Wu, Y., Bamrungsap, S. and Tan, W. 2008. Gold nanoparticle-based colorimetric assay for the direct detection of cancerous cells. Anal Chem. **80(4)**:1067-1072.

Mendelsohn, C. L., Wimmer, E. and Racaniello, V. R. 1989. Cellular receptor for poliovirus: molecular cloning, nucleotide sequence, and expression of a new member of the immunoglobulin superfamily. Cell. **56(5)**: 855-865.

Merrifield, R. B. 1963. Solid Phase Peptide Synthesis-The Synthesis of a Tetrapeptide. J. Am. Chem. Soc. **85 (14)**: 2149–2154.

Morizono, K. and Chen, I. S. 2011. Receptors and tropisms of envelope viruses. Curr Opin Virol. **1(1)**:13-18.

Murphy, F. A. and Bauer, S. P. 1974. Early street rabies virus infection in striated muscle and later progression to the central nervous system. Intervirology. **3**: 256–268.

Nadin-Davis, S. A. and Fehlner-Gardiner, C. 2008. Lyssaviruses: current trends. Adv. Virus Res.**71**: 207–250.

Nicol, M. Q., Ligertwood, Y., Bacon, M. N., Dutia, B. M. and Nash, A. A. 2012. A novel family of peptides with potent activity against influenza A viruses. J Gen Virol. **93(5):** 980-986.

Nigg, A. J. and Walker, P. L. 2009. Overview, prevention and treatment of rabies. Pharmacotherapy. **29(10)**:1182-1195.

Niidome, T., Nakashima, K., Takahashi, H. and Niidome, Y. 2004. Preparation of primary amine-modified gold nanoparticles and their transfection ability into cultivated cells. Chem Commun (Camb). **7 (17)**:1978-1979.

Ozawa, M., Ohashi, K. and Onuma, M. 2005. Identification and characterization of peptides binding to Newcastle disease virus by phage display. Virology. 1237-1241.

Pamela, R. H., Brian, H., Hadya, N., Chunyan, Y., Virginie, B. H., David, C. B., Kathleen A. K. and Richard, S. L. 2009. Phage Display selection of cyclic peptides that Inhibit Andes Virus Infection. J.Virol. **83**: 8965-8969.

Pert, C. B, Hill, J. M., Ruff, M. R., Berman, R. M., Robey, W. G., Arthur, U. O., Ruscetti F. W. and Farrar ,W. L.1986. Octapeptides deduced from the neuropeptide receptor-like pattern of antigen T4 in brain potently inhibit human immunodeficiency virus receptor binding and T-cell infectivity. PNAS. **83**: 9254-9258.

Pini, A., Giuliani, A., Falciani, C., Runci,Y., Ricci, C., Lelli, B., Malossi, M., Neri, P., Rossolini, G. M. and Bracci, L. 2005. Antimicrobial activity of novel dendrimeric peptides obtained by phage display selection and rational modification. Antimicrob Agents Chemother. **49(7)**: 2665-2672.

Pritchett, T. J., Brossmer, R., Rose, U. and Paulson, J. C. 1987. Recognition of monovalent sialosides by influenza H3 hemagglutinin. Virology. **160**: 502-506.

Pulmanausahakul, R., Li, J., Schnell, M. J. and Dietzschold, B. 2008. The glycoprotein and the matrix protein of rabies virus affect pathogenicity by regulating viral replication and facilitating cell-to-cell spread. J. Virol. **82**: 2330–2338.

Rajik, M., Jahanshiri, F., Omar, A. R., Ideris, A., Hassan, S.S. and Yusoff, K. 2009. Identification and characterisation of a novel anti-viral peptide against avian influenza virus H9N2. Virology Journal. **6**: 74-86.

Ramanujam, P., Tan, W. S., Nathan, S., Yusoff, K. 2002. Novel peptides that inhibit the propagation of Newcastle disease virus. Arch Virol. **147**: 981-993.

Real, E., Rain, J. C., Battaglia, V., Jallet, C., Perrin, P., Tordo, N., Chrisment, P., D'Alayer, J., Legrain, P. and Jacob, Y. 2004. Antiviral drug discovery strategy using combinatorial libraries of structurally constrained peptides. J Virol. **78(14)**: 7410-7417.

Roberta, G. 2009. Molecular dynamics as a tool in rational drug design: Current status and some major applications. Current Computer-Aided Drug Design. **5**: 225-240.

Roche, S., Bressanelli, S., Rey, F. A. and Gaudin, Y. 2006. Crystal structure of the low -pH form of the vesicular stomatitis virus glycoprotein G. Science. **14**: 187-191.

Roche, S., Albertini, A. A., Lepault, J., Bressanelli, S. and Gaudin, Y. 2008. Structures of vesicular stomatitis virus glycoprotein: membrane fusion revisited. Cell. Mol. Life Sci. **65**: 1716–1728.

Root, M. J. and Steger, H. K. 2004. HIV-1 gp41 as a target for viral entry inhibition. Curr. Pharm. Des. **10**: 1805-1825.

Rothan, H. A., Bahrani, H., Rahman, N. A. and Rohana, Y. 2014. Identification of natural antimicrobial agents to treat dengue infection: In vitro analysis of latarcin peptide activity against dengue virus. BMC Microbiology.**14**:140-150.

Rustici, M., Bracci, L., Lozzi, L., Neri, P., Santucci, A., Soldani, P., Spreafico, A. and Niccolai, N. 1993. A model of the rabies virus glycoprotein active site. Biopolymers. **33(6)**: 961-969.

Schnell, M. J. 1998. Requirement for a non-specific glycoprotein cytoplasmic domain sequence to drive efficient budding of vesicular stomatitis virus. EMBO J. **17**:1289–1296.

Schnell, M. J., McGettigan, J. P., Wirblich, C. and Papaneri, A. 2010. The cell biology of rabies virus: using stealth to reach the brain. Nat Rev Microbiol. **8(1)**: 51-61.

Schooley, R. T., Merigan, T. C., Gaut. P., Hirsch, M. S., Holodniy, M., Flynn, T., Liu, S., Byington, R. E., Henochowicz. S., Gubish. E., Spriggs. D., Kufe, D., Schindler, J., Dawson, A., Thomas, D., Hanson, D., Letwin, B., Liu, T., Gulinello, J., Kennedy, S. , Fisher, R. and Ho, D. D. 1990. A phase I/II escalating dose trial of recombinant soluble CD4 therapy in patients with AIDS or AIDS-related complex. Ann. Intern. Med. **112**: 247–253.

Schweighardt, B. and Atwood, W. J. 2001. Virus receptors in the human central nervous system. J. of NeuroVirol. **7**: 187-195,

Si, Y., Liu, S., Liu, X., Jacobs, J. L., Cheng, M., Niu, Y., Jin, Q., Wang, T. and Yang, W. 2012. A human claudin-1-derived peptide inhibits hepatitis C virus entry. Hepatology. **56(2)**: 507-515.

Superti, F., Derer, M. and Tsiang, H. 1984. Mechanism of rabies virus entry into CER cells. J. gen. Virol. **65**: 781-789.

Tardieu, M., Epstein, R. and Weiner, H. L. 1982. Interaction of viruses with cell surface receptors. International Review of Cytology. **80**: 27-61.

Teissier, E., Penin, F., Pécheur and E. I. 2011. Targeting cell entry of enveloped viruses as an antiviral strategy. Molecules. **16(1)**: 221-250.

Thiele, C. J. 1998. Neuroblastoma: In (Ed.) Masters, J. Lancaster, UK Kluwer Academic Publishers Human Cell Culture. **1**: 21-53.

Thorley, J. A., McKeating, J. A. and Rappoport , J. Z. 2010. Mechanisms of viral entry: sneaking in the front door. Protoplasma. **244(1-4)**: 15-24.

Thoulouze, M. I., Lafage, M., Schachner, M., Hartmann, U., Cremer, H. and Llafon. M. 1998. The neural cell adhesion molecule is a receptor for rabies virus. J.Virol. **71**: 7372-7380.

Tuffereau, C., Benejean, J., Blondel, D., Kieffer, B. and Flamand. 1998. A Low-affinity nerve-growth factor receptor(P75NTR) can serve as a receptor for rabies virus. EMBO J. **17**: 7250–7259.

Tuffereau, C., Schmidt, K., Langevin, C., Lafay, F., Dechant, G., Koltzenburg, M. 2007. The rabies virus glycoprotein receptor p75ntr is not essential for rabies virus infection. J. Virol. **81(24)**: 13622–13630.

Vlasak, M., Goesler, I. and Blaas, D. 2005. Human rhinovirus type 89 variants use heparan sulfate proteoglycan for cell attachment. J. Virol. **79**: 5963–5970.

Vodopija, I. and Clark, H. F. 1991. Human vaccination against rabies. In: Baer GM ed. The natural history of rabies. Boca Raton, FL: CRC Press, 1-94.

Ward, R. H., Capon, D. J., Jett, C. M., Murthy, K. K., Mordenti, J., Lucas, C., Frie, S. W., Prince, A. M., Green, J. D., Eichberg, J. W. 1991. CD4 immunoadhesin (CD4-IgG) can prevent infection of chimpanzees by HIV-1 IIIB. Nature. **352**: 434–436.

West, J. L. and Halas, N. J. 2000. Applications of nanotechnology to biotechnology commentary. Curr Opin Biotechnol. **11(2)**: 215-217.

WHO Fact Sheet No.99. 2010. rabies: www.who.int/mediacentre/factsheets/fs099/en/index.html

Wilde, H., Khawplod, P., Hemachudha, T. and Sitprija, V. 2002. Postexposure treatment of rabies infection: can it be done without immunoglobulin? Clin. Infect. Dis. **34**: 477–480.

Willoughby, R. E. Jr., Tieves, K. S., Hoffman, G. M., Ghanayem, N. S., Amlie-Lefond C. M., Schwabe, M. J., Chusid, M. J. and Rupprecht, C. E. 2005. Survival after treatment of rabies with induction of coma. N Engl J Med. **352 (24)**: 2508-2514.

Winfried, W., Andreas, H. and Gaudin, Y. 2007. Virus membrane fusion. FEBS Lett. **581**: 2150–2155.

Willoughby, R. E. Jr., Tieves, K. S., Hoffman, G. M., Ghanayem, N. S., Amlie-Lefond C. M., Schwabe, M. J., Chusid, M. J. and Rupprecht, C. E. 2005. Survival after treatment of rabies with induction of coma. N Engl J Med. **352 (24)**: 2508-2514.

Winfried, W., Andreas, H. and Gaudin, Y. 2007. Virus membrane fusion. FEBS Lett. **581**: 2150–2155.

Appendix

A. REAGENT USED IN ELISA

1. Coating Buffer (50mM corbonate-bicorbonate pH 9.6):

Na_2CO_3 0.0795gm (50ml DD H_2O)

$NaHCO_3$ 0.1465gm (50ml DD H_2O)

Mixed the above solution and adjusted the pH to 9.6

2. TBS

Tris-HCL 50mM (**pH 7.5**)

6.05gm of Tris Base in 900ml of DD H_2O, pH adjusted to 7.5 with 1M HCL

NaCL (150mM)

8.766gm of NaCL

Autoclaved and stored at room temperature.

3. TBST

TBS with 0.05% Twin 20 for washing of ELISA plates

B. REAGENT USED IN CELL CULTURE

1. DMEM (Gibco)

DMEM powder - 13.4 gm

Distilled water - 1000 ml

Dissolved in 950 ml of distilled water and mixed.

To this, 3.7 gm of NaHCO3 per litre of medium was added and the final volume was made up to 1000 ml. The pH was adjusted to 7.2-7.3 below desired working pH.

Sterilized by filtration.

2. Growth medium

DMEM 90 ml

FBS (Gibco) 10 ml

3. Trypsin Versene solution (2.5%)

Trypsin 2.5 gm

Versene 1.4 gm

1 X PBS was added to make the volume up to 1000 ml.

4. Phosphate Buffer Saline (PBS pH 7.4)

Sodium chloride (NaCl) 8.00gm

Pottasium dihydrogen phoshphate (KH2PO4) 0.20gm

Disodium hydrogen phosphate (Na2HPO4, 2H2O) 1.16gm

Pottassium chloride (KCl) 0.20gm

Distilled water upto 1000ml

Prepared PBS was autoclaved at 121°C, 15lb pressure for 20 min

stored at 4°C for further use.

5. Cell Fixative

Formaldehyde 4% (w/v) in PBS 1X

80% Acetone in 1X PBS

stored at room temperature.

B. REAGENTS USED IN AGAROSE GEL ELECTROPHORESIS

1. Tris-acetate-EDTA (TAE) buffer 50 X

Tris base	242 g
Glacial acetic acid	57.1 ml
0.5 mM EDTA (pH 8.0)	100 ml

Distilled water was added to make up to a final volume of 100ml.

A working solution of 1X was used.

2. Ethidium bromide stock solution (10 mg/ml)

Ethidium bromide	100 mg
Distilled water	10 ml

The solution was mixed and stored at 4^0C. A concentration of 0.5µg/ml was used in preparing agarose gel.

3. Loading dye (6X)

Bromophenol blue	0.25% (w/v)
Xylene cyanol FF	0.25% (w/v)
Sucrose	40% (w/v)

Stored at 4^0C.

Vitae

Name	:	Basavaraj Sajjanar
Father's name	:	Kotrappa Sajjanar
Mother's Name	:	Shivamma Sajjanar
Permanent Addrtess	:	C/o:Kotrappa Sajjanar, Post: Halligudi Tq: Mundaragai Dist: Gadag State: Karanataka-582115
Email	:	bksvet@gmail.com, bsajjanar@niam.res.in

Acadamic details

Degree	University	OGPA	Year
BVSc&AH	Karnataka Veterinary Animal and Fishery Sciences University	8.64	2007
M.V.Sc	Indian Veterinary Research Institute	8.64	2009